Development and Validation of Quantitative PCR Assays for DNA-Based Newborn Screening of 22q11.2 Deletion Syndrome, Spinal Muscular Atrophy, Severe Combined Immunodeficiency and Congenital Cytomegalovirus Infection

Mylene Aline Theriault

Thesis submitted to the
Faculty of Graduate and Postdoctoral Studies
in partial fulfillment of the requirements for the
Masters of Science degree in Biochemistry

Department of Biochemistry, Microbiology and Immunology
Faculty of Medicine
University of Ottawa

Abstract

The development of new high throughput technologies able to multiplex disease biomarkers as well as advances in medical treatments has lead to the recent expansion of the newborn screening panel to include DNA-based targets. Four rare disorders; deletion 22q11.2 syndrome and Spinal Muscular Atrophy (SMA), Severe Combined Immunodeficiency (SCID) and Congenital Cytomegalovirus (CMV), are potential candidates for inclusion to the newborn screening panel within the next few years. The major focus of this study was to determine whether 5'-hydrolysis assays developed for the four distinct disorders with specific detection needs and analytical ranges could be combined on the OpenArray system and in multiplexed qPCR reactions. SNP detection of homozygous *SMN1* deletions in SMA, CNV detection in the 22q11.2 critical region, and quantification of the SCID biomarker, T-cell receptor excision circles (TRECs) and CMV were all required for disease confirmation. SMA and 22q11.2 gene deletions were accurately detected using the OpenArray system, a first for the technology. The medium density deletion 22q11.2 multiplex successfully identified deletion carriers having either the larger 3 Mb deletion or the smaller 1.5 Mb deletions. Both TREC and CMV targets were detected but with a decrease in sensitivity when compared to their singleplex counterparts. Lastly, copy number detection of the *TBX1* was performed when multiplexed with the TREC assay, without a decrease in detection limit of either assay. Here, we provide proof of principal that qPCR multiplexing technologies are amenable to implementation with a newborn screening laboratory.

Acknowledgements

I would sincerely like to thank my supervisor, Dr. Pranesh Chakraborty, for giving me the opportunity to pursue graduate studies in the Newborn Screening Ontario (NSO) Laboratory at the Children's Hospital of Eastern Ontario (CHEO). His continued support and guidance throughout this process has been invaluable. I would also like to thank the members of my thesis advisory committee, Dr. Alex MacKenzie and Dr. Robert Slinger, for their assistance in initial project design, their aid in obtaining funding and their continued feedback as subject matter experts. Exceptional gratitude is extended to Dr. Osama Al-Dirbashi, Dr. Dennis Bulman and Christine McRoberts at NSO for their support, guidance and teaching during the course of this project. Special appreciation is extended to Ioana Moldovan, for sharing her expertise and practical knowledge of the OpenArray system. Thank you to all members of NSO for their support, encouragement and having the ability to make me laugh during even the most stressful times. This project was funded in part by the CHEO Scholarship Program and the Canadian Society for Medical Laboratory Science Founders Fund Award. Finally, I would also like to thank my friends and family for their unconditional support and encouragement.

Table of Contents

List of Figures

List of Tables

List of Abbreviations

aCGH	Array comparative genomic hybridization
ADA	Adenosine deaminase
ANOVA	Analysis of variance
ASA	Allele-specific amplification
BHQ	Black-hole quencher
BLAST	Basic local alignment search tool
ΔΔCq	Classical relative quantification
CI	Confidence interval
CMV	Cytomegalovirus
CNV	Copy number variation
Cq	Quantification cycle
CV	Coefficient of variation
DBS	Dried blood spot
df	Degree of freedom
DGCR	DiGeorge Critical Region
DNA	Deoxyribonucleic acid
dNTP	Deoxyrinucleotide triphosphate
E%	Amplification efficiency
ESE	Exonic splicing enhancer
ESS	Exon silencer element
F	Variation ratio
FAM	6-carboxyfluorescein
FBS	Fetal bovine serum
FISH	Fluorescent *in situ* hybridization
IRT	Immunoreactive trypsinogen
KCl	Potassium Chloride
LCR	Low copy number repeats
LOD	Limit of detection
LOQ	Limit of quantification

MeOH	Methanol
Mg^{+2}	Magnesium
MGB	Minor grove-binder
MIQE	Minimum Information for Publication of Quantitative Real-Time PCR Experiments
MLPA	Multiplex probe ligation-dependent amplification
MS	Mean of squares
MS/MS	Tandem mass spectrometry
NAHR	Non-allelic homologous recombination
NK	Natural killer cells
NPV	Negative predictive values
NTC	No template control
P	Probability
PBS	Phosphate buffered saline
PCR	Polymerase chain reaction
PEG	Polyethylene glycol
PPV	Positive predictive values
QC	Quality control
QCMD	Quality Control for Molecular Diagnostics
qPCR	Quantitative real-time PCR
Quasar-670	Indocarbocyanine (Cy5)
ΔRn	Rox-normalized fluorescent intensity
R^2	Correlation coefficient
ROC	Receiver Operating Characteristics
ROI	Region of Interest
RQ	Relative quantification
RQ_{EA}	Efficiency adjusted relative quantification
RSS	Recombination signal sequence
SCID	Severe combined immunodeficiency
SD	Standard deviation
SMA	Spinal muscular atrophy

SNHL	Sensorineural hearing loss
SNP	Single nucleotide polymosphism
SS	Sum of squares
TAMRA	Tetramethylrhodamine
Taq	*Thermus aquaticus* DNA polymerase
t-RNA	Transfer ribonucleic acid
sj TREC	Signal-joint T-cell receptor excision circle
TREC	T-cell receptor excision circle
Tx-10	Triton-X, 10%
UL	Unique long
UNG	Uracil-N-glycosylase
US	Unique short
WT	Wild-type

Introduction

1.2 History of newborn screening

1.2.1 The golden age of biochemical & metabolic screening

Wide-spread newborn screening began in early 1960's with the development of a dried blood spot (DBS) test developed by Guthrie and Susi, to detect hyperphenylalaninemia, a robust biomarker for phenylketonuria (PKU)(ACMG 2006; Dhondt, 2007; Fernhoff, 2009). While other technologies allowed a modest expansion of newborn screening, it was not until the 1990's with the introduction of amino acid and acylcarnitine profiling using tandem mass spectrometry (MS/MS) that a large number of additional conditions were added to the testing panel (Seymour et al., 1997; Schulze et al., 2003; Tarini et al., 2006). Criteria for disease inclusion are based on principles set out by Wilson and Jungner in 1968, which have been modified specifically for newborn screening purposes (Wilson and Jungner, 1968). i) There must be high incidence of the disorder within the population being screened and a significant morbidity or mortality associated with the disease. ii) The natural course of the disease must be well characterised. iii) A suitable treatment options must be available and be efficacious. iv) A pre-symptomatic period must exist so that early treatment may prevent or reverse further health decline. v) There must be an available and validated screening test for the disorder. vi) A cost-benefit assessment should be conducted prior to screening to determine the financial impact on the health care system. vii) Disease treatment facilities must be available and able to treat an increased patient load. Technological advances in both screening tools and treatment options have progressively lead to the rethink many criteria points.

With increased research delving into innovative treatment options and the development of new high throughput technologies able to multiplex disease biomarkers, non-metabolic genetic diseases have been slowly added to the disease panel. Cystic fibrosis was the first of its kind to be added to the list of core conditions with screening commencing in Ontario as of April of 2008. Severe combined immunodeficiency (SCID) was added to the American Recommended Uniform Screening panel in 2010, thanks in part to the identification of a measurable biomarker, T-cell receptor excision circles (TRECs) quantified using quantitative real-time PCR (qPCR)(ACMG 2006; Baker et al., 2010). In the United States, additional metabolic and genetic disorders are evaluated yearly by the newborn screening community to ascertain whether they should be included to the list of screening targets (Therrell Jr. et al., 2008). In recent years, relevant stakeholders have discussed deletion 22q11.2 syndrome, congenital cytomegalovirus infection (CMV) and spinal muscular atrophy (SMA). With the implementation of SCID testing in the US, a large number of screen positive infants were identified as having severe lymphopenia secondary to 22q11.2 deletion syndrome (Baker et al., 2010; Al-Tamemi et al., 2005; Bales et al., 2010; Borte et al., 2011). New research regarding hearing loss in children has demonstrated that many children who have asymptomatic congenital CMV infections are often not identified using conventional hearing tests, leading to progressive decline in both hearing and cognition over time(Jakubikova et al., 2009; Korver et al., 2009; Stehel et al., 2008). Furthermore, infants who underwent neonatal CMV screening and were treated early with antivirals drugs exhibited a halt and even reversal of sensorineural hearing loss (Barbi et al., 2006; Barbi et al., 2006b; Lombardi et al., 2009). SMA remains a controversial subject in the field of newborn

screening, as it does not classically meet some of the criteria for screening, as there are currently no approved drug treatments (Wilson and Jungner, 1968).

1.2 Overview of target diseases

1.2.1 Deletion 22q11.2 Syndrome

22q11.2 deletion syndrome, historically referred to as DiGeorge, Sphrintzen, Opitz GBBB or velocardiofacial syndrome, presents with a wide range of clinical features. The most common phenotypes included; cardiac abnormalities (>70%), immune dysfunction (>70%), hypocalcaemia (>40%), palatal defects (>40%) and behavioural issues (>90%) (Bassett et al., 2011; McDonald-Mcginn and Sullivan, 2011). Prevalence estimates vary between ~ 1 in 3 000 to 1 in 7 000 births (Driscoll et al., 1993; Óskarsdóttir et al., 2004; Sullivan, 2008). Micro-duplications within the DiGeorge Critical Region (DGCR) have also been reported with a much lower prevalence, with ~2% of suspected deletion carriers having duplications, potentially due to the milder phenotypic presentation associated with the disorder (Edelmann et al., 1999; Ensenauer et al., 2003; Blennow et al., 2008; Yobb et al., 2005; Agergaard et al., 2012; Bi et al., 2012). The DGCR at chromosome position 22q11.2 has many low copy number repeats (LCR A-H) (Figure 1, p.5) with small segmental duplication near some of the genic regions, which are thought to contribute to non-allelic homologous recombination (NAHR) (Edelmann et al., 1999; Shaikh et al., 2000; Shaikh et al., 2001). More than 90% of individuals with 22q11.2 syndrome have a ~3 Mb loss involving LCR A-D, with only 8% having the smaller ~1.5 Mb deletion involving LCR A-C and are *de novo* in nature (Driscoll et al., 1992; Driscoll et al., 1992; Carlson et al., 1997; Edelmann et al., 1999; Shaikh et al., 2000; Shaikh et al., 2001; Bittel

et al., 2009). The alteration in gene dosage, the unmasking of autosomal recessive disorders as well as the presence of modifier mutations within the remaining genes on the opposite allele, are thought to contribute to the heterogeneous nature of the 22q11.2 deletion/duplication syndrome (McDonald-McGinn et al., 2013).

There are many genes within the DGCR thought to be associated with the typical features of 22q11.2 deletion syndrome. *UFD1L*, a developmentally expressed ubiquitination protein, is responsible for the development for ectodermally derived structures contributing to the formation of palatal, thymic and aortic arch structures (Pizzuti et al., 1997; Jones and Gawronski, 2002). The transcriptional regulator, *TBX1*, involved in the normal development of the pharyngeal arch arteries, is highly linked to the cardiac abnormalities and cleft palate associated with 22q11.2 deletion syndrome (Yagi et al., 2003; Meechan et al., 2009; Lima et al., 2010b; Weisfeld-Adams et al., 2012; Maynard et al., 2013). DiGeorge Critical Region gene 2 (*DGCR2*), also known as *IDD*, is a putative membrane glycoprotein expressed in heart and brain and is thought to be involved in cell-cell mediated interactions, normal cell differentiation and migration (Dunham et al., 1999). The *HIRA* gene, previously known as *TUPLE1*, codes for a histone binding protein involved in cardiac neural crest development (Wilming et al., 1997; Magnaghi et al., 1998; Farrell et al., 1999). Catechol-O- methyltransferase, (COMT), catalyzes the methylation of catecholamines in the brain, and plays a major role in the dopamine pathway (Bearden et al., 2004; Bearden et al., 2005). Duplications and deletions in the *COMT* gene is been implicated in the development of the psychiatric disorders, learning difficulties, autism and an increased risk of developing schizophrenia (Beuten et al., 2006; Meechan et al., 2009).

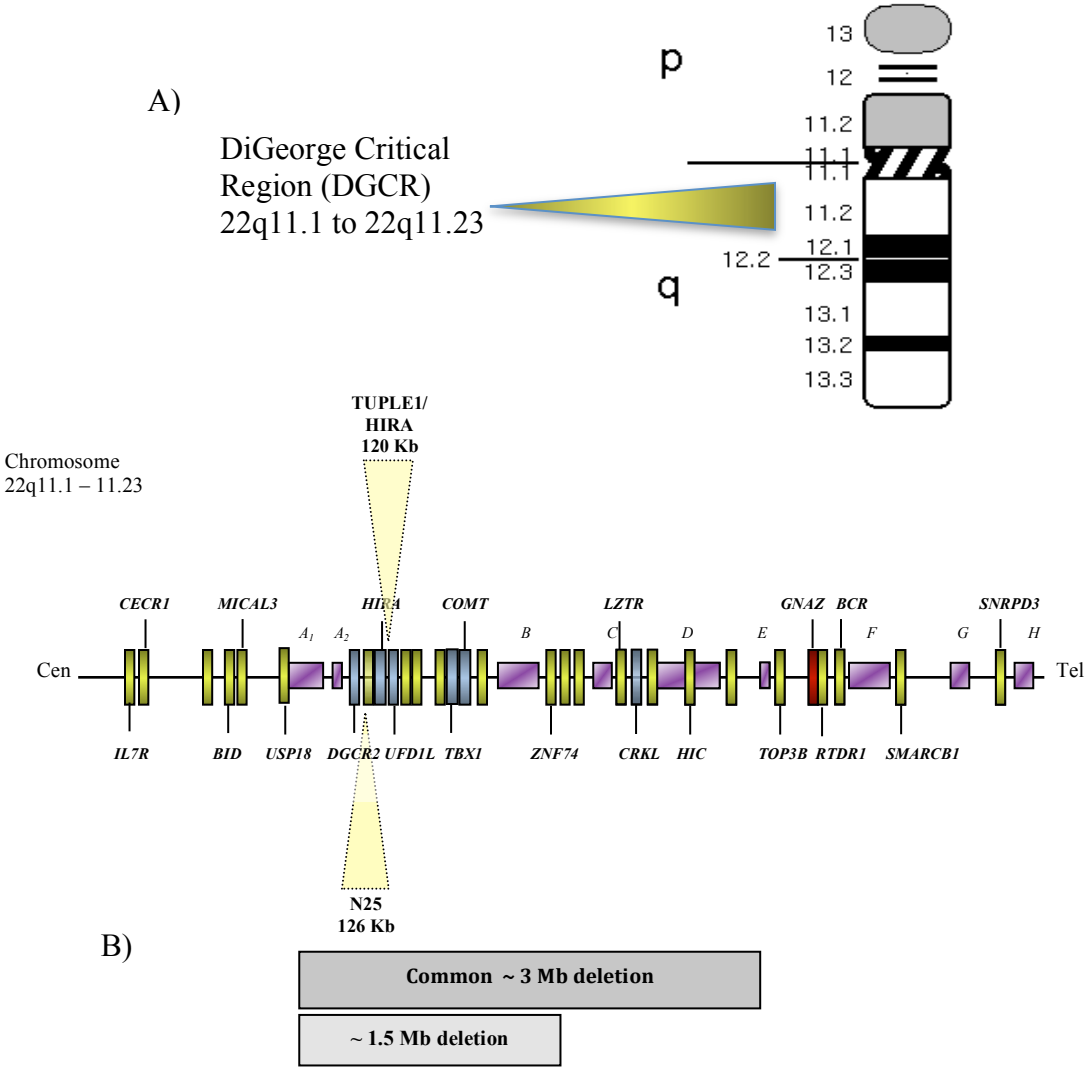

Figure 1 A-B. (A) An ideogram of chromosome 22 demarcating the different bands identified through Giemsa staining. (B) A schematic overview of the DGCR at 22q11.2 on chromosome 22. The low copy number repeats (LCR)(A-H) responsible for the genetic rearrangements in the area are depicted as shaded purple squares. The location of the TUPLE1/HIRA and N25 FISH probes commonly used to detect 22q11.2 deletions are indicated by yellow triangles. Copy number assay developed for this study are depicted in blue, with a single dropped assay *GNAZ* shown in red. Grey bars depict the common 3 Mb and the less common 1.5 Mb deletion associated with 22q11.2 deletion syndrome.

The CRKL protein has been implicated as a growth factor and focal adhesion signalling with deletions resulting in malformations of neural crest formation, aortic arch structures, thymus and parathyroid structures (Li et al., 2003; Rauch et al., 2005; Guris et al., 2006; Moon et al., 2006; Breckpot et al., 2012; Verhagen et al., 2012). GNAZ, a small Guanine nucleotide binding protein, found near the distal end of the DGCR, binds to receptors activated by neuropeptides and neurotransmitters in the opioid, melatonin and dopamine pathways, which are linked to psychiatric disorders and has been found to be absent in distal 22q11.2 deletions (Saito et al., 1999; Rauch et al., 2005; Saitta et al., 2004).

Treatment regimes for individuals with 22q11.2 deletions/duplications vary depending on the severity of the clinical manifestations, typically requiring a multidisciplinary healthcare team to evaluate and treat these children as early as possible. The most urgent presentations include major cardiac defects, severe palatal or pharyngeal insufficiencies that affect feeding, parathyroid dysfunction leading to hypocalcaemia, severe immunodeficiency or any other congenital defects that may be life threatening to the neonate (Óskarsdóttir et al., 2005; Lima et al., 2010b; Bassett et al., 2011). Minor immune dysfunction is estimated to be present in the majority of infants with 22q11.2 deletions, with 0.5% having severe T-cell abnormalities due to thymic hypoplasia (Puck, 2007; Therrell Jr. et al., 2008; Lipstein et al., 2010; Kersseboom et al., 2011; McDonald-Mcginn and Sullivan, 2011). Newborn screening programs in the United States who have implemented SCID screening have identified many infants with 22q11.2 deletion syndrome with severe T-cell lymphopenia (Baker et al., 2009; Puck, 2011; Verbsky et al., 2011).

The most widely used diagnostic test to identify 22q11.2 deletions or duplications is fluorescence in situ hybridization (FISH) using either the TUPLE1/HIRA or N25 probes carried out on lymphocyte cultures and is quite expensive and time consuming to perform (Kelly et al., 1993; McDonald-McGinn et al., 1997; Tomita-Mitchell et al., 2010; Verhagen et al., 2012). It has been estimated than nearly 6% of 22q11.2 deletions will be missed using FISH probes due to the presence of less common deletions found downstream from the binding sites or microdeletion within the probe annealing sites that do not disrupt probe binding (Yobb et al., 2005; Rauch et al., 2005; Tomita-Mitchell et al., 2010). Alternative 22q11.2 deletion/duplication detection methods are currently gaining wider acceptance in diagnostic laboratories. Multiplex probe ligation-dependent amplification (MLPA) a technique developed my MRC-Holland (Amsterdam), as well as high-density copy number microarrays and array-based comparative genomic hybridization (aCGH) are being explored (Verhagen et al., 2012; Emanuel, 2008; Jalali et al., 2008; Deng et al., 2011; Stuppia et al., 2012). Both microarrays and MLPA are not amenable to high throughput population screening as they are cost prohibitive and have a moderate turn-around time of 36-48 hours (Emanuel, 2008; Vorstman et al., 2006; Sorensen et al., 2008). Many laboratories are developing multiplexed qPCR assays to detect haploinsufficiency which have much shorter turn-around times (~ 2 hours), can be easily automated for use in population screening and are a cost-effective alternative when disease targets are multiplexed together (Yobb et al., 2005; Tomita-Mitchell et al., 2010; Kariyazono et al., 2001; Meechan et al., 2006).

1.2.2 Spinal Muscular Atrophy

Spinal muscular atrophy (SMA) is one of the most common causes of autosomal recessive neuromuscular degeneration and the leading genetic cause of sudden infant death (Lunn and Wang, 2008; Oskoui and Kaufmann, 2008; Wee et al., 2010). SMA is characterized by progressive muscle weakness caused by the destruction of the anterior horn cells of the spinal cord and motor nuclei of the brainstem (Iannaccone et al., 2004; Lunn and Wang, 2008; Oskoui and Kaufmann, 2008). The population incidence is estimated to be as high as ~1 in 6 000 infants with a carrier rate of 1 in 35 to 1 in 50 individuals (Anhuf et al., 2003; Pyatt et al., 2007). Clinical diagnosis and classification of SMA, which has a broad phenotypic spectrum, is based on the age of onset and motor function impairment (Markowitz et al., 2004; Oskoui et al., 2007; Prior, 2007; Lunn and Wang, 2008).

Both survival motor neuron genes, *SMN1* and its inverted homologue, *SMN2*, are both located on chromosome 5q12.2-q13.3. Most SMA patients have either a homozygous deletions of the entire *SMN1* gene (>95%), *SMN1* gene conversion to *SMN2* or deletions of Exon 7 in *SMN1* (Figure 2, p.9). The *SMN2* gene copy number varies from 0 to 4 copies in the general population, with individuals with SMA having a minimum of 1 *SMN2* gene copy. *SMN2* gene copy number modulates the severity of clinical SMA manifestations, as even minimal increases in the amount of full length SMN protein during early on in development and infancy can lessen the neuromuscular degeneration associated with the disorder (Lefebvre et al., 1997b; Tizzano et al., 1998; Jablonka and Sendtner, 2003; Cusco et al., 2006; Russman, 2007). Rare point mutations and small deletions in exon 7 have also been detected in individuals with SMA, with the majority

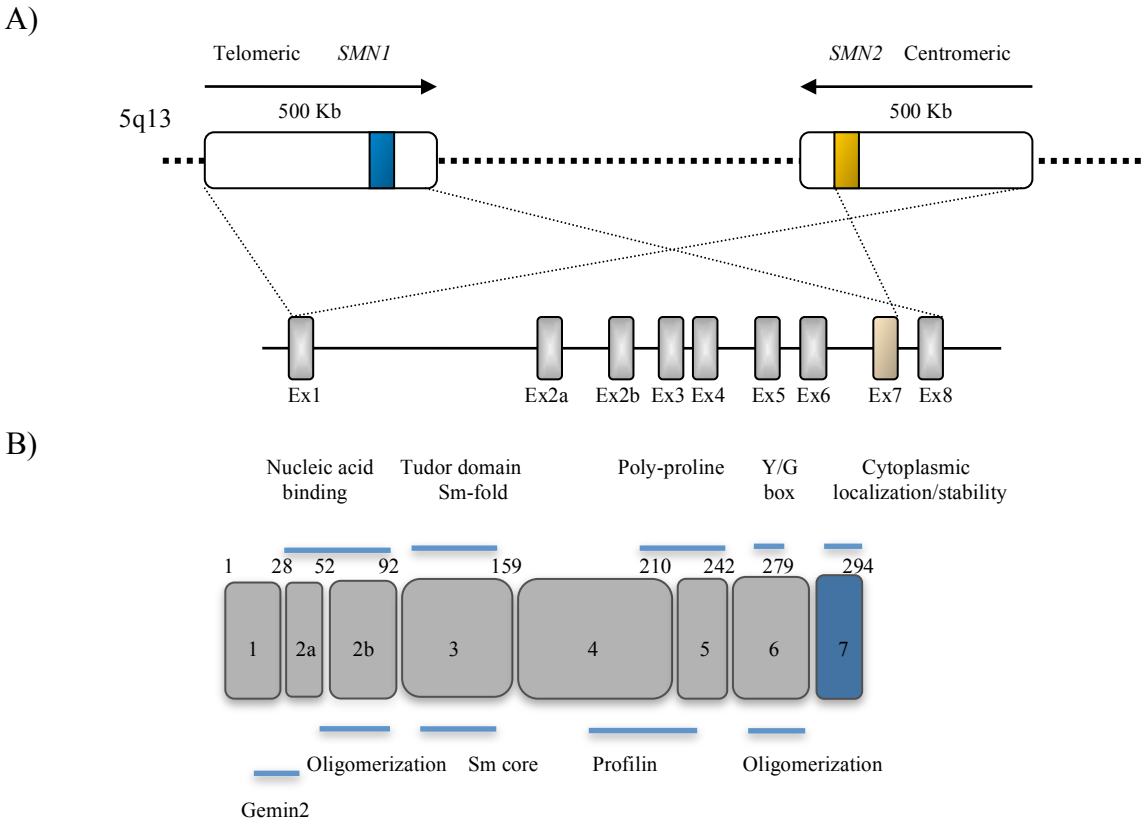

Figure 2 A-B: (A) Schematic overview of the telomeric *SMN1* and the inverted centromeric *SMN2* genes. The grey squares indicate the proximate locations of each exon, with exon 7 denoted as blue in *SMN1* and yellow in *SMN2*. The presence of the c.870C>T substitution in *SMN2* creates a stop codon, leading to the exclusion of exon 7, designated as the shaded yellow box, creating the unstable SMNΔ7 protein. (B) Full-length SMN protein with the amino acid numbers indicating the boundaries of each exon (grey box). Protein domains and functions are listed, with cytoplasmic localization and protein stability linked directly with exon 7 (adapted from Coady and Lorson, 2011).

being compound heterozygote for the deletion of one copy of exon 7 of *SMN1* with a concurrent mutation on the opposite allele (Prior, 2007; Prior et al., 2011). Both genes are nested within a 1.9Mb region filled with many inverted repeats, contributing to *SMN1* gene loss and gene conversion events (Prior, 2007; Campbell et al., 1997; Prior, 2010). Both *SMN* genes are highly homologous and differ by five base pairs only, one of which is a c.840C>T change in the coding sequence of *SMN2* (Figure 2B, p.9) (Iannaccone et al., 2004; Prior, 2007; Wee et al., 2010). The nucleotide change in exon 7 of *SMN2* was thought to either disrupt an exonic splicing enhancer (ESE) or create an exon silencer element (ESS) that leads to the preferential formation of a truncated SMNΔ7 protein that does not oligomerize efficiently, causing the protein to have a twofold shorter half-life than the full length SMN (Burlet et al., 1998; Lorson et al., 1998; Bertrandy et al., 1999; Burnett et al., 2009b; Coady and Lorson, 2011). The SMN protein is a 38 kD protein ubiquitously expressed in all cell types but is found in higher abundance in the large motor neurons of the spinal cord, as well as the neurons in the medulla oblongata, the pyramidal cells of the cortex and the Purkinje cells of the cerebellum (Tizzano et al., 1998; Prior et al., 2010). The SMN protein complex regulates the assembly of small nuclear ribonuclear proteins (snRNPs) found in spliceosomes, which are responsible for pre-mRNA splicing (Lefebvre et al., 1997a; Tizzano et al., 1998; Lorson et al., 1998; Tapia et al., 2012). Unspliced mRNA can lead to certain protein deficiencies that are necessary for neuronal growth and function, causing progressive neuronal death.

Historically, treatment options for infants with SMA centered on supportive care for both the family and the affected child. With the clear link between *SMN2* gene copy number and modulation of SMA disease phenotype, many clinical trials have begun

investigating the use of certain drugs and small molecules to increase the production of full-length SMN protein from the remaining *SMN2* gene. These treatments currently being used in clinical human trials can be subdivided into three categories; i) chemical compounds such as sodium phenylbutyrate that increase *SMN2* gene expression, thereby increasing over-all SMN protein levels; ii) compounds such as valproic acid that prevent missplicing; iii) neuroprotective compounds such as Riluzole and Gabapentin, a glutamate blocker, that prevent or halt further neurodegeneration from occurring (Oskoui and Kaufmann, 2008; Han and McDonald, 2008; Burnett et al., 2009a; Chen et al., 2010; Also-Rallo et al., 2011a). Small oligonucleotides and antisense RNA are being used to increase the inclusion of exon 7 in the *SMN2* gene product by blocking exon silencer element (ESS) (Oskoui and Kaufmann, 2008; Donnelly and Boulis, 2012). Viral gene therapy and stem cell therapies, aimed at increasing SMN production and propagation of axons, reforming the lost neuromuscular junction have shown success in rat and mouse models (MacKenzie, 2010; Corti et al., 2012; MacKenzie, 2012).

Many techniques are currently being employed in the molecular diagnosis of SMA, all using PCR-based protocols such as classical PCR-RFLP, quantitative real-time PCR (qPCR), MLPA and sequencing techniques (Cusco et al., 2001; Chan et al., 2004; Lee et al., 2004; Prior, 2007; Er et al., 2012; da Silva et al., 2013; He et al., 2013). These techniques utilize the c.870C>T single nucleotide polymorphism (SNP) in exon 7 of *SMN2* to differentiate between the two genes. Gene dosage techniques such as qPCR and MLPA are being employed more frequently, as they can determine gene copy number with similar accuracy (Alias et al., 2011; Stuppia et al., 2012; He et al., 2013). Many of

the above mentioned techniques are quite expensive and not amenable to automation for large-scale population screening.

1.2.3 Severe Combined Immunodeficiency

Severe combined immunodeficiency (SCID) is characterized by acute abnormalities in the development and function of T, B and natural killer cells leading to dysfunctional cell mediated and humoral immunity (Gaspar et al., 2001; Chan and Puck, 2005). Originally, the prevalence was estimated to be 1 in 100 000 births, but in recent years, it has increased to 1 in 60 000 births with the implementation of neonatal SCID screening in the United States (Prior, 2007; Baker et al., 2009). This increase is thought to be due to the missed diagnosis of infants with SCID who had previously died without a confirmed diagnosis, and the identification of neonates with non-SCID T-cell lymphopenias. Infants born with SCID often present with early failure to thrive, in conjunction with recurrent bacterial, viral and fungal opportunistic infections (Gaspar et al., 2001; Puck, 2012).

Mutations in more than sixteen different genes have been linked to the development of SCID, each with varying lymphocyte subpopulations. X-linked SCID, due to mutations within the γc-chain, common to multiple interluken and cytokine receptors (IL-2, IL-4, IL-7, IL-9 and IL-15), is responsible for > 50% of all cases (Gaspar et al., 2001; Buckley, 2002; Finlayson, 2008). Abnormal purine metabolism caused by deficiencies in either adenosine deaminase (ADA) or purine nucleoside phosphorylase (PNP), are also important causes of SCID, with ADA deficiency making up > 20% of all SCID cases (Gaspar et al., 2001). Deficiencies in either enzyme leads to the accumulation

of toxic purine metabolites, which initiates T cell, B cell and NK cell apoptosis. Approximately, 11% of all SCID patients have defective V(D)J (Variable, Domain, Joining) gene rearrangement in both T and B cell receptors due to mutations within recombinase enzyme genes (Gaspar et al., 2001; Buckley, 2002; Finlayson, 2008; Puck, 2012). Scarcer still are mutations or deletions of entire genes responsible for thymus development such as those within the 22q11.2 DiGeorge Critical Region (DGCR). The majority of infants with 22q11.2 deletion syndrome demonstrate different forms of immune dysfunction ranging from mild lymphopenia, delayed IgG production and classical SCID presentation (McDonald-Mcginn and Sullivan, 2011; Markert et al., 1998; Knutsen et al., 2011; Heimall et al., 2012).

The most effective long-term treatment option for individuals with SCID, regardless of the genetic cause, remains hematopoietic stem cell transplantation (HSCT) (Buckley, 2000; Buckley, 2011; Fernandes et al., 2012). Infants diagnosed with ADA deficiency have shown success with weekly PEG-ADA enzyme replacement therapy, but almost half will require regular immunoglobulin replacement (Finlayson, 2008). There has been much controversy surrounding the use of gene therapy for treating SCID patients. From 1999 to 2006, twenty ADA SCID patients were treated with CD34+ hematopoietic stem cells infected with a gamma-retroviral vector containing a functional adenosine deaminase gene (Candotti et al., 2006; Booth et al., 2011). Five of the twenty patients developed T-cell acute lymphoblastic leukemia (T-ALL) within the first 5 years post-transplant (Finlayson, 2008; Booth et al., 2011). The lympho-proliferative disorder was caused by viral vector insertion near the *LMO2* proto-oncogene promoter (Finlayson, 2008). Clinical researchers are now concentrating their efforts on developing viral vectors

with tissue specific promoters that express the transgene at normal physiological concentrations at specific developmental stages (Fernandes et al., 2012).

The common feature of all individuals with primary immunodeficiency is very low or absent peripheral T cells. In the mid-1990's, Dr. Daniel Douek and associates created a method for quantifying the amount of naïve peripheral T-cells being produced in the thymus using T-cell receptor excision circles (TRECs) as biomarkers (Douek et al., 1998). Naïve T cells undergo excisional rearrangement of the T cell Receptor alpha/delta (*TCRα/δ*) gene locus, creating an extra chromosomal, non-replicative DNA circle, comprised of the excised *TCRδ* gene, called T cell receptor excision circles (TRECs) (Figure 3, p.15). In 2005, Dr. Jennifer Puck at the University of California (San Francisco) was able to apply the technique for use as a newborn screening assay to identify infants with SCID, with the Wisconsin newborn screening program being the first laboratory to implement State-wide SCID screening in 2008 (Chan and Puck, 2005; Puck, 2007; Baker et al., 2009). Other techniques, such as performing neonatal complete blood cell count do not differentiate between naïve T-cells and maternally derived cells, which may lead to false negative results (Puck, 2012). Immunoassays used to detect and quantify IL-7 levels in dried blood spots developed at Northwester University (Chicago, IL) or T-cell specific proteins such as CD3 and CD45 using liquid bead-based technology from the Luminex corporation (Austin, TX) are still in the preliminary stages of development in newborn screening (Puck, 2012; Finlayson, 2008). Mutational analysis through direct sequencing or microarray SNP detection remains quite expensive and time consuming.

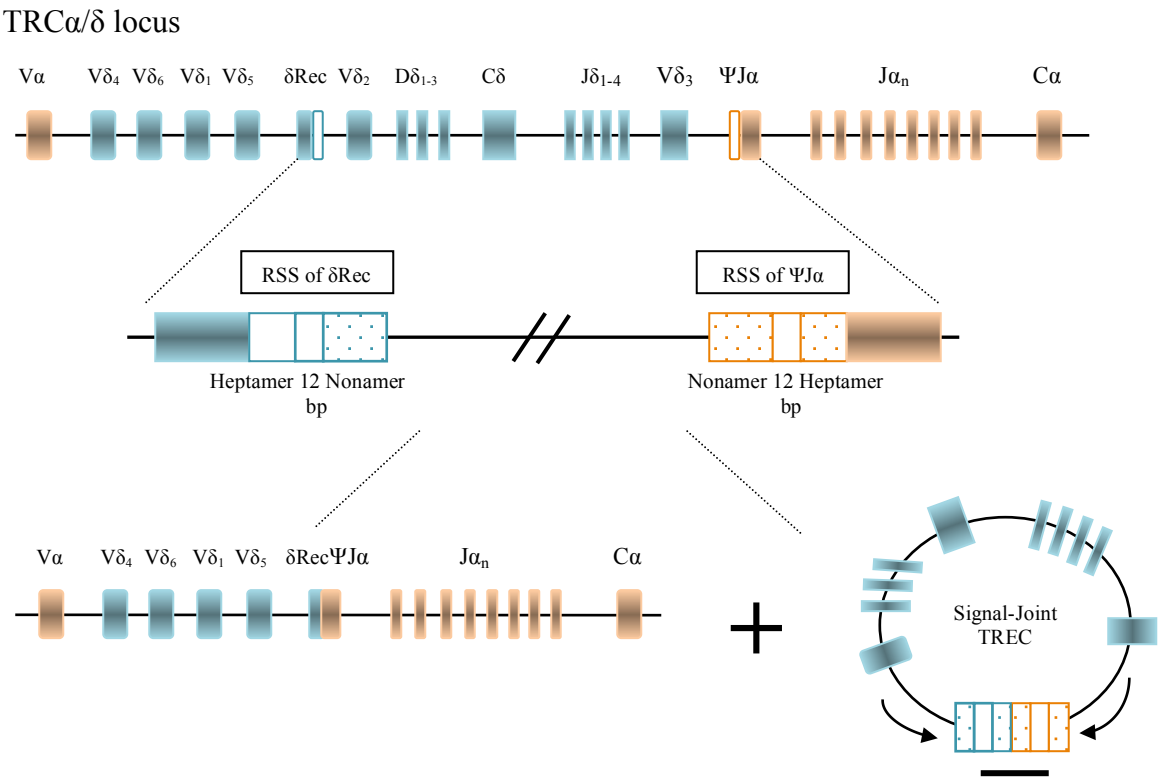

Figure 3. A schematic overview of the T-cell Receptor alpha locus and the subsequent creation of the signal-joint T-cell Receptor Excision Circle (TREC). The T-cell receptor alpha genes are denoted as orange squares, while the delta genes are denoted as blue squares. During gene rearrangement, the conserved heptamer and nonamer sequences are recognized by the recombinase enzymes, causing the excision of the intervening delta V,D,C and J gene segments. The excised fragment then circularizes to form the signal-joint TREC (Chan and Puck, 2005; Baker et al., 2009).

1.2.4 Congenital Cytomegalovirus Infection

Congenital cytomegalovirus (CMV) is the leading cause of non-syndromic sensorineural hearing loss among neonates in North America (Barbi et al., 2003; Boppana et al., 2005). Globally, approximately 0.2-2% of all newborns are congenitally infected with cytomegalovirus with current estimates suggesting that 30,000-40,000 infants are born with congenital cytomegalovirus infection annually in the United States (Walter et al., 2008; Cheeran et al., 2009). Almost 60-90% of symptomatic infants and 10-15% of asymptomatic neonates will develop progressive neurological deficits such as sensorineural hearing loss (SNHL), mental and psychomotor retardation and ophthalmological abnormalities (Scanga et al., 2006; Walter et al., 2008; Cheeran et al., 2009). Symptomatic infants present with Cytomegalovirus Inclusion Disease (CID), which is characterized by intrauterine growth retardation, hepatosplenomegaly, hematological abnormalities, and various cutaneous manifestations, including petechial and purpuric lesions (Boppana et al., 1999; Boppana et al., 2005; Walter et al., 2008; Cheeran et al., 2009). Most infants with congenital cytomegalovirus infection are born to women who are seronegative, with a small minority of seropositive women infected with new strain of CMV (Boppana et al., 2001). These infants appear clinically healthy at birth; however, they may present with progressive CNS deterioration and sensorineural hearing loss.

Cytomegalovirus is designated as human herpes virus 5 (HHV-5) and preferentially infects astrocytes and brain microvascular endothelial cells, which surround the ventricular and sub-ventricular regions of developing fetal brains (Walter et al., 2008; Coll et al., 2009). The age at which the developing infant is infected is also a major factor

dictating the severity of the disease presentation, since neonates that show early infection have more severe symptoms compared to those infected later in gestation (Boppana et al., 2005; Cheeran et al., 2009). Viral load has been linked to the development of progressive SNHL, irrespective of whether the neonates were symptomatic at birth or not, with loads > 10 000 viral copies/mL of blood having the highest risk of developing serious neurological impairment (Boppana et al., 2005; Walter et al., 2008).

Four antiviral drugs; Ganciclovir, Valganciclovir, Foscarnet and Cidofovir are in use in immuno-compromised individuals, with Ganciclovir being the first compound selected specifically to treat CMV infection (Griffiths and Walter, 2005; Cheeran et al., 2009). All of the antivirals have major side effects, including neutropenia and nephrotoxicity as well as having poor bioavailability. The recent development of drug resistance has also caused some concern among treatment centers (Barbi et al., 2006b; Walter et al., 2008). Physical interventions for those with SNHL include the use of hearing aids, cochlear implants and speech therapy, which all aid to reduce disability (Barbi et al., 2006b).

Differentiating between post-natal and congenitally acquired CMV infection is of the utmost importance, as congenital infected neonates present with more severe sequelae. Specific IgM or CMV anti-IgG antibodies in the blood can indicate congenital CMV infection but passive transfer of maternal IgG can occur leading to false positive results, with CMV IgM detected in <70% of infected infants (Boppana et al., 1997; Boppana et al., 1999; Coll et al., 2009) . Laboratory diagnosis is currently made through direct urine culture and through CMV viral load determination using urine, saliva, whole blood or plasma as sources for viral DNA (Machida et al., 2000; Sanchez and Storch,

2002; Boppana et al., 2005). Currently the "gold standard" method for confirming CMV infection is through direct detection in urine, but urine collection on filter paper for newborn screening is logistically problematic and is not conducive to viral culturing (Barbi et al., 2006b). For this reason Barbi *et al.* developed a method for detecting CMV in neonatal blood spot cards in 2000 (Barbi et al., 2000; Barbi et al., 2001). Subsequent qPCR methods using neonatal DBS developed in other laboratories have also been able to detect CMV concentrations as low as 1600 viral copies/ mL using a larger 0.5 cm to 1 cm dried blood spot, equivalent to 500-1000 µL µof whole blood(Barbi et al., 2000; Barbi et al., 2006a; Scanga et al., 2006; Walter et al., 2008). To date, CMV quantification using dried blood spot samples is not routinely being performed in any newborn screening facility.

1.3 Newborn screening in the molecular era

1.3.1 Evolution of NBS technologies

As population testing involves screening hundreds of thousand of neonates yearly, molecular-based testing methodologies have been slow to gain acceptance compared to their less expensive biochemical counterparts. Automated liquid-handlers for DNA extraction and PCR setup have proven indispensible for screening facilities, as they greatly increase the throughput, while reducing human error. Analysis instruments are now accommodating 96-well and 384-well plates, which enables high throughput screening while reducing reagent volumes and reducing the overall cost and turn-around-time of each assay.

Polymerase chain reaction (PCR) enabled the rapid amplification and detection of genomic and RNA targets, leading to the swift explosion of molecular techniques centered on PCR (Laczmanska et al., 2009). One such game changing technique is quantitative real-time PCR (qPCR), by which, the number of starting copies of a DNA sequence can be calculated. For a number of newborn screening candidate diseases, including those considered in this study, require the use of molecular-based screening assays, as they only have DNA-based disease biomarkers.

1.3.2 Quantitative real-time PCR

qPCR combines both amplification of the target gene and detection of the PCR products being created via the emission of a fluorescent signal detected in real-time by a camera capable of capturing different wavelengths of light (Laczmanska et al., 2009). Products can be quantified through end-point detection using intercalating agents such a Sybr Green, which fluoresce only upon incorporation in new forming PCR products or in real-time after each PCR cycle using fluorogenic probes (Higuchi et al., 1992; Freeman et al., 1999). We will be focusing our study on the use of 5'-nuclease probes, more commonly referred to as TaqMan assays. (Figure 4, p.20). The probes are constructed with a fluorogenic molecule attached to the 5'-end and a quencher molecule at the 3'-end. When in close proximity, the fluorophore transfers its energy to the quencher, where the light energy is either re-emitted at a different wavelength (TAMRA quencher) or converted into heat (dark quencher) by a phenomenon known as FRET (fluorescence resonance energy transfer) (Freeman et al., 1999). Different quencher molecules and fluorogenic molecules have been developed to fluoresce and quench at different

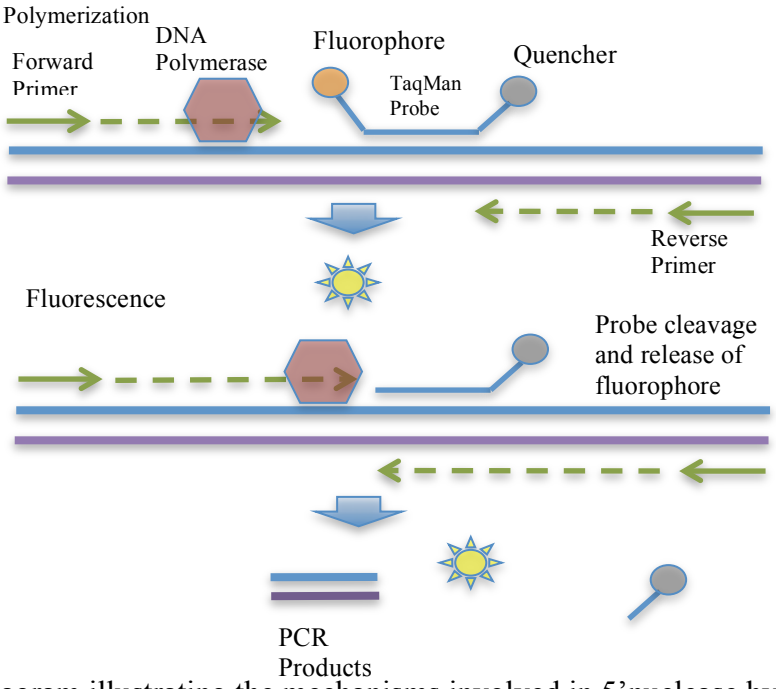

Figure 4. A diagram illustrating the mechanisms involved in 5'nuclease hydrolysis (TaqMan) –based qPCR.

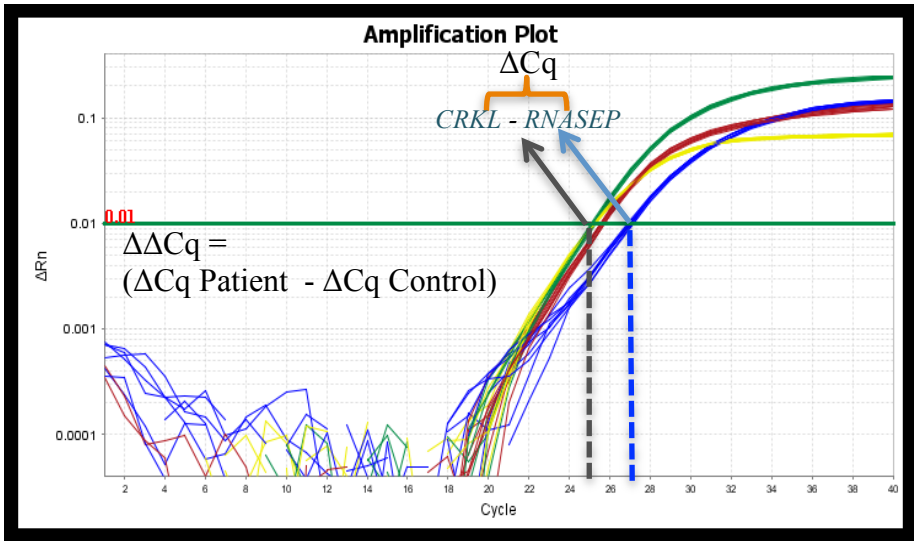

Figure 5. qPCR amplification curves of the 22q11.2 deletion quadplex (this study) depicting the use of relative quantification method, where the quantification cycle (Cq) values for both the target (*CRKL*) and the reference gene (*RNASEP*) of a WT control sample are compared to those of a patients sample to determine the relative gene copy number. The blue dashed line marks the Cq value for *CRKL*, and the black dashed line denotes the *RNASEP* Cq. Threshold is set for a ΔRn of 0.01 (green horizontal line).

wave lengths with the goal of increasing multiplexing capabilities and to reduce background fluorescence. Dark quenchers, such as black-hole quenchers (BHQ) are preferentially selected for use in multiplex reactions, as they do not re-emit light energy, reducing the background fluorescence (Kutyavin et al., 2003; Afonina et al., 2008 Laczmanska et al., 2009). Many new generation probes have additional nucleotide modifications that stabilize the probes when bound to their double-stranded DNA target, such as minor groove binder (MGB) probes (LifeTechnologies) and BHQPlus (Black-hole Quencher) probes (Biosearch Technologies) and allow for the design of much shorter probe sequences (Kutyavin et al., 2003; Kutyavin et al., 2000).

Target quantification by qPCR can be performed using absolute quantification or relative quantification. Absolute quantification requires the use of calibration curves of known starting concentrations plotted against the quantification cycle threshold (Cq). The Cq is the number of qPCR cycles needed for the normalized fluorescent signal (ΔRn) to cross a threshold point at which the amplification reaches its exponential phase, which is taken during the exponential phase, at which time the slope of the sigmoidal curve reaches ~ 1 (Figure 5, p.20). In 1996 the University of Michigan developed a method known as relative quantification ($\Delta\Delta$Cq), by which relative changes in mRNA expression or gene copy number could be quantified using qPCR (Appendix I) (Chiang et al., 1996; Livak and Schmittgen, 2001). A control gene of known gene copy number (reference assay) is used to normalize the reactions to account for differences in starting concentrations of DNA. The reference assay can be run in parallel or in a multiplexed reaction. Figure 5 (p.20) demonstrates the amplification curves created during PCR cycling of the deletion 22q11.2 multiplex reaction (this study) for which the Cq values of

the reference assay and the region of interest (ROI) of the wild-type control samples are used to calculate the gene copy number of patient samples. Recently, Yuan *et al.* created the efficiency adjusted relative quantification method (RQ_{EA}), which incorporates the amplification efficiencies of both the reference assay and the ROI assay to increase the accuracy of gene copy number quantification when using assay with widely varying amplification efficiencies (Yuan et al., 2008). If the unknown sample has two copies of the target gene, the ratio of unknown/control is 1.0. If the unknown sample is hemizygous, and has a gene deletion, then the ratio is close to 0.5. The ratio becomes > 1.5, when gene duplications are present. For the ratios to be as accurate as possible the PCR efficiencies of the target gene and the endogenous control must be similar (> 80%) or the PCR efficiencies would have to be included in the mathematical algorithm to be able to accurately calculate gene copy number (Yuan et al., 2008). Some examples of recent multiplex innovations include work by Dr. Tomita-Mitchell at the Medical College of Wisconsin who designed a multiplex assay combining *TBX1* and *RNASEP* to screen for deletion 22q11.2 syndrome in patients who have undergone cardiac surgery (Tomita-Mitchell et al., 2010). Also, the New England Newborn Screening Program developed a multiplex reaction involving the TREC-E assay with RnaseP to monitor DNA quality, reducing the need for secondary DBS punches, thereby decreasing turn-around-time (Gerstel-Thompson et al., 2010).

1.3.3 OpenArray nanofluidic platform

The need to develop qPCR technologies for high volume, low cost genetic analysis has driven the miniaturization of qPCR technologies. Such recent innovative

technologies include digital PCR (BioRad), microfluidic digital chips (Fluidigm), array cards (LifeTechnologies), bead-based PCR on a microchip (Illumina), infrared mediated microfluidic PCR (IR-PCR) and the OpenArray platform (LifeTechnologies) (Matsubara et al., 2004; Brenan et al., 2008; Liu et al., 2009; Shen et al., 2010; Hilton et al., 2012; Yu et al., 2012). The major advantage of the OpenArray system over other nano-technologies is that each TaqMan assay is developed independently before hand and optimized to amplify under the same cycling conditions, which can allow for "mixing and matching" of different primer and probe sets to create disease specific panels without having to re-optimize the entire experiment (Roberts et al., 2009). The OpenArray technology offers a high throughput, nanoliter platform, which can accommodate 48 patient samples, onto which stainless steel plates the size of a microscope slide are pre-loaded with up to 56 TaqMan assays individually designed and optimized under a uniform set of conditions, allowing for maximum sensitivity and specificity (Brenan et al., 2008; Brenan and Morrison, 2005). Each through-hole contains a volume of 33 nL of qPCR reagents and sample, reducing the reagent cost and sample volume, while maximizing the number of reactions (Figure 6, p.25).

The OpenArray system has been used for a variety of qPCR applications but has yet to be applied in clinical laboratories as it is still in its infancy. Early experiments have consisted of reverse transcription-qPCR and qPCR using Sybr Green I for real-time quantification and for melt-curve analysis (Brenan and Morrison, 2005; van Doorn et al., 2007; Brenan et al., 2009). This application has been used to determine human kinase expression levels in liver and heart samples as well as to detect virulence and marker genes within a mixed microbial environment (Stedtfeld et al., 2008; Dixon et al., 2009).

Recent advances in plate production and imaging have enabled single nucleotide polymorphism (SNP) detection using genotyping assay in which both a wild-type FAM-labelled and the mutant VIC-labelled TaqMan-MGB assays are both dispensed into the same through-hole (Roberts et al., 2009). It is the ability to mix-and-match the TaqMan assays and mode of analysis (SNP genotyping and absolute quantification) as well as the lower reagent cost that makes the OpenArray platform a potential candidate technology for use in newborn screening.

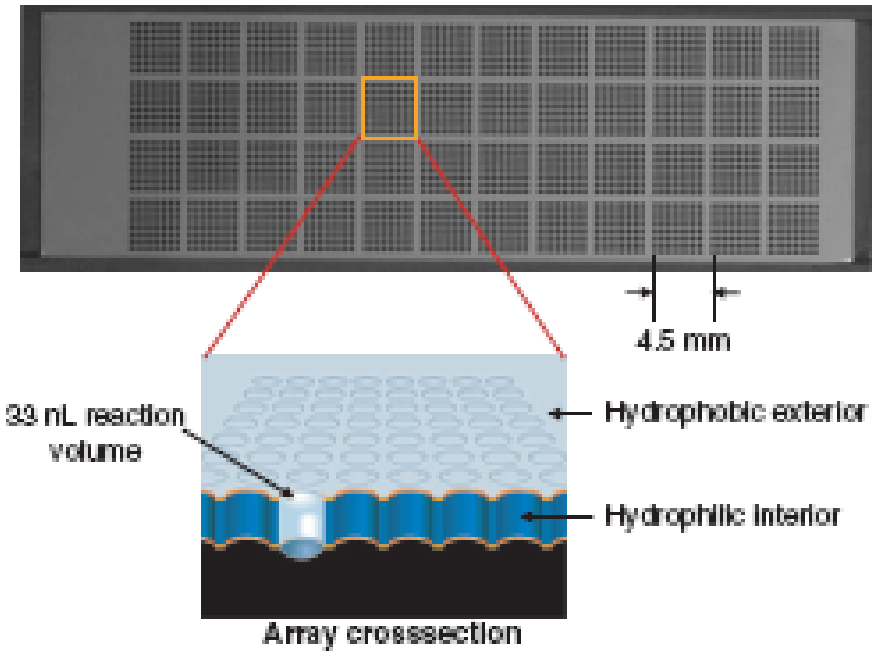

Figure 6. Image of a 48 sample x 64 assay stainless steel OpenArray plate (25 mm x 75 mm x 0.3 mm) into which an amide-coupled hydrophilic layer is applied to the center of each through-hole and a hydrophobic fluoroalkyl layer is vinyl-coupled to the exterior surface. A total of 54 separate TaqMan assays were loaded onto each array along with 8 designated quality control through-holes. The layering allows for the retention of qPCR reagents and samples to the through-holes without sample dispersion or cross-contamination. Reprinted with permission (Morrison et al., 2006).

1.4 Thesis Outline

1.4.1 Rationale

Population based screening of newborns was established with the aim of testing for diseases that are significant health burdens and where early diagnosis and intervention can prevent cognitive impairment and even death. The inclusion of certain candidate disorders such as 22q11.2 deletion syndrome, spinal muscular atrophy (SMA), severe combined immunodeficiency (SCID), and congenital cytomegalovirus (CMV) infection has been recently discussed. Each disease biomarker present distinct analytical constraints; diagnosing deletion 22q11.2 syndrome necessitates the detection of hemizygous deletions, while SMA requires the use of SNP-based assays capable of quantifying homozygous deletions of the *SMN1* gene, both confined to a very narrow dynamic quantification range of 0 to 5 genes. The quantification of extra-chromosomal TREC biomarkers for SCID necessitates a moderate dynamic range from 0 to 5 000, while congenital CMV detection requires the quantification of viral targets of upwards of a few million. Complexities arising from the heterogeneous nature of dried blood spots are also major concerns due to potential uneven blood application, creating significant inter-sample variation in DNA concentration as well as the presence PCR inhibiting substances such as heme. Identifying a technology that can quantify multiple targets using varying amounts of DNA, within precise analytical ranges, is essential. The OpenArray system accomplishes nanoliter real-time qPCR, allowing the user to analyze and quantify many different targets simultaneously using only nanoliters of reagents (Brenan and Morrison, 2005; Dixon et al., 2009). We have developed; CNV assays for deletion 22q11.2 syndrome, *SMN1*-specific SNP assays for SMA and quantification

assays for TREC and CMV that were analyzed in parallel using the OpenArray platform and in multiplexed reactions at the macro-level. By validating both the OpenArray platform and multiplexed assays, we have demonstrated the simultaneous quantification of multiple targets over variable dynamic ranges using qPCR technologies, with the end goal of applying these to large-scale newborn screening.

1.4.2 Hypothesis

Select CNV, SNP genotyping and TaqMan quantification assays requiring different analytical dynamic ranges can be combined on the OpenArray platform and in multiplex reactions to accurately identify individuals with hemizygous and homozygous gene deletions, while simultaneously quantifying levels of T-cell receptor excision circles and cytomegalovirus in neonatal dried blood samples.

1.4.3 Objectives

1. Identify and redesign 5'- hydrolysis assays for the detection of 22q11.2 and *SMN1* gene deletions, as well as assays for quantification of TREC and CMV for use on the OpenArray and in multiplexed reaction.
2. Demonstrate that relative quantification to detect CNVs can be successfully performed on the OpenArray platform.
3. Develop dried blood spot calibrators and QC material for use in both relative and absolute qPCR reactions.
4. Demonstrate that the OpenArray platform and multiplexing assays at the macro-level can accurately quantify assays with different dynamic ranges.

PART A: Development of Disorder Specific 5'-hydrolysis Assays

2. Deletion 22q11.2 Syndrome

2.1 Introduction

Diagnosis of deletion 22q11.2 syndrome involves detecting the hemizygous deletions of gene within the DGCR (Figure 1, p.5). The primary goal of this study was to identify and re-design qPCR assays targeting genes within the 22q11.2 deletion region for use in relative gene copy number quantification. Gene targets that span the entire DGCR linked to the associated phenotypes were selected. These targets included *DGCR2*, *HIRA*, *UFD1L, TBX1*, *COMT*, *CRKL* and *GNAZ*, which allowed us to detect the large 3 Mb deletion and the smaller less common nested deletions or duplications. TaqMan MGB (minor-groove binder) probes were selected over traditional TAMRA-based probes due to their increased stability when bound to single-stranded DNA and their lower background fluorescence (Kutyavin et al., 2003; Afonina et al., 2008; Kutyavin et al., 2000). The redesigned assays were then selected for use on the OpenArray system, a nanoliter high-throughput qPCR technology, and in multiplexed qPCR reactions, with each methodology compared to the singleplex assays to ascertain whether these techniques were sensitive enough to detect hemizygous deletions and amenable for use in newborn screening.

2.2 Materials and Methods

2.2.1 qPCR 5'-hydrolysis probe and primer design

Primer and Probe Design:

An extensive literature search was performed to identify assays that are currently in use to detect gene copy number within the 22q11.2 DGCR. We selected seven assays for the following genes; *UFD1L* (Kariyazono et al., 2001), *COMT* (Beuten et al., 2006), *CRKL* and *GNAZ* (Rauch et al., 2005), as well as three proprietary copy number (CNV) assays from LifeTechnologies for *DGCR2* (Hs01576261_cn), *TBX1* (Hs01313390_cn) and *HIRA* (Hs02290153_cn). The proprietary copy number assays were used as control assay by which to compare the other custom assays for efficiency and ability to determine accurate gene copy number. The published primer and probe sequences were mapped to their corresponding genomic location using GenBank sequence NC_000022.10. All custom primers and probes selected, except for *GNAZ* and the proprietary assays, were redesigned to be TaqMan FAM-labelled MGB assays using the PrimerExpress 3.0 software (LifeTechnologies) (Table 1, p.29). Reference assays needed for normalization during relative quantification (RQ) were selected from our literature search based on their current use in CNV quantification. These genes consisted of *Albumin* at position 14467569 on chromosome 4q13.3 (NW_004078021.1) (Anhuf et al., 2003), *β-Actin* at position 5539095 overlapping Exon 3 and Intron 4 on chromosome 7 (NW_004078029.1) (Baker et al., 2009) and the commercially available reference assay *RNASEP* at position 20811565 on chromosome 14q11.2 (NC_000014.8) (LifeTechnologies). The *RNASEP* assay will be used as a standard from which to compare the other reference assays.

Table 1. A list of all functional primers and probes developed for copy number quantification of the 22q11.2 region. Assays that were redesigned to be FAM-labeled MGB assays are underlined.

qPCR Assay	Sense Primer (5'→3')	Antisense Primer (5'→3')	FAM MGB Probe (5'→3')	Size (bp)
Deletion 22q				
UFL1D	GAGGCAGATTCGTCGCTTTC	CAATCAGCCAACAGTCCTCACTT	TCTGGAGAAGGACAGTCAT	85
CRKL	TAGAGAAGCCTGAAGAACAGTGG	CTTTTCGACATAAGGGACAGGAAT	CCGGAACAAGGATG	83
GNAZ	CGGGCATTGTGGAGAACAA	CCCACGTCCACCATCTTGA	TTCACCTTCAAGGAGCTC	61
COMT	CAGTTGTGGTTACTTTCTGGAGAGAG	GGCCGCCCAGGAAGAC	CATGTGGCATGCAGGA	70
TBX1	Hs01313390_cn			80
DGCR2	Hs01576261_cn			110
HIRA	Hs02290153_cn			130
Reference Assays				
RNASEP	Ribonuclease P RNA component H1 (H1RNA) gene (RPPH1)			87
B-Actin	ATTTCCCTCTCAGGCATGGA	CGTCACACTTCATGATGGAGTTG	CCTGTGGCATCCACGAA	70
Albumin	ATGCTGCACAGAATCCTTGGT	TCATCGACTTCCAGAGCTGAAA	AACAGGCGACCATGC	60

Primer and probe sequences were assessed against the human genome using the BLAST program to ensure 100% homology to only the sequence from which they were derived and also to guarantee that the primer and probe annealing sites were free from single nucleotide polymorphisms.

2.2.2 DNA extraction from whole blood

To ensure robustness of amplification, high quality DNA extracted from whole blood was used to validate all TaqMan assays. Whole blood from a single adult donor known to have both copies of the DGCR was collected in sodium heparin blood collection tubes and used as the DNA source. QIAmp DNA mini kits (QIAGEN) were used to extract genomic DNA following the provided protocol. The extracted DNA elutions were pooled into a single tube and quantified using the NanoDrop2000 spectrophotometer (Thermo Scientific). The resulting DNA had a concentration of 342 ng/ul with a 260/280 ratio of 1.92. The sample was then diluted using molecular grade water first into a 50 ng/uL concentration to initially validate presence or absence of amplification and then subsequently diluted into multiple concentrations consisting of 25, 50, 75, 100 and 125 ng/uL aliquots to be used as calibrators to determine the amplification efficiencies of all of the developed assays for this study. The DNA sample was also used as the wild-type control during all copy number quantification assays.

2.2.3 Assay validation and selection of reference assays

qPCR was performed in a total volume of 20 uL containing 1X TaqMan Universal Master Mix without UNG (Uracil-N-glycosylase) (LifeTechnologies), 1 ul single-tube TaqMan-MGB Assay (900 nM primers and 250 nM FAM-labeled probe)

(LifeTechnologies), molecular grade water (VWR), and 100 ng of DNA. The reactions were carried out on a ViiA 7 Real-Time PCR System (LifeTechnologies). Cycling conditions were as follows; 1 cycle of 10 minutes at 95°C and 45 cycles of 30 seconds at 95°C and 60 seconds at 60°C.

2.2.4 Assay efficiency (E%) calculation

Using the prepared serially diluted wild-type DNA calibrators ranging from 50 ng, 100 ng, 150 ng, 200 ng and 250ng total DNA, we subsequently prepared each sample in triplicate and performed qPCR on the ViiA 7 instrument using the above mentioned cycling conditions for each assay to calculate amplification efficiency, compared slope values, Y-intercept values and correlation coefficient (R^2). The amplification efficiency (E%) (E% = [10(-1/slope) - 1] *100%) is determined through the use of serially diluted calibrators of known concentrations (log of concentration) plotted against the quantification cycle (Cq) values, which is directly linked to the slope of the calibration curve. The Y-intercept indicates the theoretical limit of detection, while the R^2 value indicating the sureness of fit of the calibrators along the regression line of the calibration curve.

2.2.5 Relative quantification method

DNA from six deletion 22q11.2 syndrome samples from Coriell were used throughout the validation, each one having been previously confirmed by FISH analysis (NA17942, NA17938, NA13325, NA05401, NA07939, NA03479). Sample NA13325, NA17942, NA17938 and NA07939 have the common 3 Mb deletion of the DGCR; NA03479 has classical deletion 22q phenotype but no deletions in the DGCR were

detected by FISH probes N25 and D22S39 (Scambler et al., 1992); NA05401, with a complex translocation involving chromosome 22 [45,XY,der(4)t(4pter>4q35::22q11>22qter)mat,-22]. Each sample was analyzed in triplicate along with the wild-type DNA control sample and a NTC. The mean cycle threshold (Cq) for each sample was used to calculate the RQ in the region of the target probe using the comparative ΔΔCq method, using with the mean Cq value of the *RNASEP* reference assay for normalization. The ViiA 7 analysis software was used to calculate both RQ and RQ_{EA} values, which subsequently, were compared using the ANOVA analysis method to ascertain if there are any statistically significant differences between both quantification methods. Additional replicate plates of the same test samples were analyzed for each 22q11.2 assay using multiple independent qPCR plates to allow for assay cut-off determination using the area under the Receiver Operating Characteristic (ROC) curves as well as to calculate specificity and sensitivity.

2.2.6 Statistical analysis

Statistical analysis was performed using the MedCalc® statistical software (http:/www.medcalc.org) to determine the means, standard deviations and to perform one-way ANOVA analysis for all deletion 22q assays. The area under the ROC curve was calculated using non-parametric methods by Delong *et al.* (Delong et al., 1988). All data is presented according to the Minimum Information for Publication of Quantitative Real-Time PCR Experiments (MIQE) to enable accurate evaluation of qPCR experimental parameters and results (Bustin et al., 2009; Bustin, 2010).

2.3 Results

2.3.1 Assay validation

Initial validation employing simple presence or absence of qPCR amplification was performed using the Qiagen extracted DNA with all assays showing successful amplification (data not shown). Calibration curves were generated for each of the 22q11.2 TaqMan assays to check for E%, slope and the R^2. Each calibrator was setup in triplicate with the DNA concentrations plotted against the Cq values (Figure 7, p.34). All of the custom TaqMan assays (*UFD1L, COMT, CRKL* and *GNAZ*) demonstrated excellent amplification efficiency when compared to the three commercial CNV assays (*DGCR2, TBX1* and *HIRA*). The *GNAZ* assay was omitted from further analysis as both the forward and reverse primers (16 out of 19 bp) were discovered through BLAST search to bind non-specifically to the glycosyltransferase-like protein *LARGE1* gene, located also on chromosome 22 but at position 22q12.3, leading to falsely elevated *GNAZ* gene copy number.

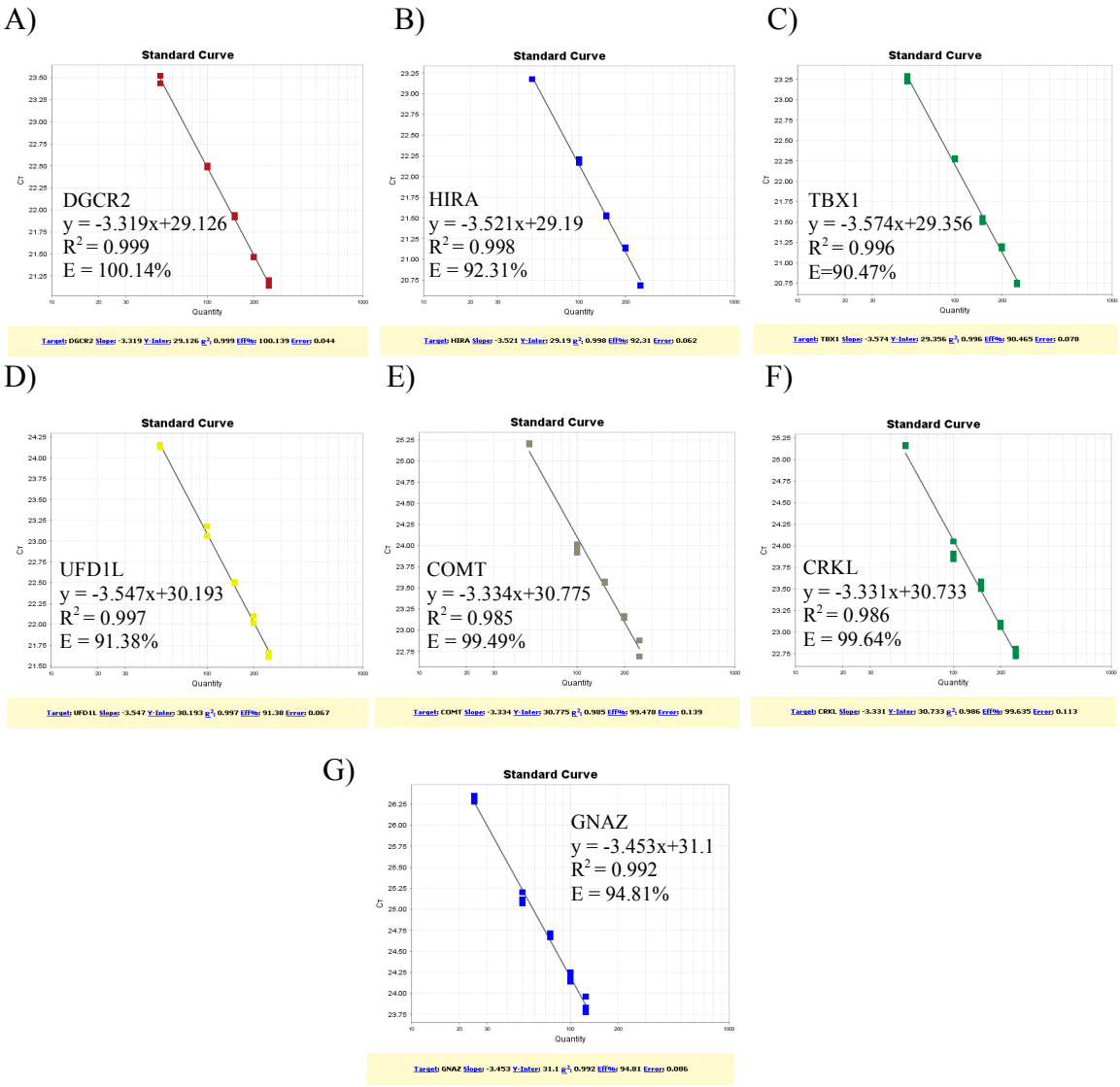

Figure 7 A-G. Calibration curves for each of the seven 22q11.2 TaqMan assays. Assays were cycled on a ViiA 7 Real-Time PCR system. No calibrator data points were omitted and amplification was absent from all NTC wells for each assay.

2.3.2 Selection and validation of a reference assay

Three reference assays were selected and validated for use in copy number quantification. Both custom assays, B-actin and Albumin, were evaluated against the commercial *RNASEP* reference assay used in CNV calculations. Calibration curves were generated for each of the reference assays to calculate E%, slope and the R^2 (Figure 8, p.36). Each calibrator was setup in triplicate with the DNA concentrations plotted against the Cq values. The linear regression curves demonstrated good linearity over all DNA concentrations. The β-actin primers were created to overlap an intron-exon boundary to prevent non-specific amplification of any of the 19 actin pseudogenes, which demonstrate considerable homology. The Albumin gene is known to harbor as many as 449 different single nucleotide polymorphisms (SNP) found in different frequencies amoung the general population. Due to the possability of non-specific β-actin pseudogene detection and mis-priming of the Albumin gene due to the presence of SNPs, both potentially leading to variable gene copy number quantification, we selected the *RNASEP* assay as the main reference assay for use in RQ of the singleplex assay and for multiplexing, but will also include the B-Actin assay on the OpenArray system to perform further comparisons.

A)

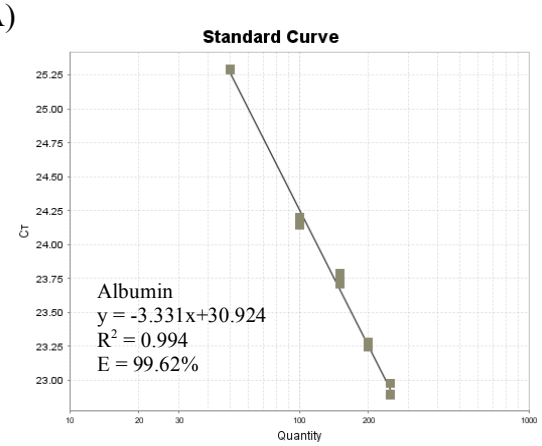

Target: ALBUMIN Slope: -3.331 Y-Inter: 30.924 R^2: 0.994 Eff%: 99.623 Error: 0.071

B)

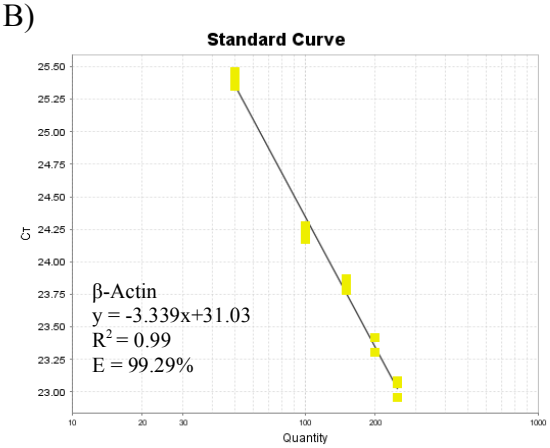

Target: B-ACTIN Slope: -3.339 Y-Inter: 31.03 R^2: 0.99 Eff%: 99.292 Error: 0.093

C)

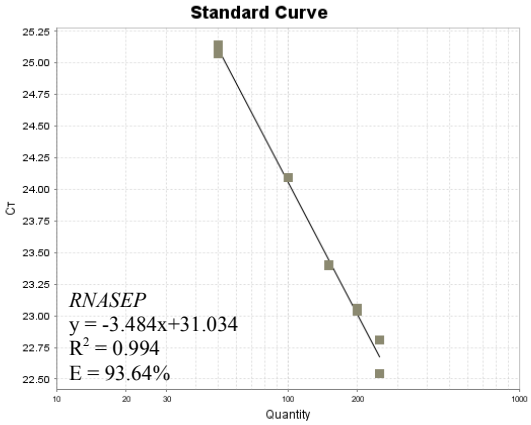

Target: RNASEP Slope: -3.484 Y-Inter: 31.034 R^2: 0.994 Eff%: 93.643 Error: 0.098

Figure 8 A-C. Calibration curves for each of the reference assays. Assays were cycled on a ViiA 7 Real-Time PCR system. No calibrator data points were omitted in the calibration curves and amplification was absent from all NTC wells.

2.3.3 Validation of relative gene quantification

We chose to calculate the RQ using both the classical ΔΔCq relative quantification method and using the efficiency adjusted method, which takes into account the amplification efficiencies of both the target and reference assays (Livak and Schmittgen, 2001; Yuan et al., 2008; Yuan et al., 2007). Results from both methods would be expressed similarly with non-deleted subjects having Relative Quantity (RQ) of 1.0; hemizygous deletion carriers having an RQ of 0.5; homozygous deletion carriers demonstrating an RQ of 0; and an individual with a gene duplication will have a RQ of 1.5. (Appendix I).

The RQ values obtained for each 22q11.2 target using the *RNASEP* as the reference assay setup in parallel with the target assays are shown in figures 9 A and B (p.38). All samples, except for NA03479, had values ranging from ~0.4 to 0.66, showing hemizygous deletions for all targets. Interestingly, sample NA03479 shows gene triplication for *HIRA*, with an RQ value of 1.42 (RQ_{EA} = 1.77) but shows no gene deletion for any other target (Figure 9B, p.38). Interestingly, sample NA05401 has two copies of the distal *CRKL* gene with an RQ value of 1.02. The presence of two copies of *CRKL* suggests the identification of the smaller ~ 1.5 Mb deletion.

A)

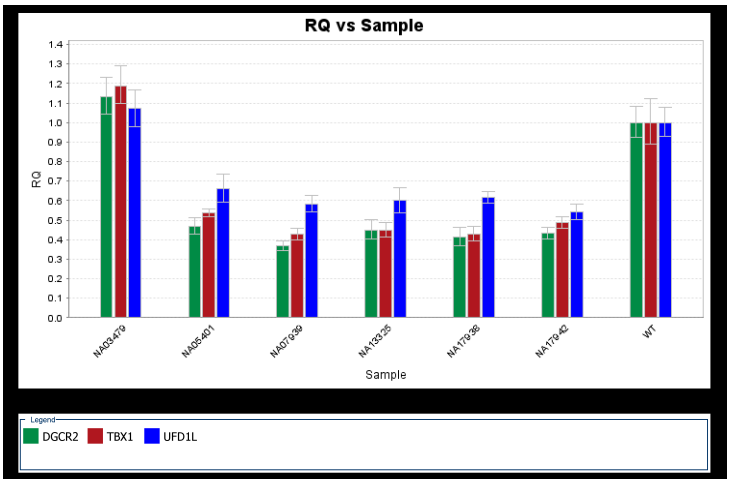

B)

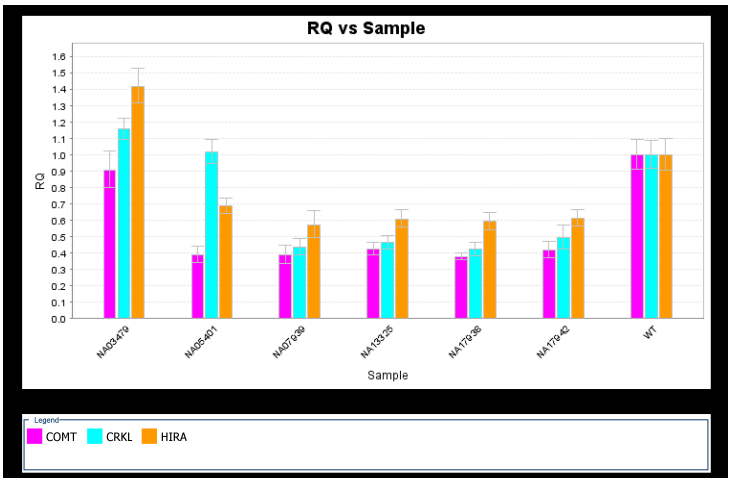

Figure 9 A-B. Bar graph and corresponding results table showing the RQ values for each samples. Error bar indicate ± 1SD for the RQ values calculated by the ViiA 7 analysis software. Two copies of *CRKL* were detected for NA05401, which suggestive of the smaller ~1.5 Mb DGCR deletion.

The values of both the RQ and RQ_{EA} calculation methods were compared by one-way ANOVA to determine if the differences in CNV are statistically different from one another. The RQ and RQ_{EA} means of all test samples for each individual assay were compared through one-way ANOVA analysis using the MedCalc® software (Appendix II), with each sample setup in triplicate on two concurrent plates, which allows determination of inter- and intra-qPCR variability of each sample and assay. Increased intra-sample gene copy number variation was observed, with little variation detected between statistical methods. The variation ratio (F) of all assays except for *HIRA*, show little to no method variation between the mean RQ and RQ_{EA} values. The P- value used to demonstrate the probability of statistically significance differences between analytical methods was >0.55 for every assay, demonstrating good correlation between the RQ numbers obtained using the classical ΔΔCq and the efficiency adjusted ΔΔCq method. Based on the results obtained through ANOVA analysis, we chose to rely on the classical ΔΔCq for subsequent experiments using the 22q11.2 deletion assays.

2.3.5 Statistical analysis of the deletion 22q11 assays

Further replicate experiments using the same samples were repeated over several days to enable additional statistical analysis using MedCalc®. Mean, standard deviation and CV for the RQ values of the WT (2 gene copies) and hemizygous deletion Coriell samples were calculated for each assay and represented in Table 2 (p. 41). There are no overlapping 95% CI for the normal and deletion samples amongst all of the 22q11.2 assays. As sample NA03479 is the only example of potential gene duplication, additional samples with known DGCR duplications would need to be analyzed to confirm the presence of the duplicated *HIRA* gene. Therefore, the results for NA03479 were treated as outliers and were excluded during analysis.

The resulting RQ data was further analyzed using the area under the Receiver Operating Characteristic (ROC) curve method, which plots the true positive rate (sensitivity) against the false positive rate (specificity) of each assay, allowing the selection of an assay cut-off that maximizes both specificity and sensitivity (Obuchowski et al., 2004; Hillis et al., 2005; Obuchowski, 2006). ROC analysis identified cut-off values for the 22q11.2 assay with a 100% sensitivity and 100% specificity for all six TaqMan assays (Table 3, p. 41). Subsequently false positive and false negative rates along with the positive (PPV) and negative (NPV) predictive values were also tabulated. Cut-off values are well above the mean for the deletion samples to enable high assay accuracy. Gaussian distribution plots (Appendix III) demonstrate the separate bi-modal distribution of the deletion and the normal samples, in between which the ROC cut-off values were chosen to maximize the accuracy of disease detection.

Table 2. Statistical calculations of the mean, standard deviation (SD), coefficient of variation (CV) and 95% confidence interval calculated for each 22q11.2 copy number assay. There were no overlapping 95% CI for the WT (2 copies) and the deleted (1 copy) results indicating high accuracy of copy number quantification.

Assay	Result	N	Mean RQ	95% CI	SD	CV
DGCR2	WT	7	1.001	0.975 - 1.028	0.0291	0.0291
	Deletion	21	0.436	0.416 - 0.457	0.0457	0.1046
HIRA	WT	7	1.000	0.946 - 1.054	0.0436	0.0436
	Deletion	21	0.550	0.506 - 0.594	0.1067	0.1940
UFD1L	WT	7	1.051	0.977 - 1.126	0.0803	0.0764
	Deletion	22	0.642	0.610 - 0.674	0.0719	0.1119
TBX1	WT	7	1.001	0.962 - 1.040	0.0422	0.0421
	Deletion	21	0.494	0.463 - 0.525	0.0681	0.1377
COMT	WT	7	1.003	0.935 - 1.072	0.0653	0.0651
	Deletion	21	0.455	0.407 - 0.503	0.0996	0.2191
CRKL	WT	10	1.010	0.971 - 1.049	0.0549	0.0544
	Deletion	17	0.498	0.456 - 0.540	0.0812	0.1631

Table 3. Assay cut-off determination using the area under the ROC curve analysis method for which the cut-off was selected to maximize specificity and sensitivity. All assays had 100% specificity and sensitivity with no false negative or false positive results.

Single Assays	RQ Cut-Off (ROC)	Specificity	False -ve	False +ve	Sensitivity	PPV	NPV
DGCR2	≤0.62	100%	0%	0%	100%	100%	100%
HIRA	≤0.69	100%	0%	0%	100%	100%	100%
UFD1L	≤0.78	100%	0%	0%	100%	100%	100%
TBX1	≤0.63	100%	0%	0%	100%	100%	100%
COMT	≤0.73	100%	0%	0%	100%	100%	100%
CRKL	≤0.67	100%	0%	0%	100%	100%	100%

2.4 Discussion

During the initial deletion 22q11.2 validation phase we were able to demonstrate the high specificity and sensitivity of each of the custom deletion 22q11.2 assays with comparable results to commercially available CNV assays. Three reference assays, β-Actin and Albumin, commonly used during relative gene quantification, were also with similar results to their commercial *RNASEP* counterpart. Amplification efficiencies of each reference assay were quite similar to those of the 22q11.2 target assays, allowing for accurate gene copy number calculation using either the classical ΔΔCq method or by way of the efficiency adjusted quantification method as shown by the high P-value calculated by one-way ANOVA (Appendix II). Each 22q11.2 assay successfully showed predicted hemizygous deletions in the positive control samples, including the identification of a sample with a previously unknown smaller 1.5 Mb deletions. Interestingly, sample NA03479 known to have two copies of FISH probe N25 (Figure 1, p. 5) near the *CLCTL1* gene (46,XY.ish 22q11.2(N25,D22S39)x2.arr(1-22)x2,(XY)x1), was found to harbour a gene duplication involving *HIRA* (Figure 9B, p.38). The infant from whom the cell line was derived, presented with classical 22q11.2 deletion/duplication phenotype including absent thymus, tracheoesophageal fistula, bilateral cleft lip, profound lymphocytopenia, hypocalcemia, Tetralogy of Fallot with infundibular pulmonary stenosis, ventricular septal defect and patent ductus arteriosus (Scambler et al., 1992; Mulder et al., 1995). Such small duplications or deletions may be missed when using single target methods such as FISH or singleplex qPCR. Such findings support our decision to use multiple DGCR targets in either a multiplex reaction or run

simultaneously on the OpenArray, enabling the reduction of false negative cases potentially seen during large-scale population screening.

The re-design and validation of the TaqMan MGB assays has enabled us to employ the 22q11.2 singleplex assays as the "gold standard" for which we have compared results obtained through multiplexing and through miniaturization on the OpenArray system. The *UFD1L, COMT* and *CRKL* assays were selected for use in our multiplexing experiments, as the primers and probes could be purchased separately, which was required during optimization of the reaction conditions. All six 22q11.2 assays along with both the *RNASEP* and B-Actin reference assays were spotted on array plates and used to establish the sensitivity of the dynamic range of the OpenArray needed for the detection of hemizygous gene deletions.

3. Spinal Muscular Atrophy (SMA)

3.1 Introduction

Spinal muscular atrophy is predominantly caused by the homozygous deletion of the Survival of Motor Neuron (*SMN1*) gene (Figure 2A, p. 9). Diagnostic assays must differentiate between both *SMN1* and its inverted homologue, *SMN2.* Significantly, the homozygous deletion of exon 7 of *SMN1* is diagnostic for SMA, while *SMN2* gene copy number modulates the severity of the disease. The two genes differ in their coding region due to a c.840C>T change in *SMN2* leading to the formation of a detectable single nucleotide polymorphism (SNP).

The primary goal of this portion of the study was to identify and re-design qPCR assays targeting the *SMN1* c.840C>T SNP for relative quantification. Allele-specific amplification (ASA) and SNP genotyping assays were selected and compared to establish which assay was the most sensitive and specific. The redesigned assays were then used to determine if the OpenArray platform can be used to detect homozygous deletions of *SMN1* for the diagnosis of SMA as well as to ascertain whether this new technology is accurate and amenable for use in newborn screening.

3.2 Materials and Methods

3.2.1 qPCR 5'-hydrolysis probe and primer design

Primer and Probe Design:

An extensive literature search was performed to identify assays that are currently in use to detect gene copy numbers of the *SMN1* gene. Assays were identified as either having i) *SMN1* ASA primers and a non-specific probe or having ii) non-specific *SMN* primers that amplify both *SMN1* and *SMN2* but have an *SMN1* SNP genotyping specific probe. Two of each type of assay were selected for validation referred to as SMN1-A (Watterson et al., 2004), B(Anhuf et al., 2003), C (Chan et al., 2004)and G (Lee et al., 2004). The primer and probe sequences were mapped to their corresponding genomic location using their GenBank sequence (NT_006713.15). All primers and probes selected were redesigned to be TaqMan FAM-labeled MGB assays with similar melting temperatures using the PrimerExpress 3.0 software (LifeTechnologies) (Table 4, p.46). Primer and probe sequences were compared to the human genome using the BLAST program to ensure 100% homology to only the sequence from which they were designed, therefore able to amplify (ASA primers) or detect (SNP probe) *SMN1* only, as well as to guarantee that the primer and probe annealing sites were free of single nucleotide polymorphisms. The reference assay, *RNASEP*, was chosen for gene copy number quantification of *SMN1* based on the initial findings during the validation *RNASEP*, Albumin and β-Actin assays for copy number detection of the deletion 22q11 assays.

Table 4. A list of all functional primers and probes developed for copy number quantification of the *SMN1* gene. Non-specific amplification of certain *SMN1* assays was noted for two of the re-designed assays.

qPCR Assay	Sense Primer (5'→3')	Antisense Primer (5'→3')	MGB Probe (5'→3')	Size (bp)
SMA				
SMN1-A	CAATGCTTTTTAACATCC ATATAAAGCT	TCTGCCAGCATTATGA AAGTGAAT	CAGGGTTTCAGA CAAAA	NA
SMN1-B	AATGCTTTTTAACATCCA TATAAAGCTATC	CCTTAATTTAAGGAAT GTGAGCACC	CAGGGTTTCAGA CAAA	146
SMN1-C	TTCCTTTATTTTCCTTACA GGGTTTC	GCTGGCAGACTTACTC CTTAATTTAA	AATCAAAAAGAA GGAAGGTGC	NA
SMN1-G	CTTCCTTTATTTTCCTTAC AGGGTTTC	TGATTGTTTTACATTAA CCTTTCAACTTTT	AAGTCTGCCAGC ATTAT	204
Reference				
RNASEP	Ribonuclease P RNA component H1 (*H1RNA*) gene (*RPPH1*)			87

NA = non-specific amplification and detection of both *SMN1* and *SMN2*

3.2.2 Assay validation

The TaqMan copy number assays were synthesized by LifeTechnologies (Carlsbad, CA). Initial validation of the copy number assays was performed using both Qiagen purified human DNA as well as SMA control DNA samples (Coriell, Camden, NJ). SMA samples include a *SMN1* deletion carrier (NA03814) and two *SMN1* homozygote deletions SMA samples (NA09677 and NA10684). Each sample was analyzed in triplicate along with a wild-type DNA control sample and an NTC. SMA control samples were used to assure *SMN1*-specific detection. Real-time quantitative PCR was performed following the same protocols and cycling conditions as previously mentioned (Section 2.2.3, p.30).

3.2.3 Assay efficiency calculation

We compared slope values, Y-intercepts and efficiencies for all assays using the serially diluted DNA calibrators created in Section 2.2.2 (p.30), calculated using the ViiA 7 software. Amplification efficiencies were used for further RQ_{EA} calculations.

3.2.4 Relative quantification method

RQ was calculated using the aforementioned Coriell control samples as well as the wild-type DNA sample. Each sample was analyzed in triplicate along with a wild-type DNA control sample and an NTC containing water instead of DNA. The mean Cq value for each sample was used to calculate the RQ in the region of the target probe using the comparative ΔΔCq method, with the mean Cq value of the *RNASEP* reference assay to normalize. Individual assay efficiencies were used to determine RQ_{EA} values, which

we then compared to classically calculated RQ values using one-way ANOVA. Additional replicate of the same test samples analyzed in duplicate over multiple independent qPCR plates were evaluated to allow for assay cut-off determination using the area under the ROC curves as well as calculating specificity and sensitivity for each the SMA assay.

3.2.5 Statistical analysis

Statistical analysis was performed using the MedCalc® statistical software (http:/www.medcalc.org) as described in section 2.2.6 (p.32).

3.3 Results

3.3.1 Assay validation

Initial validation employing simple presence or absence of qPCR amplification was performed using the Qiagen extracted DNA and the SMA control samples with only SMN1-B and SMN1-G demonstrating *SMN1* specific amplification and detection (data not shown). Calibration curves of both of the *SMN1* assays were generated to determine amplification E%, slope and the R^2 value (Figure 10 A-B, p.50). Each calibrator was set-up in triplicate with the DNA concentrations plotted against the Cq values to create a regression plot. Assays were cycled on a ViiA 7 Real-Time PCR system. Both *SMN1* assays have comparable efficiencies, slopes and y-intercept values compared to the commercial *RNASEP* reference assay, which has a slope of -3.484 and an efficiency of 93.64% (Figure 8C, p.36).

A)

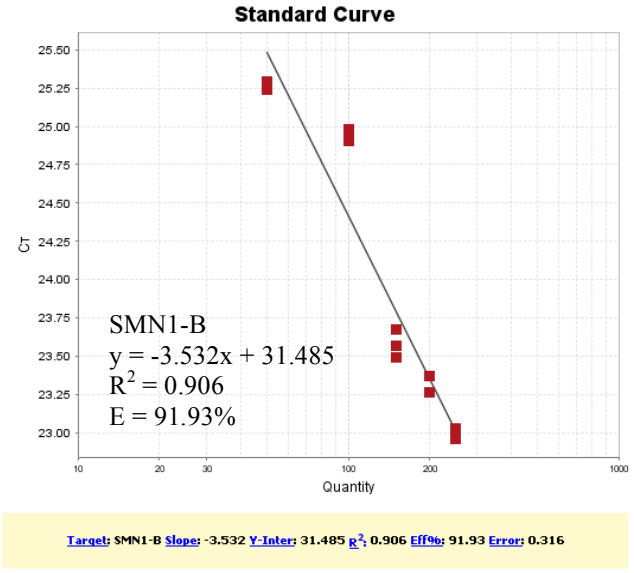

B)

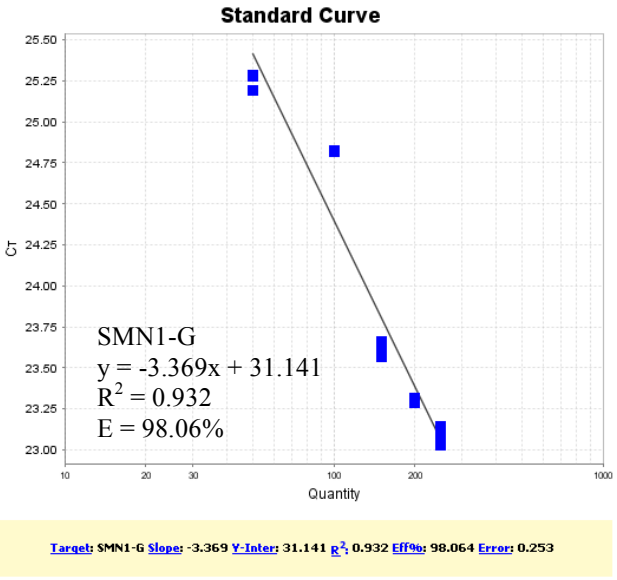

Figure 10 A-B: Calibration curves for two *SMN1* TaqMan assays, SMN1-B (A) and SMN1-G (B). SMN1-G has slightly better slope due to the higher amplification efficiency of the assay and the increased R^2 value (0.932). A single 100 ng calibration data point was omitted for SMN1-G and amplification was absent from all NTC wells for each assay

3.3.2 Validation of relative gene quantification

We chose to calculate the relative gene copy number using both the classical ΔΔCq method and the efficiency adjusted calculations as previously described in Section 2.3.4 (p.40) (Livak and Schmittgen, 2001; Yuan et al., 2008; Yuan et al., 2007). The bar graph reveals the gene copy number of SMN1-B and SMN1-G for samples NA09677, NA10684, NA03814 and the wild-type control DNA sample (Figure 11, p.53). Amplification was absent for the *SMN1* homozygous gene deletion samples (NA09677 and NA10684) using the SMN1-B assay. The same assay displayed clear hemizygous deletion of exon 7 of *SMN1* with a mean RQ of 0.41 for the SMA carrier and an RQ of 1.0 for the WT sample. Small amplification products (RQs of 0.09 - 0.12) were detected from both homozygous deletion samples using the SMN1-G assay, well below the RQ value (RQ of 0.63) obtained from the SMA carrier (NA03814).

The values of both the classical and efficiency adjusted relative quantification methods were compared by one-way ANOVA to determine if the differences in gene copy number were statistically different from one another and were in fact affected greatly by the differences in amplification efficiency of the selected assays. The RQ and RQ_{EA} means of all test samples for each individual assay were compared using MedCalc® (Appendix IV), with each sample set-up in triplicate on two independent qPCR plates, which enables the determination of inter- and intra-qPCR variability of each sample and assay. Increased intra-sample gene copy number variation was observed compared the variations found between the gene copy numbers calculated using different statistical methods. Variation in sample loading, caused by pipetting irregularities, is the main cause of intra-sample and inter-plate differences. The variation ratio (F) of both

SMN1 assays (SMN1-B and SMN1-G) demonstrated little to no statistical difference between the mean RQ and RQ_{EA} values. The P- value was determined to be >0.86 for every assay, displaying good correlation between the relative gene copy numbers obtained using the classical ΔΔCq and the efficiency adjusted ΔΔCq method. Based on the results obtained through ANOVA analysis, we chose to rely on the classical ΔΔCq for subsequence experiments using the *SMN1* developed TaqMan assays.

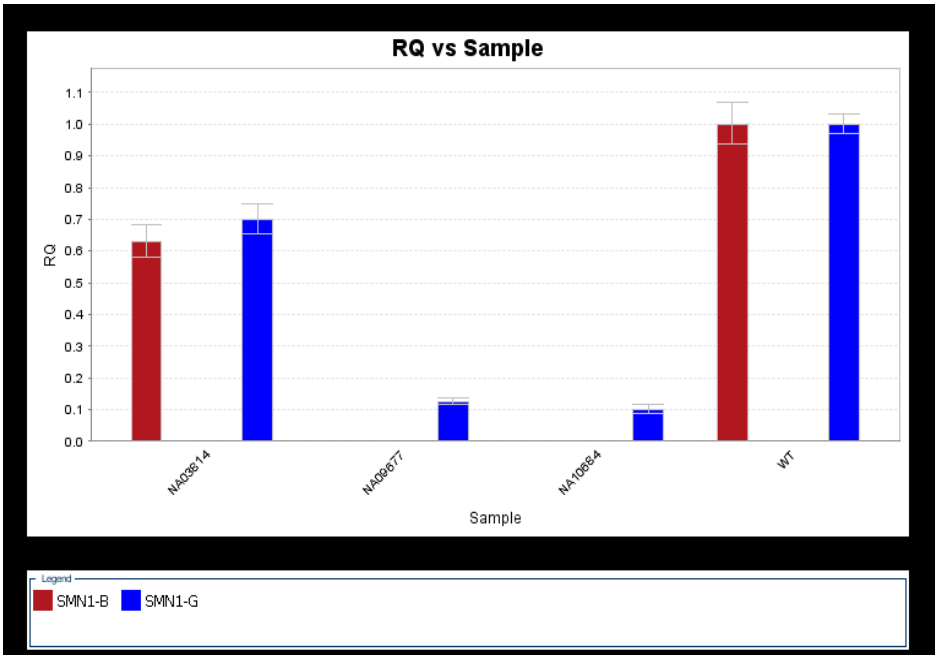

Figure11. Bar graph and corresponding results table showing the mean RQ values for each sample. Very little RQ variations were noted for each Coriell sample, indicated by the small error bars. Error bar indicate ± 1SD for the RQ values calculated by the ViiA 7 analysis software.

3.3.3 Statistical analysis of the *SMN1*-specific assays

Further replicate experiments using the same Coriell and wild-type samples set-up over several days were performed to allow for statistical analysis using MedCalc®. Mean, SD and CV for the RQ values of for the WT (2 gene copies) sample, hemizygous deletion carrier and homozygous *SMN1* deletion samples were calculated for each assay and presented in Table 5 (p.55). There are no overlapping 95% CI for the normal and deletion samples amongst either *SMN1* assay, demonstrating excellent sensitivity. Large CV's were noted for both carrier detection using the SMN1-B assay (CV >0.44) and for homozygous *SMN1* deletion detection using SMN1-G (CV >1.29) due to the slightly dispersed range of RQ values calculated between replicates and plates.

The resulting RQ data was further analyzed using the area under the ROC curve method which identified cut-off values for both the SMN1-B and SMN1-G assays, with a 100% sensitivity and 100% specificity for both assays (Table 6, p.55). Subsequently false positive and false negative rates along with the positive (PPV) and negative (NPV) predictive values were tabulated as well. Gaussian distribution plots demonstrate the multimodal distribution of the deletion samples and the normal samples in between which the ROC cut-off values were calculated to maximize disease detection (Appendix V).

Table 5. Statistical calculations of the mean, standard deviation (SD), coefficient of variation (CV) and 95% confidence interval calculated SMN1-B and SMN1-G copy number assay. There were no overlapping 95% CI for the WT, carrier and SMA results indicating high accuracy of copy number quantification.

Assay	Results	N	Mean RQ	95% CI	SD	CV
SMN1-B	WT	7	1.003	0.946 - 1.060	0.0613	0.0611
	Carrier	7	0.290	0.170 - 0.410	0.1300	0.4483
	SMA	10	0.000	0.000 - 0.000	0.0000	0.0000
SMN1-G	WT	12	0.990	0.941 - 1.039	0.0772	0.0780
	Carrier	13	0.563	0.489 - 0.636	0.1221	0.2171
	SMA	15	0.047	0.013 - 0.080	0.0607	1.2966

Table 6. Assay cut-off determination using the area under the ROC curve analysis method for which the cut-off was selected to maximize specificity and sensitivity. Both SMN1 assays had 100% specificity and sensitivity with no false negative or false positive results.

Single Assays	RQ Cut-off (ROC)	Specificity	False -ve	False +ve	Sensitivity	PPV	NPV
SMN1-B	≤0	100%	0%	0%	100%	100%	100%
SMN1-G	≤0.15	100%	0%	0%	100%	100%	100%

3.4 Discussion

For the accurate quantification of *SMN1* gene deletions, designing primers and probes that are gene specific, which will not falsely detect the centromeric *SMN2* gene copies is of the utmost importance. During the initial development phase, we were able to demonstrate the high specificity and sensitivity of each of the *SMN1* assays. The comparable amplification efficiencies, similar to that of the commercially available *RNASEP* reference assay, allowed for accurate gene copy number calculation using both the classical ΔΔCq method and the efficiency adjusted quantification method. SMN1-B and SMN1-G successfully showed predicted hemizygous and homozygous deletions in the positive control samples NA09677, NA10684 and NA03814 (Figure 11, p.53).

Low-level amplification of the homozygous deletion SMA samples was observed using the SMN1-G assay but not the SMN1-B assay. The ASA SMN1-G assay was created with an *SMN1* allele-specific forward primer with a 3' mismatch to destabilize non-homologous binding to *SMN2*, which must bind perfectly to its complementary sequence for amplification to occur. The SMN1-G assay shows slight amplification of the *SMN2* gene, which also competes for biding of the non-specific SMN probe leading to a detectable signal but with a much higher Cq (> 28). The SMN1-B SNP assay, on the other hand, creates amplification products for both *SMN1* and *SMN2* genes but has an *SMN1* specific probe created with a mismatched C in the ninth base pair, destabilizing annealing to the *SMN2* PCR product. Both the *SMN1* and *SMN2* qPCR products must compete for binding of the same probe causing a reduction in end-point fluorescence (Tong et al., 2008). With the possibility of either PCR product or primer binding competition occurring with both *SMN1* assays, we chose to run both on the OpenArray

system, allowing us the opportunity not only to validate the new technology for use in gene copy number quantification but to compare both types of *SMN1* deletion detection methods; allele-specific amplification and SNP genotyping using TaqMan assays. We have utilized the results obtained for both SMN1-B and SMN1-G assays as the "gold standard" by which we have compared results obtained by way of the OpenArray system.

4. Severe Combined Immunodeficiency (SCID)

4.1 Introduction

Severe combined immunodeficiency (SCID) is a genetically heterogeneous disorder characterised by defects in T-cell maturation and proliferation, hindered B-cell activation and variable natural killer cell (NK) activity (Chan and Puck, 2005; Buckley et al., 1997). During T-cell maturation in the thymus, extra-chromosomal circular DNA molecules known as T-cell receptor excision circles (TRECs) are formed through T-cell Receptor α/δ V(D)J rearrangement events (Figure 3, p.15). Current SCID diagnostic assays use quantitative real-time PCR (qPCR) to determine the number of TRECs per mL of whole blood, thereby estimating the number of naïve T-cells generated in the thymus. Individuals with classical forms of SCID will have little to no detectable TRECs in their blood throughout their life, making the absence of TRECs an essential biomarker for early identification of infants with the disorder. Early diagnosis will allow neonates to quickly receive a life-saving bone marrow transplant before the onset of opportunistic infections.

The primary goal of this portion of the study is to identify and re-design pre-existing qPCR assays currently being used in newborn screening laboratories to quantify TRECs extracted from dried blood spots. The 5'-hydrolysis assays will be compared to determine the most optimal assay for use in further multiplexing assays and for use on the OpenArray system. The secondary goal is to create reliable dried blood spot calibrators that will be then used to accurately quantify TREC copy numbers extracted from neonatal DBS.

4.2 Materials and Methods

4.2.1 qPCR 5'-hydrolysis probe and primer design

Primer and Probe Design:

An extensive literature search was performed to identify assays that are currently in use to quantify TREC numbers, with assays designed by Baker *et al.*(Baker et al., 2009) (TREC-B) and by Gerstel-Thompson *et al.* (Gerstel-Thompson et al., 2010) (TREC-E) selected for comparison, as they are currently being used in State newborn screening labs in both Wisconsin and New England, respectively. Three additional 5'-hydrolysis assays used in the detection signal-joint TREC (sjTREC) were also tested during the validation process (Yamanaka et al., 2005; Just et al., 2008; Lima et al., 2010a). The published primer and probe sequences were mapped to their corresponding genomic location using the GenBank sequence (NG_001332.2). Four of the assays (TREC-A, TREC-B, TREC-C and TREC-D) were redesigned to incorporate FAM-labeled MGB probes using the PrimerExpress 3.0 software (LifeTechnologies). Assay TREC-E (New England) did not require any re-designing (Table 7, p. 60). Final primer and probe sequences were compared to the human genome using the BLAST program to ensure 100% homology to only the sequence from which they were designed and also to guarantee that the annealing locations of the primers and probes were free of single nucleotide polymorphisms.

Table 7. A list of all signal-joint TREC assays that were tested during the initial validation. Underlined assays (TREC-A to TREC-D) were originally created with TAMRA-based probes and were redesigned as FAM-labeled MGB TaqMan probes, which increased the stability of probe hybridization.

qPCR assay	**Sense Primer (5'→3')**	**Antisense Primer (5'→3')**	**MGB Probe (5'→3')**	**Size (bp)**
TREC-A	CCCTTTCAACCATGCT GACA	TTGCAACTCGTGAGAA CGGA	TTGTAAAGGTGCC CACTC	NA
TREC-B	CTTTCAACCATGCTGA CACCTC	CGTGAGAACGGTGAA TGAAGAG	TTGTAAAGGTGCC CACTC	NA
TREC-C	CACATCCCTTTCAACC ATGCT	GTGCCAGCTGCAGGG TTTAG	CTCTGGTTTTTGT AAAGGT	111
TREC-D	ACCATGCTGACACCTC TGGTT	CTCGTGAGAACGGAG AATGAAG	ATGCATAGGCAC CTGC	NA
TREC-E	TGCTGACACCTCTGGT TTTTGTAA	GCCAGCTGCAGGGTTT AGG	ATGCATAGGCAC CTGC	81

4.2.2 DBS DNA Extraction Methods

Initial DBS DNA Extraction Method:

DNA was extracted from dried blood spots using an extraction method developed in our lab based on a previously published method (Lin et al., 2005). Blood spot cards were punched using the BSD 600 Duet semi-automated dried blood post puncher (Luminex, Austin, TX) which punched 3.2mm diameter DBS into 96-well PCR plates (VWR). The blood spots were completely submerged in 50 uL LC-MS grade 100% MeOH and then placed under an EVX-192 Evaporex (Apricot Designs, Finland) to evaporate the methanol completely. Once dry, 50 uL of 1X Platinum Taq PCR Buffer (20 mM Tris-HCl (pH 8.4), 50 mM KCl) (LifeTechnologies, CA) made in molecular grade water (VWR) was added to each well. The sealed plates were then placed in a DNA Engine DYAD Thermocycler (BioRad, CA) and incubated. Thermocycler conditions consisted of a 15 minute incubation at 99°C, followed by a hold at 4°C. Plates were then quickly pulse vortexed and centrifuged at 3000 rpm using the Beckman GS-15R Centrifuge (Beckman Coulter) for 1 minute, and 8 uL of the supernatant was used to set-up each qPCR reaction.

Modified DBS DNA Extraction Method:

Blood spot cards were punched and washed twice using 100 uL 0.5% Triton X-10 (Tx-10) solution (Astoria Pacific, Clackamas, OR) diluted in PBS (Gibco, LifeTechnologies), followed by a single 100 uL wash with 20 mM Tris pH. 8.0 (Gibco, LifeTechnologies), with subsequent mixing on a nutator for 15 minutes at ambient temperature. The Tris wash was removed and 50 uL of 1X Platinum Taq PCR Buffer (20

mM Tris-HCl (pH 8.4), 50 mM KCl) with 0.05% yeast tRNA (Invitrogen) (LifeTechnologies, CA) was added to each well. The sealed plates were then placed in a DNA Engine DYAD Thermocycler using the same cycling conditions as mentioned above. Plates were then quickly pulse vortexed and centrifuged at 3000 rpm using the Beckman GS-15R Centrifuge (Beckman Coulter) for 1 minute, with 8 uL of the supernatant used to set up each qPCR reaction.

4.2.3 Assay validation

SCID DBS samples

The Newborn Screening and Molecular Biology Branch of the Center for Disease Control (Atlanta, GA), led by Dr. Robert Voght, kindly provided us with a array of both TREC dried blood spot calibrators and quality control material with varying amounts of signal-joint TRECs. Additional CDC samples with unknown TREC concentrations were also received as part of a trial Model Performance Evaluation Survey (MPES) on T-cell receptor excision circle assay for SCID testing performed in newborn screening laboratories. The unknown samples were used to determine assay cut-off values for normal and SCID positive patient identification.

Initial assay functionality testing:

All TREC assays (TREC-A to TREC-E) were synthesized by LifeTechnologies (Carlsbad, CA). Real-time quantitative PCR for gene copy number detection was performed in a total volume of 20 uL containing 1X TaqMan Universal Master Mix without UNG (LifeTechnologies), 1 uL single-tube TaqMan-MGB Assay (900 nM primers and 250 nM FAM-labelled probe), 8 uL of extracted DNA from the CDC

reference material which. Each sample was analyzed in triplicate along NTC containing molecular grade water instead of DNA. Real-time quantitative PCR was performed following the same protocols and cycling conditions as previously described (Section 2.2.3, p.29). Cq values were noted for each assay developed, with only the newborn screening assays TREC-C and TREC-E having successful amplification (data not shown).

4.2.4 Assay efficiency calculation

We compared slope values, Y-intercept values and efficiency values for both TREC-C and TREC-E assays using the dried blood spot calibrators provided by the CDC extracted using the modified DBS DNA extraction method. The TREC copy numbers for each of the calibrators were not revealed, as calibrator B (Cal B) was simply deemed as having TREC copy numbers representing the mean values obtained by the Center for Disease Control for healthy neonates calculated using flow cytometry to determine the number of TREC containing naïve T-cells. We therefore assigned percentages to the calibrators with each having a 2-log dilution between each based on the limited information given by the CDC. We assigned the following arbitrary values of 200% (Cal A), 100% (Cal B), 50% (Cal C), 25% (Cal D), 12.5% (Cal E), 6.25% (Cal F) and 3.125% (Cal G). Each sample was analyzed in duplicate, and included an NTC control used as a negative control. We compared slope values, Y-intercept values and efficiency values for all assays using the CDC DBS TREC calibrators.

4.2.5 Creation of TREC DBS calibrators

Bacterial transformation and plasmid prep:

We obtained bacterial plasmids containing the T-cell receptor excision circle signal-joint region (sjTREC), which was kindly provided by Dr. Daniel Douek from the National Institutes of Health (Bethesda, MD) to enable the creation of the in-house DBS calibrators (Figure 12, p. 65). The insert is comprised of an 111bp sequence and cloned into the pGem-T-Easy plasmid (Promega) forming a 3.126 Mb plasmid (Al-Harthi et al., 2000). The provided plasmid was diluted to 10 ng/ul and used to transform One Shot TOP10 chemically competent *Escherichia coli* (Invitrogen) using the accompanying manufacturer protocol. Plasmid extractions, using the GenElute HP Plasmid Maxiprep syringes (Sigma Aldrich), were performed following previously described protocols (Sigma Aldrich). The TREC plasmid maxiprep elutions were pooled and quantified using the NanoDrop2000 spectrophotometer (Thermo Scientific). The average of five separate readings was used to give a final concentration of 89.3 ng/ul with a 260/280 ratio of 1.83. Plasmid concentration and insert size was independently confirmed through *Eco*RI restriction enzyme digestion of the plasmid, which was then run on a 1.5% agarose gel along with High DNA Mass Ladder (Invitrogen) (Appendix VI).

Creation of a TREC-free blood diluent:

As signal-joint TRECs are present in diminishing quantities as we age, 80 mL of whole blood was collected in sodium heparin blood collection tubes from a single adult donor who was in their early fifties. The plasma layer was removed and the remaining red blood cells and buffy coat were washed 3X with saline and resuspended to a 50%

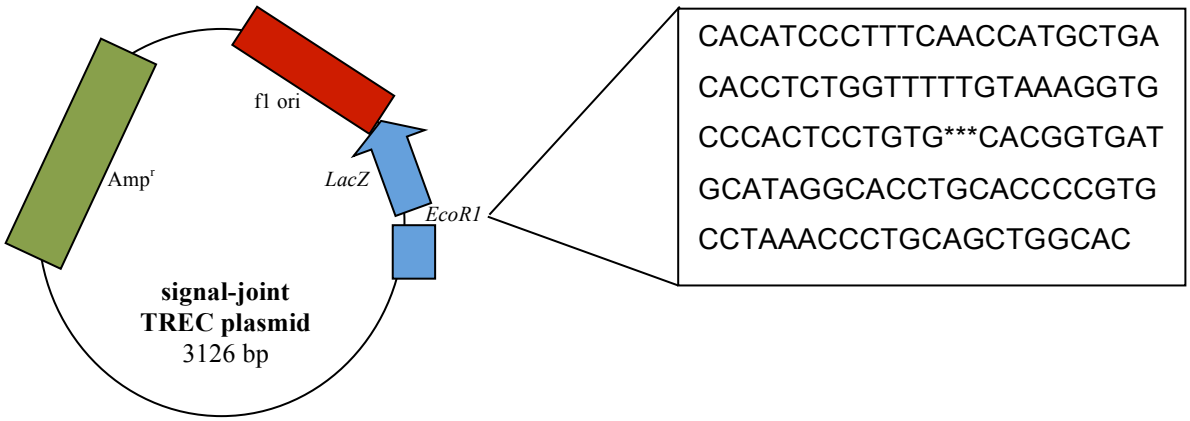

Figure12. A diagram of the pGem-T-Easy plasmid containing the ampicillin selectable marker (green square) and the *LacZ* reporter gene (blue arrow) into which part of the signal-joint TREC sequence was cloned by way of the *Eco* RI restriction cut site. The white box to the right contains the s-j TREC sequence confirmed by sequencing. *** Denotes the δRec-ΨJα joint site which is detected by the TaqMan probe.

hematocrit level in fetal bovine serum (FBS). Packed red blood cells, devoid of all lymphocytes, plasma and platelets, obtained through the blood bank at the Children's Hospital of Eastern Ontario was processed in the same fashion as the whole blood. We then proceeded to dilute the whole blood sample in a 4:1 ratio with the washed packed red blood cells, both reconstituted to a 50% hematocrit level, to create a blood diluent that is free of detectable TREC levels.

Dried blood spot calibrators:

Dried blood spot calibrators were created by using the equation described by Whelan *et al.* (2003) to obtain the desired absolute TREC copy number for each 3.2 mm. dried blood spot, which is equivalent to 3 uL of whole blood (Whelan et al., 2003). We created ten individual calibrators ranging from 100 000, 50 000, 10 000, 5 000, 2 500, 1 000, 500, 100, 50 and 25 TREC copies/ 3.2 mm DBS using the stock plasmid solution with each serial dilution left to mix on a nutator mixer for 4 hours at room temperature to enable for adequate distribution of the plasmids within the blood matrix. Once all the dilutions were adequately mixed, blood spots using 75 uL of the calibration material were spotted onto Whatman 903 Protein Saver cards (VWR) using a pipette and allowed to dry for 4 hours.

Validation of TREC in-house calibrators:

We validated the calibrators by first punching the calibrators in triplicate into a 96-well plate and extracting the DNA using the modified DBS extraction protocol as described above. DNA from each calibrator was pooled and 8ul of extracted DNA was

setup in triplicate for both the TREC-C and TREC-E assays on the ViiA 7, with the slope, amplification efficiency and Y-intercepts compared against the values obtained by the TREC DBS calibrators from the CDC.

4.2.6 TREC quantification and analysis of CDC samples

Blinded dried blood spot samples containing varying amounts of endogenous TREC, including samples with reduced lymphocyte numbers mimicking unsatisfactory samples and SCID positive samples, were provided by the CDC every four months from July 2011 till March 2012 as part of a trial MPES program. Each sample was analyzed in triplicate along with the calibrators to calculate absolute TREC copies per microliter of whole blood, which included NTC control using the above-mentioned setup and cycling conditions. The final results were then compared to the qualitative results provided by CDC for each of the participating laboratories, which consisted of samples being deemed either SCID positive, SCID negative or as having unsatisfactory DNA.

4.2.7 Statistical analysis

Statistical analysis was performed using the MedCalc® statistical software (http:/www.medcalc.org) as described in section 2.2.6 (p.32).

4.3 Results

4.3.1 Optimization of TREC assay parameters

Initial assay validation resulted in only TREC-C and TREC-E, developed for use on dried blood spots, demonstrating amplification of the CDC quality control dried blood spot material; low2, low, high and MNC-D (data not shown). Further validation was performed using DNA extracted from CDC dried blood spot calibrators following the initial DNA extraction procedure (Figure 13A, p.69). Poor amplification was noted with a slope value of -2.618 and an efficiency of 1.41, suggesting amplification inhibition during cycling caused either by reduced DNA quantity or by the presence of PCR inhibitors (Freeman et al., 1999). Further review of the extraction methods used by both the Wisconsin and Massachusetts newborn screening labs allowed us to develop a new extraction procedure which reduced the amount of contaminating heme, while increasing the yield of the extra chromosomal TREC circular DNA, allowing for accurate quantification at lower concentrations. The dried blood spot washing steps in PBS with 0.5% Triton-X eluted the heme and removed the remaining plasma and plasma associated proteins that have been known to inhibit qPCR amplification (Tichopad et al., 2003). DNA elution is performed using a Tris-based PCR buffer, which includes 50 ng/ul of yeast t-RNA, acting as a carrier molecule during extraction, thereby increasing the overall yield of genomic and TREC DNA. The increase in both DNA purity and quantity is self-evident by the amplification of Cal F and Cal G, as well as an improvement in both slope value and amplification efficiency (Figure 13B, p.69) (Shaw et al., 2009). All future DNA extractions from dried blood spots for all assays will use the modified protocol.

A)

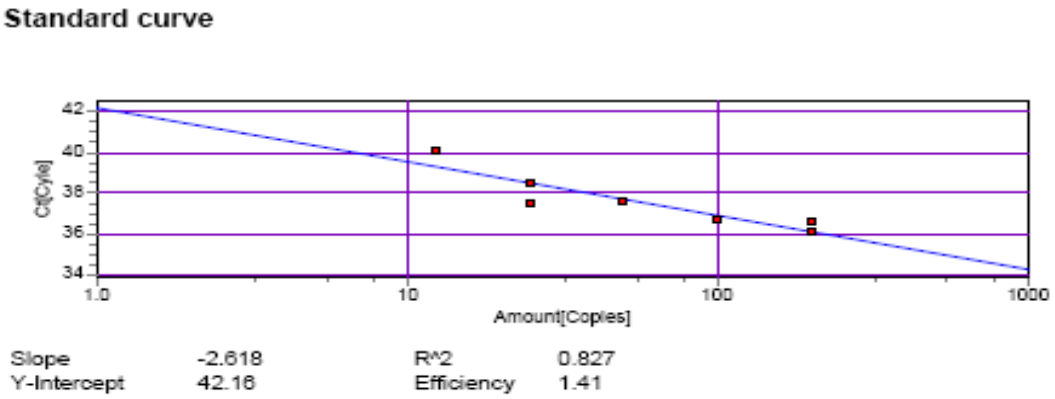

B)

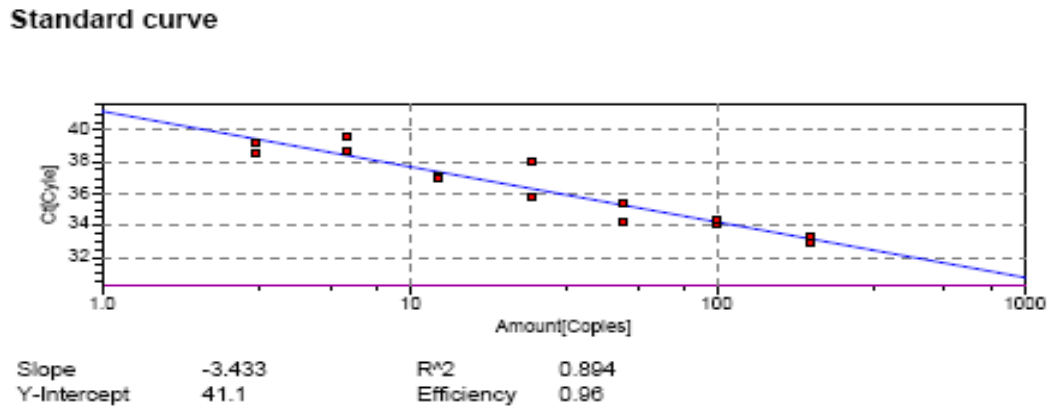

Figure 13 A-B. TREC DNA extraction method comparison of CDC calibrators extracted using the original in-house developed method (A) and the modified extraction method (B) run in duplicate using the TREC-C assay on the Eppendorf real-plex^2. All samples were eluted in 50ul 1X Platinum Taq PCR buffer without (A) or with 50 ng/ul yeast t-RNA (B) in the case of the modified protocol. Single points for Cal B and Cal fE were removed, with no amplification noted for Cal F or Cal G. Note the significant improvement in both slope value and efficiency using the modified extraction protocol, with amplification of each calibrator replicate.

4.3.2 TREC assay comparison

Once an efficient DNA extraction method from dried blood spots was validated, we wanted to determine the amplification efficiency of both TREC TaqMan assays (TREC-C and TREC-E), originally developed for use in newborn screening, and compare the results obtained. Pooled DNA extracted from triplicates of each of the CDC calibrators was used to reduce potential differences in extraction efficiencies that may occur between dried blood spots. Samples were analyzed in triplicate on the ViiA 7 instruments and regression curves were created to calculate efficiencies (Figure 14 A-B, p.71). Both assays demonstrated good linearity with slope values of -3.531 and -3.318 for TREC-C and TREC-E respectively. The TREC-E calibration curve displayed increased amplification efficiency (100%) and a lower Y-intercept (44.31) compared to the TREC-C curve, which had an efficiency of 92% with a high Y-intercept of 46.21. The increased efficiency of the TREC-E assay can be attributed to the amplification of a smaller, 81 bp, PCR product compared to the larger 111 bp product created by the TREC-C TaqMan assay (Table 7, p.60). Further confirmation of assay efficiency using our in-house DBS calibrators is necessary before selecting a SCID assay for additional validation studies.

A)

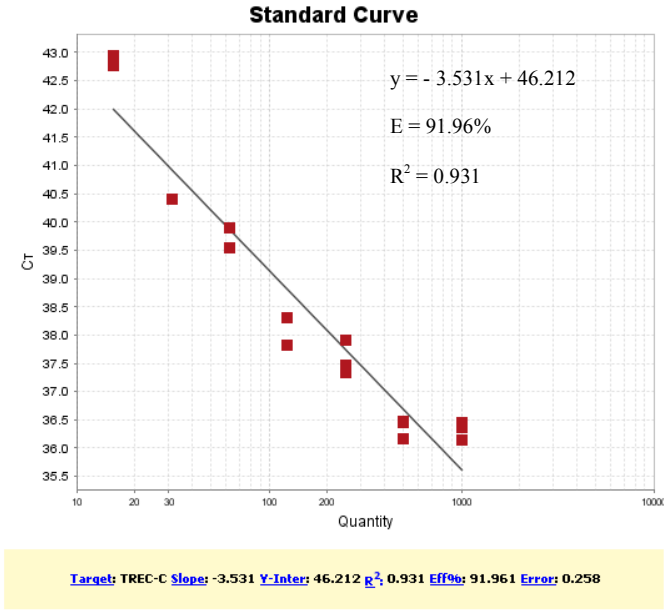

B)

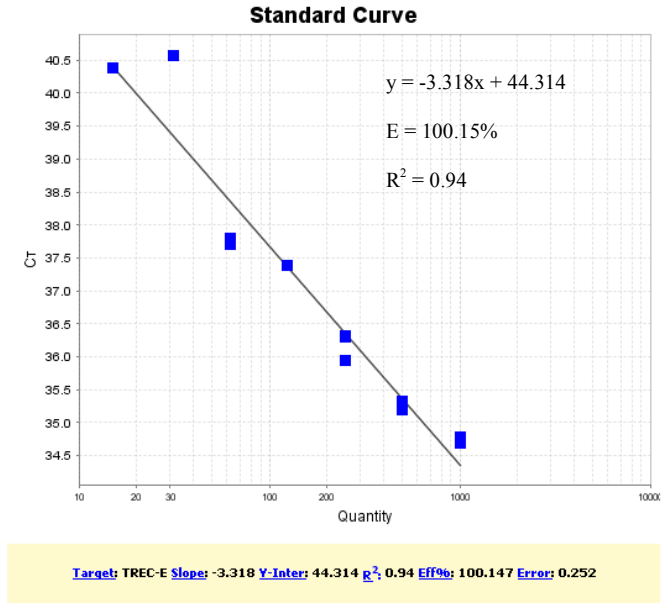

Figure 14 A-B. Standard curves of the CDC dried blood spot calibrators for TREC-C (A) and for TREC-E (B). Both TREC assays had comparable slope values and R^2 values, with TREC-E having slightly better amplification efficiency (E= 100%). TREC-C had single data points were removed for Cal D, Cal E and two data points removed for Cal F. TREC E had two data points removed for Cal D, Cal F and Cal G.

4.3.3 Validation of DBS calibrators

The creation of DBS calibrators for TREC quantification is of utmost importance, as the dried blood stabilizes the plasmids for long-term storage and eliminates the possibility of plasmid contamination. Using both SCID assays (TREC-C and TREC-E) we wanted to verify the linearity of the dried blood calibrators which had the following absolute TREC copies/ 3.2 mm DBS; 25, 50, 100, 500, 1 000, 2 500, 5 000, 10 000, 50 000 and 100 000 (Figure 15 A-B, p.73). Pooled DNA extracted from each of the new calibrator was used to normalize possible differences in extraction efficiencies. Samples were analyzed in triplicate on the ViiA 7 instruments and regression curves were created to access efficiency. The DBS calibrators demonstrated excellent linearity, similar to that obtained from the CDC calibrators (Figure 15 A-B, p.73). The TREC-E assay demonstrated higher amplification efficiency (E=99%) and a lower Y-intercept (Y= 42.26) with the new calibrators compared to the TREC-C assay (Y=46.21), comparable to the results using the CDC calibrators. We therefore chose to proceed with further DBS calibrator validations using only the TREC-E TaqMan assay.

Summary data from ten consecutive regression curves, each set-up in triplicate, confirmed that Cq values for each calibrator stay within ± 1SD from the mean, with very low variation within the replicates and between separate plates (Figure 16, p.74). A 1 Cq change in the mean Cq value for each of the 2-fold dilutions was noted, indicating optimal amplification efficiency was maintained in all thirteen curves. Increasing amplification failures was observed for the smallest three calibrators (100, 50 and 25 TRECs/ 3.2 mm DBS) as we neared the possible limit of detection of the assay.

A)

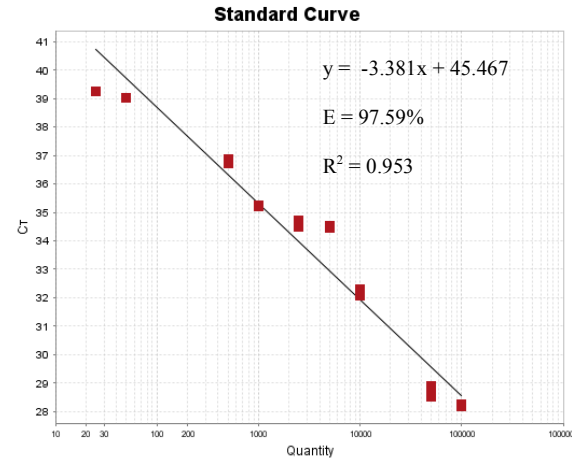

B)

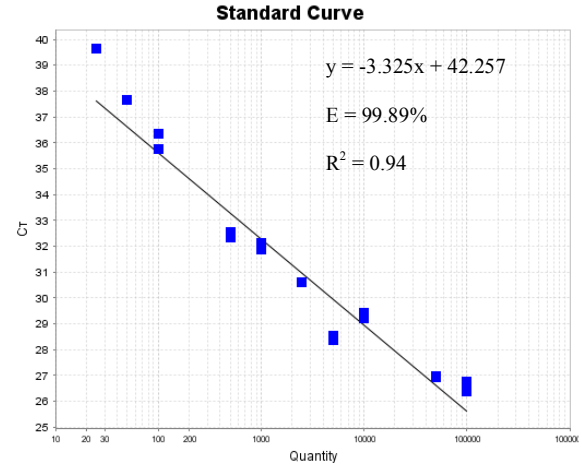

Figure 15 A-B. Standard curves of the in-house dried blood spot calibrators for TREC-C (A) and for TREC-E (B). Both TREC assays had identical slope values and R^2 values, with TREC-E having slightly better amplification efficiency (E= 99%) and smaller Y-intercept (Y= 44.314). TREC-C had single data points were removed for the 50 TRECs/3.2 mm DBS calibrators. TREC E had single data points removed for the 25, 50 and 2 500 TRECs/3.2 mm DBS calibrators.

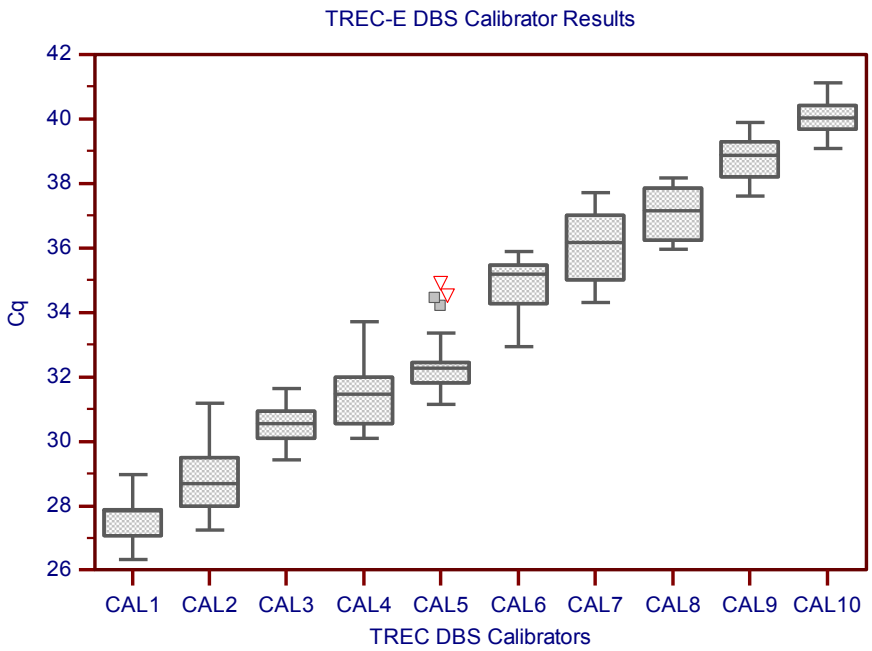

In-House Calibrators	TRECs/3.2 mm DBS	N	Mean Cq	95% CI	SD	CV
CAL1	100 000	23	27.660	27.365 - 27.956	0.682	0.025
CAL2	50 000	28	28.838	28.440 - 29.236	1.027	0.036
CAL3	10 000	15	30.572	30.199 - 30.945	0.674	0.022
CAL4	5 000	27	31.400	31.004 - 31.795	1.000	0.032
CAL5	2 500	26	32.462	32.051 - 32.873	1.017	0.031
CAL6	1 000	24	34.814	34.424 - 35.204	0.924	0.027
CAL7	500	19	35.993	35.416 - 36.569	1.195	0.033
CAL8	100	10	37.108	36.464 - 37.752	0.900	0.024
CAL9	50	16	38.811	38.447 - 39.175	0.683	0.018
CAL10	25	12	40.076	39.729 - 40.423	0.546	0.014

Figure 16. Box-and-whisker plot and data summary of Cq values for each in-house dried blood spot TREC calibrator set up in triplicate and analyzed in 10 consecutive reactions using TREC-E. Center horizontal lines represent the mean Cq values, with grey error bars indicating ± 1SD and outlier shown as individual coloured data points.

4.3.4 Determination of assay accuracy and statistical analysis

To determine the accuracy of both the TREC-E assay and our in-house DBS calibrators we analyzed dried blood spot samples with unknown TREC concentration that had been kindly provided by the CDC. Forty-eight de-identified samples were analyzed in triplicate using the TREC-E assay, with all samples whose TREC levels fell below Cal 8 (100 copies/ 3.2 mm DBS) repeated again in duplicate using in tandem with the TREC-E assay to confirm TREC values and with the RnaseP assay to ensure sample quality (data not shown). Using the final qualitative results obtained by the CDC, we were able to subdivide the samples into SCID positive or SCID negative and calculate the mean TREC/uL of whole blood values (Figure 17, p. 76). We successfully identified all 21 SCID positive samples with the majority of them showing complete amplification failure (mean=7.62 TREC/uL). Conversely, the normal samples had a mean of 303.96 TREC/uL of whole blood, with a wide distribution range of TREC values similar to those obtained in other newborn screening laboratories (Baker et al., 2009; Chan and Puck, 2005; Gerstel-Thompson et al., 2010).

The resulting data was further analyzed using the area under the ROC curve method. ROC analysis identified a cut-off value of ≤ 46 TREC/uL for the TREC-E assay, with 100% sensitivity and 100% specificity (Appendix VII). Subsequently, false positive and false negative rates along with the positive (PPV) and negative (NPV) predictive values were tabulated as well and included in Table 8 (p.77). The box-and-whisker plot visually demonstrates the clear separation observed between the SCID positive and the normal CDC samples, with all twenty-one SCID samples having been positively identified using the predicted ≤ 46 TREC/uL cut-off value.

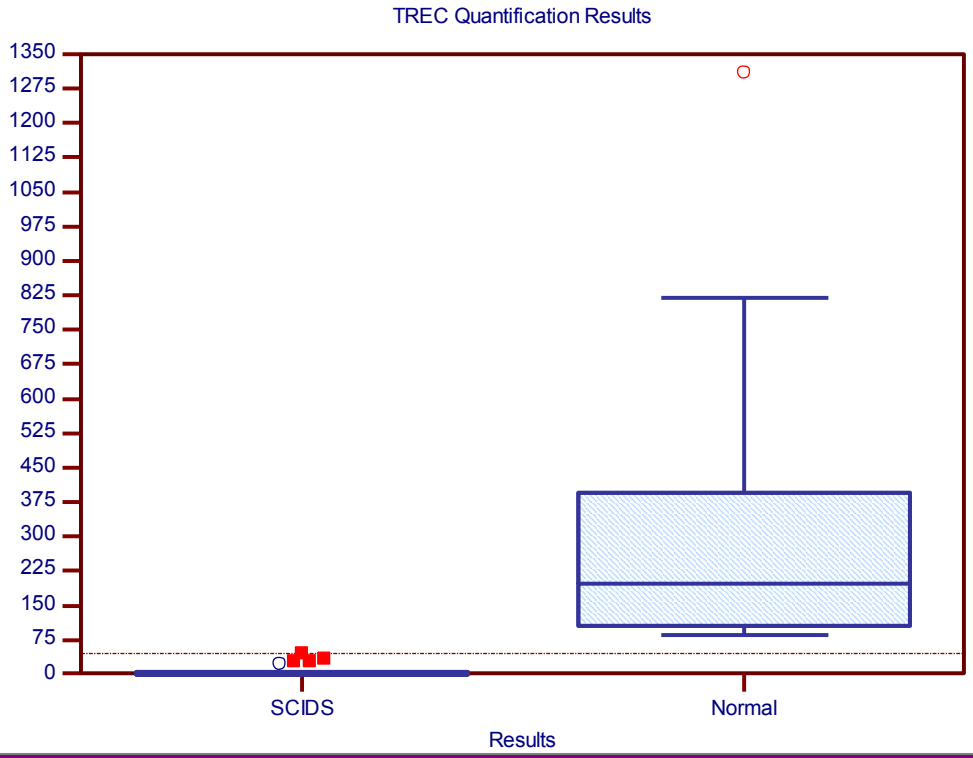

Results	N	Mean TRECs/uL	95% CI	SD	CV
Normal	27	303.96	196.08 - 411.84	272.72	0.90
SCID	21	7.62	0.998 - 14.240	14.54	1.91

Figure 17. Box-and-whisker plot and data summary of the mean TREC/ul observed for each unknown CDC sample analyzed with the TREC-E assay with green error bars representing the TREC ranges and the blue horizontal line demonstrating the mean TREC/uL. The cut-off value of ≤ 46 TREC/uL of whole blood is identified by the orange dotted line.

Table 8. Assay cut-off determination using the area under the ROC curve analysis method for which the cut-off was selected to maximize specificity and sensitivity. The TREC-E assay had 100% specificity and sensitivity with no false negative or false positive results.

Assay	TREC/uL Cut-Off (ROC)	Specificity	False +ve	False -ve	Sensitivity	PPV	NPV
TREC-E	≤46	100%	0%	0%	100%	100%	100%

4.4 Discussion

The identification and comparison of different SCID assays enabled us to ascertain the TaqMan primer and probe set with the greatest amplification efficiency, further enhanced by the new DNA extraction method, which increased the accuracy of TREC detection in dried blood spots by increasing the limit of detection. Carrier molecules such as yeast t-RNA and carrier (poly-A) RNA, added to the DNA extraction buffer have previously demonstrated the ability to increase DNA, plasmid and viral DNA concentrations in low-yield and degraded samples (Kishore et al., 2006; Shaw et al., 2009). The use of t-RNA as a carrier molecule during DNA extraction of the DBS calibrators facilitated the precipitate of additional TREC circular molecules, thus increasing the overall yield as demonstrated by the improved amplification efficiency and increase in the lower limit of detection in Figure 13B (p.69). Dried blood spot calibrators, extracted along side patient samples, ensured that each sample had the same DNA extraction efficiency and therefore, the same amplification efficiency during cycling, providing an accurate TREC concentration for each patient sample. The calibrator concentration encompassed the expected normal and abnormal ranges with a limit of quantitation (LOQ) of 25 TRECs/uL of blood and a limit of detection (LOD) of 14 TRECs/uL (Figure 17, p.76).

The TREC-E assay, developed in the newborn screening laboratory by Gerstel-Thompson *et al.* at the New England Newborn Screening Program demonstrated excellent sensitivity and specificity. We have pursued further qPCR research using only the TREC-E 5'-hydrolysis assay, as the smaller product size and increased amplification efficiency makes it more amenable to other technologies. We continued to use the dried

blood spot calibrators for TREC quantification, employing the singleplex assay as the "gold standard" for which we compared results from the OpenArray system and from the multiplex reactions.

5. Congenital Cytomegalovirus Infection

5.1 Introduction

Congenital infection with the human cytomegalovirus (CMV) is the leading cause of progressive non-syndromic sensorineural hearing loss in neonates (Barbi et al., 2003; Boppana et al., 2005). More than 10% of infants born with congenital CMV infection will be asymptomatic at birth and will develop hearing loss within the next few years (Scanga et al., 2006; Walter et al., 2008; Cheeran et al., 2009). Such numbers demonstrate the importance of early identification and initiation of treatment can occur before permanent hearing loss can develop. Clinically significant viral loads can range from a little as 10 viral copies/mL of blood to as much as $1x10^7$ viral copies/mL (Boppana et al., 2005). As there is a clear link between increased viral load and severity of neurological impact, quantification assays using qPCR, amenable to both high throughput and multiplexing. Multiple genomic targets are often used in parallel to increase detection sensitivity and specificity of clinical strains of CMV (Binda et al., 1999; Habbal et al., 2009).

The principal aim of this portion of the study was to identify and re-design pre-existing qPCR assays used to determine CMV viral load in human blood samples. Primer sets, previously deemed to be highly specific and sensitive for CMV detection were selected and compared to determine the most optimal target for use in further multiplexing assays and for use on the OpenArray system. We sought to further create reliable, non-infectious dried blood spot CMV calibrators that were then used to quantify viral copy numbers in dried blood spots.

5.2 Materials and Methods

5.2.1 qPCR 5'-nuclease hydrolysis probe and primer design

An extensive literature search was performed to identify assays that are currently in use to detect viral copy number and that have been proven to be the most sensitive (Habbal et al., 2009). The published primer and probe sequences selected were for cytomegalovirus specific targets; the trans-membrane protein gene *US17* (Sanghavi et al., 2008), the DNA polymerase gene, *UL54* (Sanchez and Storch, 2002) and the glycoprotein gB gene, *UL55* (Zweygberg Wirgart et al., 1998). Each assay was mapped to their corresponding genomic location using the GenBank sequence (NC_006273.2) All primers and probes, except for *US17*, were redesigned to be TaqMan FAM-labelled MGB assays with similar melting temperatures, using the PrimerExpress 3.0 software (LifeTechnologies) (Table 9, p.82). Primer and probe sequences were compared to the human genome using the BLAST program to ensure 100% homology to the sequence for which they were designed, and also to guarantee that the primer and probe annealing sites were free of single nucleotide polymorphisms amongst the different clinical strains of human cytomegalovirus.

5.2.2 DNA extraction methods

DNA extraction from Dried Blood Spots:

All DNA extractions were performed using the modified extraction method previously mentioned (Section 4.2.2, p. 61) An 8uL aliquot of the supernatant was used to set up each qPCR reaction.

Table 9. A list of all functional primers and probes developed for hCMV viral load quantification. Re-designed TaqMan assays are underlined in the table.

qPCR assay	Sense Primer (5'→3')	Antisense Primer (5'→3')	MGB Probe (5'→3')	Size (bp)
UL55	GTTGCCCAACAG GATTTCG	CCCGTGGTCATCTTTAA TTTCG	TTGACCGTACTGCACGT AC	61
UL54	GCTGACGCGTTTG GTCATC	ACGATTCACGGAGCAC CAG	ATCGGCGGATCACCA	61
US17	CCATGGCGTAAT AGCCCAA	CCATAATCACCGTCGAT GGC	TTGCAGGTAAAGTGCG ATC	126

Viral DNA Extraction from Human Plasma:

A commercially available human CMV high sample from AcroMetrix (LifeTechnologies) was used to initially validate the CMV TaqMan assays. The positive control sample contained an unknown amount of intact, encapsulated viral particles from CMV strain $AD_{169,}$ aliquoted into human plasma. Viral DNA was extracted from 250 uL of the control sample using the iPrep Purelink Virus kit (Invitrogen) on the iPrep Purification Instrument (Invitrogen) following kit instructions. The extracted DNA was eluted using molecular grade water into a final volume of 50 uL.

5.2.3 Assay validation

Each TaqMan assay was synthesized by LifeTechnologies (Carlsbad, CA). Real-time quantitative PCR was performed in a total volume of 20 uL containing 1X TaqMan Universal Master Mix without UNG (LifeTechnologies), 1 uL single-tube TaqMan-MGB Assay (900 nM primers and 250 nM FAM-labelled probe), 2 uL of iPrep extracted viral DNA or 8 uL DBS extracted DNA. The reactions were carried out on an Eppendorf RealPlex2 Real-Time PCR System (Eppendorf) or a ViiA 7 Real-Time PCR System (LifeTechnologies). Cycling conditions were as follows; 1 cycle of 10 minutes at 95°C and 45 cycles of 30 seconds at 95°C and 60 seconds at 60°C. Quantification cycle values (Cq) were noted for each assay developed.

5.2.4 Creation of CMV DBS calibrators using an hCMV BAC

Creation of a CMV-free blood diluent:

To enable the production of accurate calibrators to use in calculating the absolute hCMV copy numbers, we had to create a blood diluent free of any detectable hCMV

virus but with detectable *RNASEP* levels. A total of 40 mL of whole blood were drawn in sodium heparin blood collection tubes from a single adult donor and treated in a similar fashion as previously described (Section 4.2.5, p.62). A small 75 uL volume of blood from the washed whole blood was applied to Whatman 903 Protein Saver cards (VWR) using a pipette and allowed to dry for 4 hours. Using the modified DNA extraction method, a small aliquot of extracted DNA was used to confirm the blood was hCMV negative using both *UL54* and *UL55* assays (data not shown). Once proven negative for any hCMV viral DNA, the blood was then used as a diluent to create the calibrators.

hCMV BAC calibrators:

Cytomegalovirus standard reference material consisting of certifiable genomic copies of a bacterial artificial chromosome (BAC) known as CMV $Towne_{\Delta 147}$ BAC was purchased from the National Institute of Standards and Technology (NIST, Gaithersburg, MD) (Wang et al., 2004). The BAC contained nine cloned CMV fragments, three of which could be amplified and detected with the selected CMV assays (Table 10, p.83). Three vials labeled A, B and C contained 150 uL of the following mean CMV copies per microliter; 420 copies/uL (A), 1 702 copies/uL (B) and 19 641 copies/uL were diluted using the hCMV-free blood diluent to create seven calibrators ranging from 10 000, 1000, 500, 250, 100, 50 and 25 viral copies/uL. The dilutions were allowed to mix on a nutator mixer for 4 hours at room temperature to allow for adequate distribution of the BACs within the blood matrix. Once all the dilutions were adequately mixed, blood spots using 75 ul of the calibration material were spotted onto Whatman 903 Protein Saver cards (VWR) using a pipette and allowed to dry for 4 hours.

Table 10. A list of all CMV genes cloned into the CMV Towne$_{\Delta 147}$ BAC used to make the in-house calibrators (Wang et al., 2004).

Genes	Nucleotide Range	# of Bases
UL54	**77695 - 79992**	**2298**
UL55* to *UL56	**80848 - 82731**	**1884**
US17	**198929 – 199312**	**384**
UL34	**43202 - 44971**	**1170**
UL80	**114401 - 116793**	**2393**
UL83	**118890-119937**	**1048**
UL97	**140784-142090**	**1307**
UL122* to *UL126	**170525 - 173182**	**2658**
UL132	**176380 - 177192**	**813**

Validation of hCMV in-house calibrators:

We validated the calibrators by first punching the calibrators in triplicate into a 96-well plate and extracting the DNA using the modified DBS extraction protocol. A total of 8 uL of each of the pooled extracted DNA was analyzed in triplicate for the *US17, UL54* and *UL55* assays on either the Eppendorf realPlex or the ViiA 7 to enable the comparison of slope values, amplification efficiencies and Y-intercepts of all three assays.

5.2.5 CMV quantification of QCMD samples

Commercially available blinded dried blood spot samples made with different concentration of the CMV AD_{169} strain for 2011 were purchased from the Quality Control for Molecular Diagnostics (QCMD) External Quality Assessment program headed by the European Society for Clinical Virology and European Society for Clinical Microbiology and Infectious Disease (Qnostics, UK) (Barbi et al., 2008). All ten samples (CMVDBS11-01 to CMVDBS11-10) were analyzed in duplicate along with an NTC control and the results converted into CMV viral copies/mL. The final results were then compared to the qualitative results provided by Qnostics, which consisted of samples being deemed either CMV positive, CMV negative or as not determined. The manufacturer provided predefined sample concentrations for internal reference purposes only. We will use the quantitative results solely for the purpose of inter-assay comparisons between *US17* and *UL54.* These two assays were selected due to the limited CMV dried blood spot material availability and the increased sensitivity of *UL54* to detect clinical CMV strains (Habbal et al., 2009).

5.3 Results

5.3.1 Validation of the CMV DBS calibrators

Using all three CMV assays (*US17, UL54* and *UL55*), we sought to determine the linearity of the dried blood calibrators with the following concentrations; 25, 50, 100, 250, 500, 1 000, and 10 000 CMV copies/ 3.2 mm DBS (Figure 18 A-C, p.86). Pooled DNA extracted from each calibrator was used to validate the new calibrators as to normalize the possible differences in extraction efficiencies. Samples were analyzed in triplicate on either the Eppendorf realPlex^2 or the ViiA 7 instruments and regression curves were created to access efficiency. The DBS calibrators demonstrated excellent linearity in all three assays, and consequently, we chose to proceed with further DBS calibrator validations by comparing individual assay performance. The mean E%, slope values, Y-intercept and R^2 were calculated for each assay, with *US17* and *UL55* having > 90% efficiency and all three having similar slope values.

Summary data from three consecutive amplifications, each set-up in triplicate, demonstrated that Cq values for each calibrator stay within ± 1 SD from the mean, with very low variation within the replicates and between separate plates (Table 11, p. 89). A change of ~1Cq for each of the 2-fold dilutions was observed, indicating optimal amplification efficiency was maintained in all three assay replicates. *UL54* failed to amplify the smallest calibrator 25 CMV copies/uL in all three separate plates, indicating a higher limit of detection (LOD) for that assay compared to *UL55* and *US17*.

A)

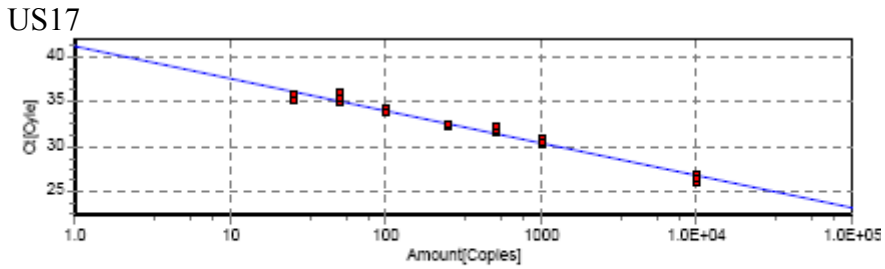

Slope	-3.575	R^2	0.976
Y-Intercept	41.11	Efficiency	0.90

B)

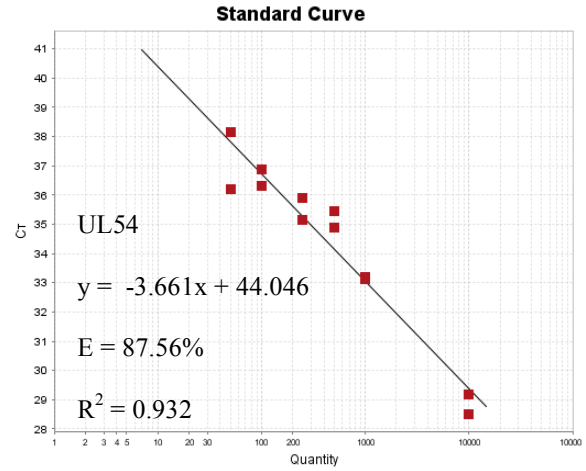

C)

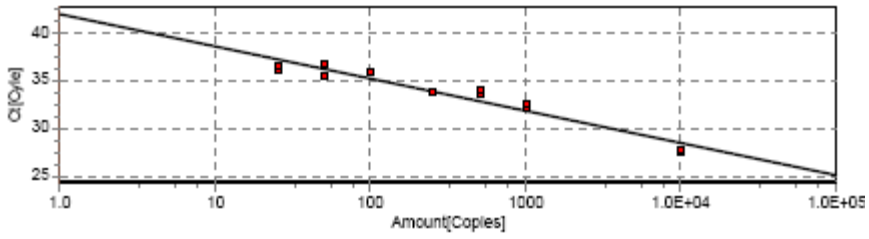

Slope	-3.383	R^2	0.934
Y-Intercept	42.1	Efficiency	0.98

Figure 18 A-C. Standard curves of the in-house CMV BAC dried blood spot calibrators for *US17* (A), *UL54* (B) and for *UL55* (C). Amplficiation failures were noted for *UL54* in some of the relpicates for the 50 and 100 CMV copies/uL calibrators, with the 25 CMV copies/uL calibrator having no amplification at all. *US17* and *UL55* were cycled on the Eppendorf realPlex^2 and *UL54* was analyzed on the ViiA 7.

Table 11. Summary data of mean Cq values for each in-house dried blood spot CMV calibrator setup in triplicate and analyzed in 3 consecutive reactions using *US17, UL54* and *UL55*. A ~ 1 Cq difference is noted for calibrators with a 2-log difference in viral concentration indicating optimal amplification efficiencies for all three CMV assays.

Assay	N	CAL1	CAL2	CAL3	CAL4	CAL5	CAL6	CAL7
		25 CMV copies/uL	50 CMV copies/uL	100 CMV copies/uL	250 CMV copies/uL	500 CMV copies/uL	1 000 CMV copies/uL	10 000 CMV copies/uL
US17	**9**	**36.81 (± 0.18)**	**36.097 (± 0.55)**	**35.013 (± 0.64)**	**34.02 (± 0.00)**	**33.09 (± 0.57)**	**32.235 (± 0.09)**	**27.685 (± 0.16)**
UL54	**9**	**NA**	**39.161 (± 1.41)**	**38.109 (± 0.48)**	**37.215 (± 0.36)**	**36.578 (± 0.16)**	**34.673 (± 0.03)**	**30.474 (± 0.45)**
UL55	**9**	**35.815 (± 0.06)**	**35.08 (± 0.32)**	**33.985 (± 0.26)**	**32.627 (± 0.43)**	**31.73 (± 0.25)**	**31.34 (± 0.74)**	**27.232 (± 0.65)**

Table 12. Summary data from the ten 2011 QCMD samples analyzed in duplicate using the *UL17* and *UL54*. The singleplex *UL17* has the highest sensitivity compared to UL54.

Samples	Sample Con. Copies/mL	Core Proficiency	*US17* (Copies/mL)	*UL54* (Copies/mL)
BS11-06	**0**	**core**	0	0
BS11-04	**625**		**NA**	**NA**
BS11-07	**1 250**		5 200	2 803
BS11-02	**2 500**	**core**	3 633	**NA***
BS11-09	**2 500**	**core**	1 823	2 775
BS11-01	**5 000**	**core**	5 733	10 517
BS11-05	**5 000**	**core**	8 833	12 819
BS11-08	**10 000**	**core**	34 667	23 612
BS11-10	**10 000**	**core**	52 000	30 309
BS11-03	**20 000**	**core**	25 000	20 000

NA = no amplification, NA*= non-amplification of core samples

5.3.2 Determining assay accuracy

To determine the accuracy of the CMV assays, ten QCMD dried blood spot samples were analyzed in duplicate using only the *US17* and *UL54* assays due to limited sample quantity, the high accuracy of CMV detection for both gene targets reported for other laboratories listed in the QCMD report and to the increased sensitivity to clinical strains determined by Habbal *et al.* (Habbal et al., 2009). Using the qualitative and quantitative results obtained from Qnostics, we sought to compare the expected values with the observed concentrations from both CMV assays (Table 12, p.89). Both *US17* and *UL54* identified the six core samples with clinically significant concentrations of CMV virion, with *US17* detecting concentration well below previously published detection levels of 1 600 CMV copies/ uL (Walter et al., 2008; Scanga et al., 2006; Barbi et al., 2000; Barbi et al., 2006a). We were able to attain these values and identify the core samples with a single 3.2 mm dried blood spot using the CMV BAC dried blood spot calibrators. Our qualitative results correlate well with results obtained from other clinical laboratories which use both liquid calibrators for quantification and laboratories who also use larger 50mm DBS (Barbi et al., 2006; Barbi et al., 2000; Binda et al., 2004; Choi et al., 2009). Based on these results we have accessed the limit of detection for both *US17* and *UL54* to be < 1 200 CMV copies/ mL of blood, which is equivalent to ~ 4 CMV copies/ 3.2 mm dried blood spot.

5.4 Discussion

The creation of dried blood spot DBS for CMV quantification is of highest importance. Currently all laboratories performing CMV analysis are using diluted live CMV strains extracted from whole blood or bacterial plasmids containing CMV viral DNA, which pose both a high risk of potential infection and the possibility of surface contamination (Barbi et al., 2006b; Scanga et al., 2006; Habbal et al., 2009). CMV DBS calibrators made using the non-infectious BAC eliminate the possibility of laboratory acquired infection and plasmid contamination. Differences in extraction efficiencies between the calibrators and DBS samples can lead to inaccurate viral quantification. Therefore, utilizing dried blood spot calibrators to determine CMV viral load would increase the precision of viral load determination.

Through CMV assay comparison, we were able to ascertain which assay had the greatest sensitivity using DBS calibrators. The *US17* assay was the most accurate of the three assays allowing for CMV detection well below the previous published limit of detection of 1600 CMV copies/mL (Walter et al., 2008; Scanga et al., 2006; Barbi et al., 2000; Barbi et al., 2006a). We noted a large variation in observed CMV concentrations compared to predicted values in the QCMD samples. This variation is most likely due to the use of the smaller dried blood spot sample (3.2 mm punch) for DNA extraction. Concentration disparities could have also arisen during time of DBS material preparation, as whole blood was first spotted then dried into the filter paper, after which the liquid CMV dilutions were then applied, potentially leading to an uneven application of virus over the 0.5 cm sample surface.

All three assays were selected for OpenArray analysis, thereby maximizing the number of CMV specific targets used for detection. We have attempted to multiplex a CMV target with both TREC-E and RnaseP and will continue to use the dried blood spot calibrators for CMV quantification, using the singleplex assay as the "gold standard" for which we will compare results obtained from the OpenArray system and from multiplex reaction.

Part B: Multiplexing using the OpenArray System

6.1. Introduction

The OpenArray platform was developed in the early 2000's by Dr. Tom Morrison and Dr. Colin Brenan. The assay plates consist of a stainless steel plate with dimensions similar to that of a microscope slide (25 mm x 75 mm x 0.3 mm), photolithographically etched to form 48 sub-arrays each with 64- 320 μm diameter holes (Figure 18, p.94). An amide coupled polyethylene glycol hydrophilic layer is applied to the interior, while a hydrophobic fluoroalkyl is then applied to the exterior surfaces. Interactions between the hydrophilic center and hydrophobic exterior allow for isolated fluid retention within the center of each through-hole, preventing cross-contamination (Brenan, 2002; Brenan and Morrison, 2005; Brenan et al., 2008; Brenan et al., 2009). Primers and probes are spotted into specific hole of each sub-array and samples are then loaded onto the array by simple capillary action using an auto-loader. Each through-hole contains 33 nL of DNA sample mixed with qPCR reagents, with a minimum DNA concentration of 50 ng/ul required (Roberts et al., 2009). Up to 56 different targets can be analyzed simultaneously on 48 samples, with the ability to increase the throughput to a maximum 144 samples per array plate (Figure 6, p. 24). The loaded arrays are then placed into a glass cassette containing an immiscible perfluorinated liquid and UV-sealed to prevent sample evaporation during cycling. The OpenArray NT cycler has the ability to analyze three plates in under 2.5 hours, thus greatly reducing the price per sample for each disease target and reducing the turn-around-time.

The main purpose of this section was to develop a newborn screening specific OpenArray panel, which would combine three separate qPCR techniques; absolute

quantification, SNP detection and relative gene copy number quantification in a single plate. Selected pre-validated TaqMan assays for TREC, CMV, SNP-based *SMN1* assays and deletion 22q11.2 copy number assays were spotted onto the OpenArray plates along with two reference assays. Additionally, we have assessed, for the first time ever whether the OpenArray platform is sensitive enough to detect single gene deletions and duplications needed for accurate CNV detection.

6.2 Material and Methods

6.2.1 OpenArray plate design and assay selection

TaqMan assay selection was based on the results obtained from the initial validations. The following assays were selected; (del22q) – *DGCR2, HIRA, TBX1*, *UFD1L, COMT* and *CRKL*; (SMA) – SMN1-B and SMN1-G; (CMV) – *US17, UL54* and *UL55*; (SCID) TREC-C and TREC-D; (reference assays) – B-Actin and *RNASEP* (Table 13, p.96). Due to the inclusion of quality control through-holes on the array plates, only 54 holes were available in each of the 48 sub-arrays for assay spotting. Each of the copy number assays (deletion 22q11.2 and SMA) and reference assays were spotted in triplicate, where as the assays for absolute quantification (CMV and TREC) were spotted in six consecutive through-holes to increase precision of quantification.

OpenArray Cycling:

Amplification of the samples was performed in real time with an OpenArray NT Cycler (LifeTechnologies). Samples were loaded into the OpenArray plates with the OpenArray NT Autoloader according to the manufacturer's protocols. Each sub-array was loaded with 5 uL of master mix containing 1.2 uL of target DNA at a concentration of 75 ng/uL and reagents in a mixture of 1X GeneAmp Fast PCR Master Mix (LifeTechnologies), 1X OpenArray Remix solution (LifeTechnologies), 0.05 mg/mL UltraPure Bovine Serum Albumin (LifeTechnologies) and molecular grade water. Thermal cycling parameters consisted of initial enzyme activation at 95°C for 10 min, 40 cycles of the following program were used for amplification: denaturation at 95°C for 10

Table 13. List of validated TaqMan assays spotted onto the OpenArray plates used during this study. Each assay was dispensed in the following number of triplicate through-holes; deletion 22q11.2 assays (1x), SMA assays (1x), CMV assays (2x), TREC (2x) and reference assays (1x) for a total of 54 spotted assays.

qPCR Assay	Sense Primer (5'→3')	Antisense Primer (5'→3')	FAM MGB Probe (5'→3')	Size (bp)
Del 22q				
UFL1D	GAGGCAGATTCGTCGCTTTC	CAATCAGCCAACAGTCCTCACTT	TCTGGAGAAGGACAGTCAT	85
CRKL	TAGAGAAGCCTGAAGAACAGTGG	CTTTTCGACATAAGGGACAGGAAT	CCGGAACAAGGATG	83
COMT	CAGTTGTGGTTACTTTCTGGAGAGAG	GGCCGCCCAGGAAGAC	CATGTGGCATGCAGGA	70
TBX1	Hs01313390_cn			80
DGCR2	Hs01576261_cn			110
HIRA	Hs02290153_cn			130
SMA				
SMN1-B	AATGCTTTTTAACATCCATATAAAGCTATC	CCTTAATTTAAGGAATGTGAGCACC	CAGGGTTTCAGACAAA	146
SMN1-G	CTTCCTTTATTTTCCTTACAGGGTTTC	TGATTGTTTTACATTAACCTTTCAACTTTT	AAGTCTGCCAGCATTAT	204
CMV				
UL55	GTTGCCCAACAGGATTTCG	CCCGTGGTCATCTTTAATTTCG	TTGACCGTACTGCACGTAC	61
UL54	GCTGACGCGTTTGGTCATC	ACGATTCACGGAGCACCAG	ATCGGCGGATCACCA	61
US17	CCATGGCGTAATAGCCCAA	CCATAATCACCGTCGATGGC	TTGCAGGTAAAGTGCGATC	126
SCID				
TREC-C	CACATCCCTTTCAACCATGCT	GTGCCAGCTGCAGGGTTTAG	CTCTGGTTTTTGTAAAGGT	111
TREC-E	TGCTGACACCTCTGGTTTTTGTAA	GCCAGCTGCAGGGTTTAGG	ATGCATAGGCACCTGC	81
Reference Assays				
RNASEP	Ribonuclease P RNA component H1 (*H1RNA*) gene (*RPPH1*)			87
B-Actin	ATTTCCCTCTCAGGCATGGA	CGTCACACTTCATGATGGAGTTG	CCTGTGGCATCCACGAA	70

sec, annealing at 60°C for 10 sec, and elongation at 72°C for 10 sec, with real-time fluorescent data collection occurring after each cycle

6.2.2 Copy number quantification for deletion 22q11.2 and SMA

Deletion 22q11.2 Samples:

The same six 22q11.2 deletion samples (Coriell); NA17942, NA17938, NA13325, NA05401, NA07939, NA03479 were used to validate the OpenArray. Wild-type DNA used during initial assay validations will be used as the control sample during copy number quantification. Each sample was diluted to 75 ng/uL for loading onto the arrays.

SMA Samples:

SMA control samples included an SMN1 deletion heterozygote (NA03814) and two SMN1 homozygote deletions (NA09677 and NA10684). Similarly, the same WT DNA extracted from whole blood used during the initial assay validations was used as the control sample for gene copy number calculation. Dr. Alex Mackenzie (University of Ottawa) graciously gifted us with nineteen human DNA samples confirmed by MLPA to have varying *SMN1* and *SMN2* gene copy numbers which we used to compare expected *SMN1* copy number with observed values on the OpenArray and to determine if varying *SMN2* copy number will affect results. DNA was quantified by UV spectrophotometry using the NanoDrop (Thermo Scientific, Wilmington, DE), quality tested by optical density (OD) 260/280 nm ratios and normalized to a starting concentration of 75 ng/ul in 20mM Tris HCL (pH 8.4) (LifeTechnologies, Carlsbad, CA).

Data Analysis and Relative Gene Copy Number Calculations:

Each deletion 22q11.2 sample was positioned in eight consecutive sub-arrays, which were repeated on three separate plates. Each SMA sample was placed in three consecutive sub-arrays repeated on three separate plates. We chose to calculate the relative gene copy number both the classical ΔΔCq method and the efficiency adjusted ΔΔCq method (Livak and Schmittgen, 2001; Yuan et al., 2008; Yuan et al., 2007). Two no template controls (NTC) were included on each plate to detect sample carry-over during auto-loading. The OpenArray Real-Time qPCR Analysis Software (LifeTechnologies) allows for automatic calculation of relative expression level used to determine gene copy number using the classical ΔΔCq method, where as the efficiency adjusted values were calculated independently using the sample Cq values.

6.2.3 Validation and optimization of TRECs and CMV

Calibrator Samples:

The TREC in-house and CMV in-house calibrators were extracted using the modified DNA extraction protocol using one, two or three 3.2 mm dried blood spot punches. Each sample was analyzed in duplicate on a single OpenArray plate using DNA extracted from one, two and three 3.2 mm DBS.

DNA concentration and clean up:

In an attempt to remove PCR inhibitors and concentrate the DNA extracted from the dried blood spot calibrators, Zymo DNA Clean & Concentrator – 5 kits (Zymo Research, Irving, CA) were used on all TREC calibrators punched from a single dried

blood spot using the modified DNA extraction method. Following the manufacturer's protocols, samples were finally eluted in 20 uL of 1X PCR buffer containing 50 ng/uL yeast t-RNA.

6.2.4 Statistical analysis

Statistical analysis was performed using the MedCalc® statistical software (http:/www.medcalc.org) as described in section 2.2.6 (p.32) to determine the means, standard deviations, ROC curve analysis, Passing and Bablok method comparison, Bland-Altman bias assessment and as well as one-way ANOVA analysis for all deletion 22q assays. Passing and Bablok regression analysis, a non-parametric method, enabled the comparison of two separate methods to determine assay concordance (Bilio-Zulle, 2011; Passing et al., 1983). Bland-Altman plots enabled determination of systemic biases that might occur in one or both methods through visualization of the difference of the method means (Y axes) plotted against the averages of the mean (X axis) (Bland et al., 1986).

6.3 Results

6.3.1 Selecting a reference assays for use in relative quantification

Two reference assays previously validated for use in gene copy number quantification were selected and validated for use on the OpenArray. The assay efficiency and slope value for β-Actin (-3.21, E=105%) was slightly better than that of the *RNASEP* assay (-3.86, E=82%) (Table 14, p.103). Calibration curves are located in Appendix IIX. The re-designed β-Actin and the commercial *RNASEP*, assay were compared, looking at mean Cq values (±1SD) and mean RQ values (±1SD). A wild-type sample was loaded in duplicate on twelve consecutive array plates for statistical analysis (Figure 19, p. 101). Greater variations in Cq (21.41 ±1.06) and corresponding RQ (0.981 ±0.14) values were noted for the β-Actin assay compared to the *RNASEP* assay, as demonstrated by the higher coefficient of variation (CV=14%). We therefore selected *RNASEP* as reference assay for copy number quantification for the deletion 22q11.2 and SMA assays. Maintaining the same reference assay for use in relative gene copy number quantification on the OpenArray as in the singleplex reactions has provided us with a means by which to compare the accuracy of both methods.

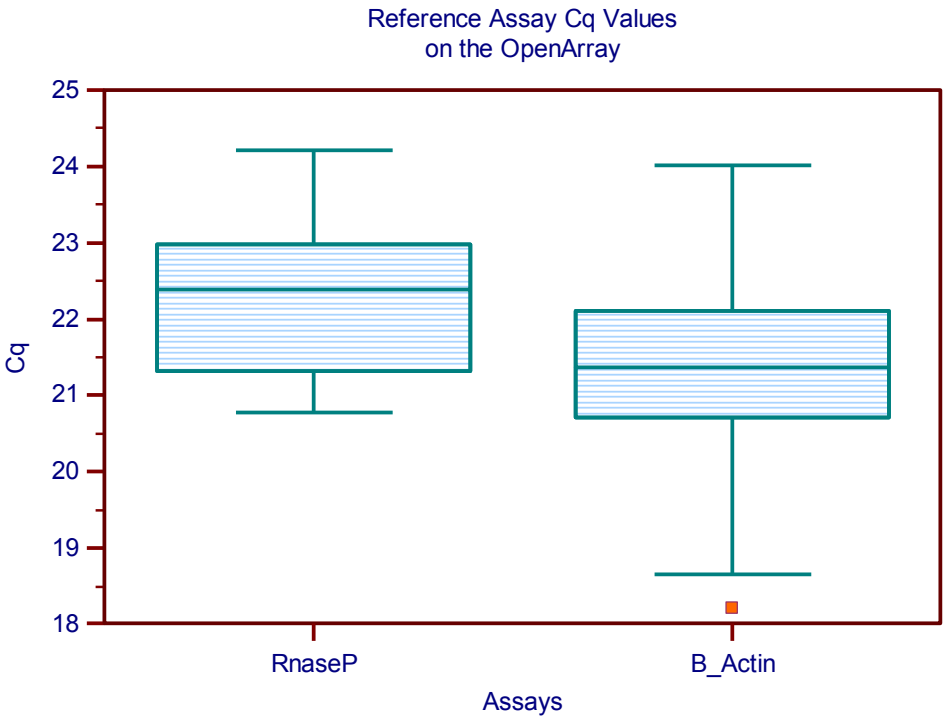

Assay	N	Mean Cq ±SD	Mean RQ ±SD	CV
B-Actin	204	21.41 ±1.06	0.981 ±0.14	0.1419
RNASEP	208	22.27 ±0.91	1.008 ±0.05	0.05432

Figure 19. Box-and-whisker plots and corresponding results table of mean Cq values and relative gene copy number (RQ) of both reference assay; β-Actin and *RNASEP*. Whiskers represent ± 1SD from the mean Cq value and the mean Cq values are represented by the centerline in the boxes.

6.3.2 Deletion 22q11.2 assay validation

Calibrations curves were generated for each of the 22q11.2 TaqMan assays to check for amplification efficiency , slope and the correlation coefficient (Appendix Figure IX). Assays were cycled on a OpenArray NT cycler and results were compared to those obtained from the singleplex reactions (Table 14, p.103). An increase in the slope value along with a corresponding decrease in the amplification efficiency was observed for all OpenArray assays compared to their singleplexed counterparts. The presence of PCR inhibitors in the DNA samples as well as potentially unequal sample loading using the autoloader may have contributed to the decreased efficiency. Only β-Actin continued to maintain a similar slope and efficiency in both the macro and micro-qPCR formats. High correlation coefficients are maintained on the OpenArray due to the precision of the autoloader with $R^2 > 0.95$ for all assays except for *COMT*.

Table 14. Summary data comparing the efficiencies, slopes and the coefficient of determination of the deletion 22q11.2 assays analyzed in singleplex and on the OpenArray system. Note the increasing slopes and the decrease in amplification efficiency for all OpenArray assays except for β-Actin, which maintained its excellent efficiency.

TaqMan Assays									
	Platforms	***DGCR2***	***HIRA***	***TBX1***	***UFD1L***	***COMT***	***CRKL***	**B-Actin**	***RNASEP***
Slope	Singleplex	-3.32	-3.52	-3.57	-3.55	-3.33	-3.33	-3.34	-3.48
	OpenArray	-3.83	-3.67	-3.79	-3.97	-3.75	-4.00	-3.21	-3.86
E%	Singleplex	100.14%	92.31%	90.47%	91.38%	99.49%	99.64%	99.29%	93.64%
	OpenArray	82.50%	87.10%	83.50%	78.70%	84.90%	77.90%	104.90%	81.60%
R^2	Singleplex	0.999	0.998	0.996	0.997	0.985	0.986	0.99	0.994
	OpenArray	0.985	0.949	0.959	0.973	0.927	0.959	0.963	0.968

6.3.3 22q11.2 gene copy number calculation

The RQ and the efficiency adjusted RQ_{EA} mean gene copy number of all test samples for each individual assay were compared through one-way ANOVA analysis using the MedCalc® software (Appendix X), with each sample set-up in three independent OpenArray plates, which allows determination of inter- and intra-qPCR variability of each sample and assay (Livak and Schmittgen, 2001; Yuan et al., 2008). The variation ratio (F) of all assays showed little to no variation in data points used to calculate the mean RQ and RQ_{EA} values. The p- value used to demonstrate the statistical probability of statistically significance differences between analytical methods was determined to be >0.58 for every assay, showing good correlation between the relative gene copy numbers obtained using the classical ΔΔCq and the efficiency adjusted ΔΔCq method.

Based on the results obtained through ANOVA analysis, we chose to only present the gene copy number data calculated for the Coriell samples using the classical ΔΔCq method (Figure 20, p.105). The smaller 1.5 Mb deletion in NA05401 (pink) was detected by both methods (Figure 8B, p.38), with visible hemizygous deletions for all proximal targets except for the distal *CRKL* gene. Sample NA03479 consistently has higher RQ values for most targets except for *COMT* using both methods. No amplification was ever detected in the NTC sub-arrays for any plate.

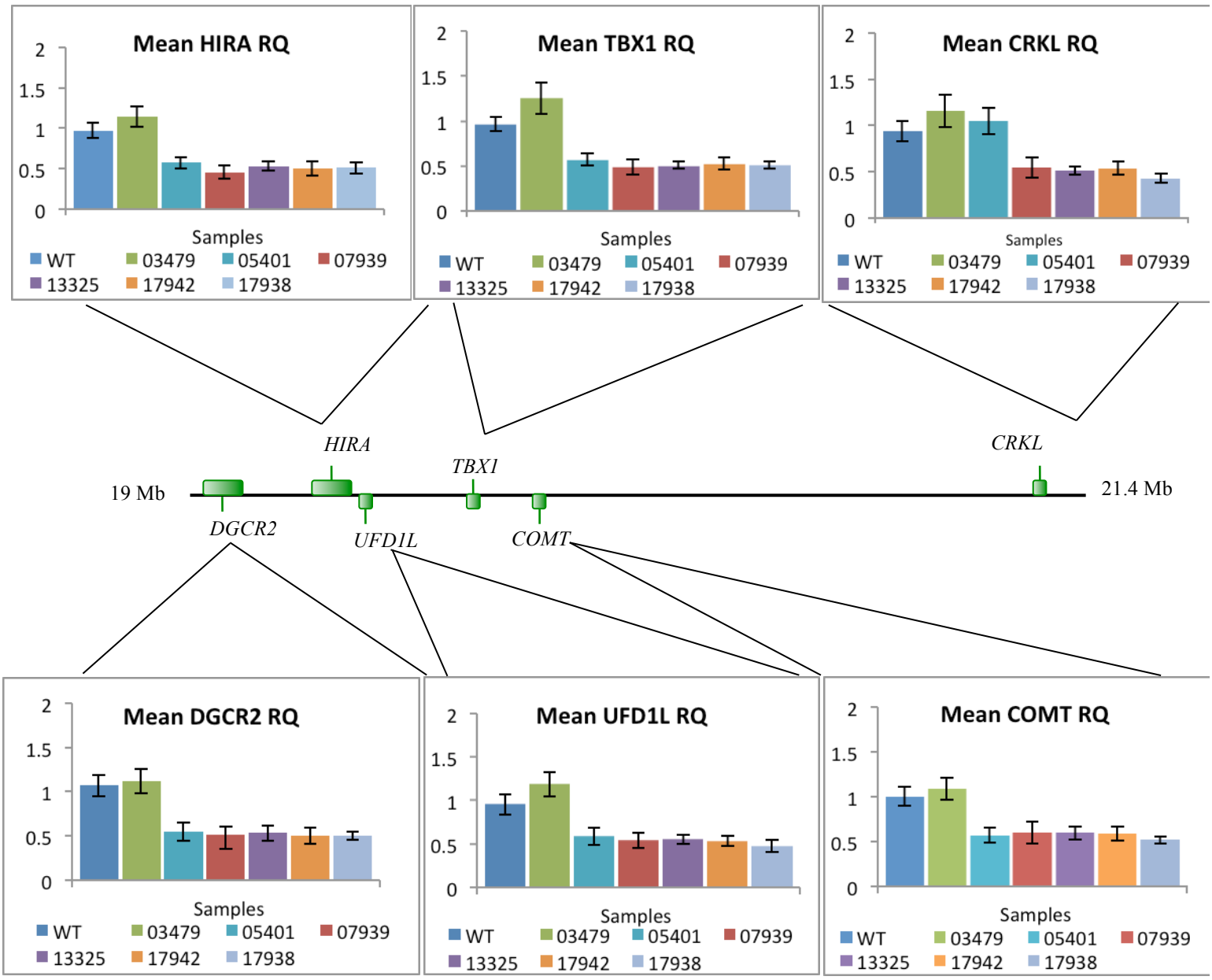

Figure 20. Bar graphs of the mean RQ values for the 22q11.2 samples using the OpenArray system. Each sample was analyzed in eight replicates per array and repeated on three consecutive arrays. Mean results for the wild-type sample (dark blue), NA03479 (green), NA05401 (aqua), NA07939 (red), NA13325 (purple), NA17942 (orange) and NA17938 (light blue) are displayed in the assay specific bar graphs (± 1SD).

6.3.4 Statistical analysis of the deletion 22q11 assays

Multiple experiments using the same Coriell and wild-type samples were performed to allow for statistical analysis using MedCalc®. Mean, standard deviation (SD) and coefficient of variation (CV) for the RQ values of both wild-type samples and 22q11.2 deletion samples were calculated for each assay and represented in Table 15 (p. 107). There are no overlapping 95% CI for the normal and deletion samples amongst all of the 22q11.2 assays, demonstrating the high accuracy of the copy number calculations. The mean RQ values for the wild-type samples vary from 0.952 (*UFD1L*) to 1.015 (*DGCR2*), and the mean RQ values for the deleted samples vary from 0.498 (*CRKL*) to 0.571 (*COMT*), both well within expected ranges for accurate copy number assays.

The resulting RQ data was further analyzed using the area under the Receiver Operating Characteristic (ROC) curve method. ROC analysis identified cut-off values for the 22q11.2 assay with a 100% sensitivity and 100% specificity for all six TaqMan assays. Subsequently false positive and false negative rates along with the positive (PPV) and negative (NPV) predictive values were tabulated as well and included in Table 16 (p.107). Gaussian distribution plots (Appendix XI) demonstrate the separate bi-modal distribution of the deletion and the normal samples, in between which the ROC cut-off values were chosen to maximize the accuracy of disease detection.

Table 15. Statistical calculations of the mean, standard deviation (SD), coefficient of variation (CV) and 95% confidence interval calculated for each 22q11.2 copy number assay analyzed on the OpenArray. There were no overlapping 95% CI for the wild-type (2 copies) and the deleted (1 copy) results indicating high accuracy of copy number quantification.

Assays	Results	N	Mean RQ	95% CI	SD	CV
DGCR2	WT	31	1.015	0.987 - 1.042	0.0757	0.0746
	Deletion	116	0.530	0.515 - 0.546	0.0835	0.1574
HIRA	WT	32	0.979	0.953 - 1.005	0.0712	0.0727
	Deletion	111	0.523	0.510 - 0.537	0.0697	0.1332
UFD1L	WT	31	0.952	0.924 - 0.980	0.0764	0.0802
	Deletion	109	0.535	0.523 - 0.547	0.0652	0.1218
TBX1	WT	32	0.974	0.956 - 0.992	0.0511	0.0524
	Deletion	114	0.525	0.513 - 0.537	0.0649	0.1236
COMT	WT	33	0.987	0.950 - 1.024	0.1048	0.1061
	Deletion	115	0.571	0.556 - 0.585	0.0783	0.1372
CRKL	WT	53	0.976	0.948 - 1.005	0.1034	0.1060
	Deletion	91	0.498	0.482 - 0.514	0.0750	0.1506

Table 16. Assay cut-off determination using the area under the ROC curve analysis method for which the cut-off was selected to maximize specificity and sensitivity. All assays had 100% specificity and sensitivity with no false negative or false positive results.

OpenArray	RQ Cut-Off (ROC)	Specificity	False +ve	False - ve	Sensitivity	PPV	NPV
DGCR2	≤0.75	100%	0%	0%	100%	100%	100%
HIRA	≤0.67	100%	0%	0%	100%	100%	100%
UFD1L	≤0.68	100%	0%	0%	100%	100%	100%
TBX1	≤0.72	100%	0%	0%	100%	100%	100%
COMT	≤0.76	100%	0%	0%	100%	100%	100%
CRKL	≤0.75	100%	0%	0%	100%	100%	100%

6.3.5 Deletion 22q11.2 method comparison

The Passing and Bablok regression analysis is a statistical procedure that allows valuable estimation of analytical methods agreement and possible systematic bias between them. We chose this method over classical Deming Regression as this method is not sensitive to data outliers and is non-parametric, which would prevent variables such as automated OpenArray sample loading and manual qPCR set-up from skewing the method comparison. Regression analysis revealed excellent method agreement for *DGCR2, HIRA, UFD1L, TBX1* and *CRKL* (Figure 21 A-F, p.109). For method agreement, the 95% C.I. for the slope values must encompass 1, while the 95% C.I. for the intercept must include 0 (Bilio-Zulle, 2011). Both the ranges for the intercept (0.07-0.0184) and slope (0.7691-0.944) for *COMT* suggest slight differences between the results obtained on the OpenArray and as a singleplex assay, but the data maintains its linearity across many RQ values (Figure 21E, p.109).

To further calculate method correlation as well as to determine proportional and fixed bias, we chose to analyze the data using Bland-Altman plots. All assays demonstrated excellent method agreement with their singleplex counterparts, as the mean differences of each of the assays (Figure 22 A-D and F, p.110) were at or near 0 demonstrated by the solid center blue line, flanked by the 95% limits of agreement (dashed red lines).

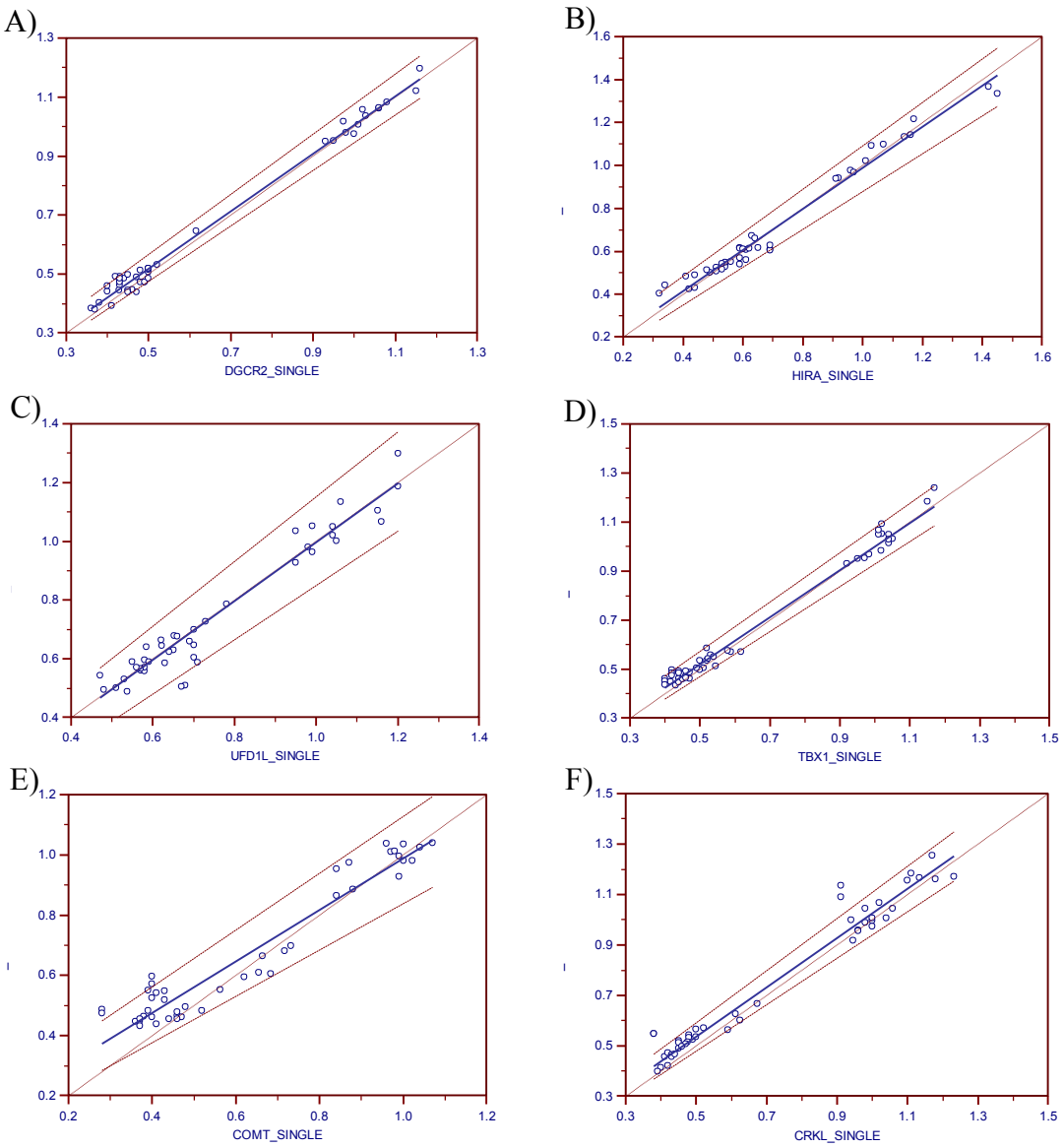

Figure 21 A-F. Passing and Bablok regression analysis of the deletion 22q11.2 singleplex and OpenArray assays. The scatter diagram shows the regression line (solid blue line) and confidence bands (dashed red lines). Cusum test for linearity indicates no significant deviation from linearity for all assays (P >0.05).

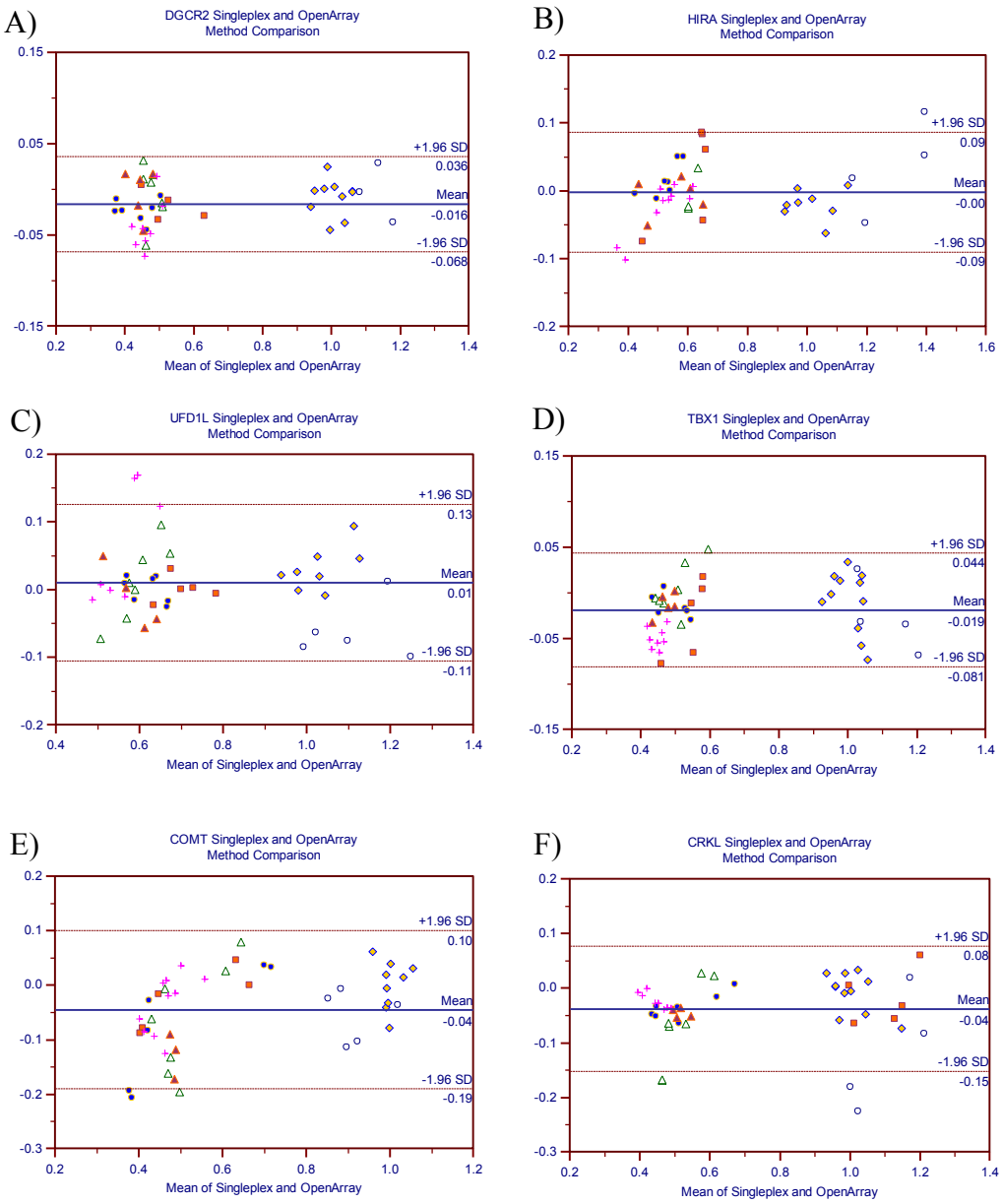

Figure 22 A-F. Bland-Altman plots of sample RQ values for the 22q11.2 assays obtained for the singleplex reaction versus the OpenArray, used to detect proportional and fixed biases during method comparison. Solid blue line represents the mean RQ ratio and the dashed red lines represent ±1.96 SD from the mean. Solid yellow diamonds= wild-type, open circles=NA03479, solid orange squares=NA05401, open green triangles=NA07939, solid purple triangles=NA13325, pink plus signs= NA17942 and solid blue circles=NA17938

6.3.6 *SMN1* assay comparison

The OpenArray plates were spotted with both the SMN1-B assay, a SNP based assay with non-specific SMN primers and an *SMN1* specific probe; and SMN1-G, which has an *SMN1* allele-specific primer pair and a non-specific SMN probe for comparison.

Nineteen donated samples with known *SMN1* and *SMN2* gene copy number, along with the three Coriell control samples (NA09677, NA10684 and NA03814) and our wild-type sample were loaded in triplicate on a single plate, repeated in three independent experiments. No amplification was ever detected in the NTC sub-arrays on any of the OpenArray plate. Cq values were unobtainable for any SMN1-B through-hole for any sample or plates analyzed. Further investigation revealed that the fluorescent signals for even the wild-type and triplication samples recorded by the NT cycler did not meet the minimum confidence value of >300 (Figure 23, p.112) compared to through-hole containing the SMN1-G assay. The OpenArray software calculates Cq based on a confidence algorithm that combines the baseline intercept and numerical exponential amplification modeling to determine the sureness of fit (Morrison et al., 2006; Van Doorn et al., 2009). Co-amplification of both *SMN1* and *SMN2* with detection of *SMN1* only is thought to contribute to the lower amplification and recognition of the *SMN1* specific product, thereby reducing the overall fluorescence intensity.

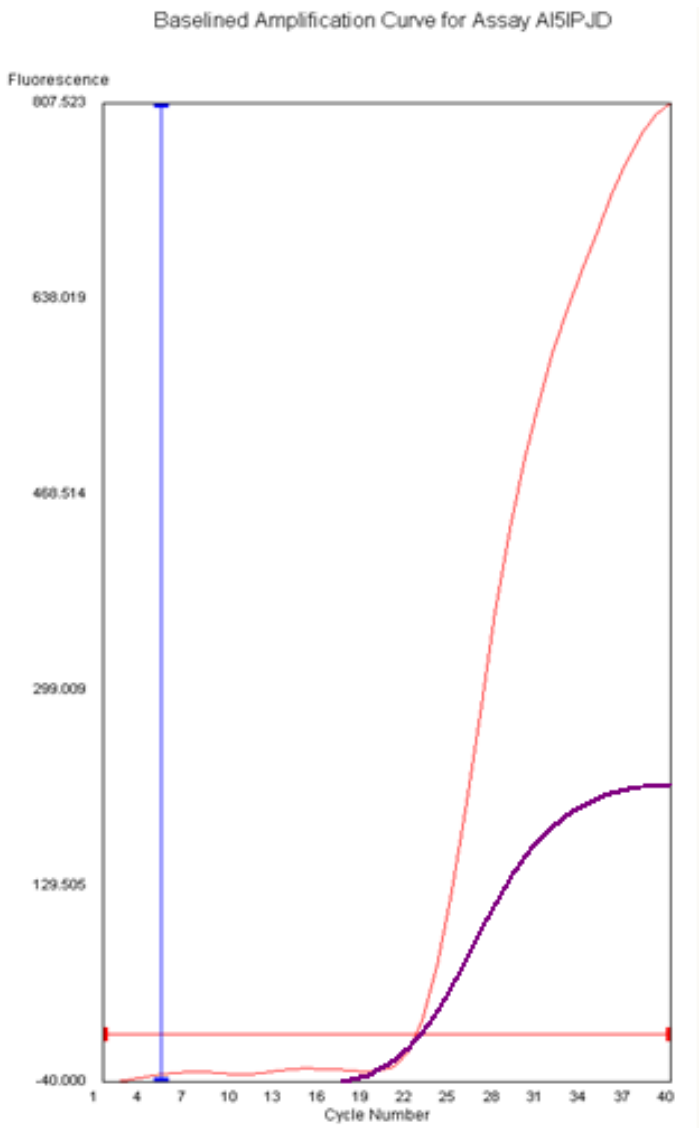

Figure 23. Exponential amplification curves of fluorescence versus cycle number drawn to scale for SMN1-B (purple) and SMN1-G (red) analyzed on the OpenArray. The fluorescent intensity detected for SMN1-B (170.77) is well below the minimum pre-set detection confidence level of the OpenArray NT cycler of >300. Baseline intercept (blue vertical line) and exponential amplification (red horizontal line) are used to determine Cq confidence levels.

6.3.7 Statistical analysis of SMN1-G on the OpenArray

Assay reproducibility was determined using the nineteen donated samples with known *SMN1* and *SMN2* copy number, along with the WT and abnormal control, which were set-up in triplicate and analysed on three separate array plates to allow for statistical analysis of means, standard deviations and variation (Table 17, p.116). We chose to calculate the RQ value using only the classical ΔΔCq method, as we were unable to generate a standard curve for RQ_{EA} efficiency comparison due to the limited availability of OpenArray plates. Based on the data obtained from the deletion 22q11.2 assays analyzed on the OpenArray and the statistical results from the SMN1-G singleplex reaction, we were quite confident that the RQ and the RQ_{EA} for the SMN1-G assay would be quite similar as well. There are no overlapping 95% CI for the SMA, carrier, normal and triplication samples, indicating high accuracy during copy number calculations, results supported by the Gaussian distribution plots found in Appendix XII.

We furthermore sought to determine whether additional copies of *SMN2* would affect the accuracy of RQ calculations due to the possibility of both annealing of the non-specific SMN reverse primer and probe of the SMN1-G assay. Figure 24 (p.115) depicts the mean RQ values obtained for the donated samples with *SMN1*copy number*: SMN2* copy number indicated for each sample. No significant difference in *SMN1* RQ value was noted in samples with increasing *SMN2* copy number. Samples 8 (1:3), 9 (1:1) and 24 (1:2) with single copies of *SMN1* and had mean RQ values of 0.481, 0.411 and 0.476 respectively, demonstrating the similarities of results, regardless of their *SMN2* status.

The results observed for all 19 samples using the SMN1-G assay on the OpenArray substantiated the MLPA findings.

The corresponding RQ values were analyzed using the area under the ROC curve method to determine the assay cut-offs for the SMN1-G assay on the OpenArray (Table 18, p.116). ROC analysis determined RQ cut-off values of 0 for an individual with zero copies of *SMN1*, and RQ of greater than zero but ≤0.685 for an SMA carrier, individuals with two *SMN1* copies had greater than 0.685 but ≤ 1.22, while samples with triplications had an RQ cut-off of ≥ 1.22. Sensitivity and specificity were all near 100%, with only the carrier cut-off demonstrating a few outliers that would fall under the lower range for normal.

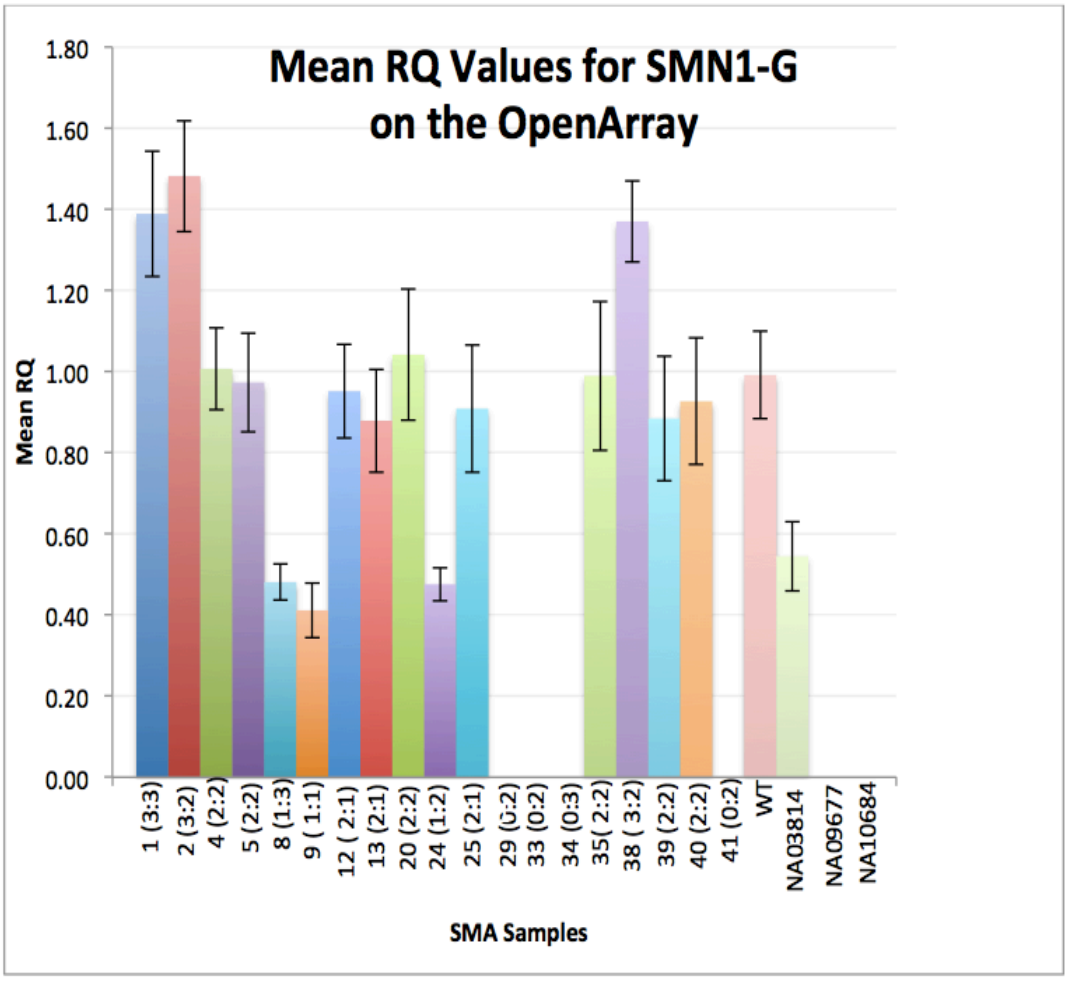

Figure 24. Bar graph depicting the mean RQ values calculated for the SMA samples. Sample number and *SMN1: SMN2* gene copy numbers calculated using MLPA (MRC-Holland) are indicated below each bar. Error bars show ± 1SD.

Table 17. Statistical calculations of the means, standard deviations (SD, coefficient of variation (CV) and 95% C.I. for SMA samples (0 copies), deletion carriers (1 copy), normal individuals (2 copies) and *SMN1* gene duplication (3 copies).

SMN1-G	N	Mean RQ	95% CI	SD	CV
SMA	74	0.000	0.000 - 0.000	0.0000	0.0000
Carrier	49	0.480	0.458 - 0.501	0.07397	0.1542
Normal	109	0.955	0.932 - 0.979	0.1250	0.1309
Duplication	32	1.435	1.393 - 1.477	0.1156	0.08054

Table 18. SMN1-G assay cut-off determination using the area under the ROC curve analysis method for which the cut-off was selected to maximize specificity and sensitivity.

OpenArray Assay	Result	RQ Cut-Off (ROC)	Specificity	False +ve	False –ve	Sensitivity	PPV	NPV
SMN1-G	SMA	≤0	100%	0%	0%	100%	100%	100%
	Carrier	0 > X ≤ 0.685	100%	0%	1%	99%	100%	100%
	Normal	0.685 > x <1.22	100%	0%	0%	100%	100%	100%
	Duplication	≥ 1.22	100%	0%	0%	100%	100%	100%

6.3.8 SMA method comparison

We chose to analyze a limited number of the donated SMA samples; 1 (3:3), 13 (2: 1), 24 (1:2) and 38 (3:2), using the singleplex SMN1-G assay due to the limited sample volume. Gaussian distribution plot of the SMN1-G singleplex assay is located in Appendix XII. The Passing and Bablok regression analysis was performed to determine method agreement between the SMN1-G singleplex and OpenArray qPCR. Regression analysis revealed excellent method agreement between the two analytical platforms (Figure 25A, p.118). For method agreement, the 95% CI for the slope values must encompass 1.0, while the 95% CI for the intercept must include 0 (Bilio-Zulle, 2011). Both the ranges for the intercept (-0.055 - 0.000) and slope (0.923 – 1.00) are near perfect values across all sample results.

To further calculate method correlation as well as to determine proportional and fixed bias, we chose to analyze the data using Bland-Altman plots (Figure 25B, p.118). Outstanding method agreement between their singleplex counterparts, as the mean difference of the assay was near 0 (0.06) demonstrated by the solid center blue line, flanked by the 95% limits of agreement (dashed red lines). No data outliers were noted for either method either above or below the ± 1.96 SD limits (dashed red lines).

A)

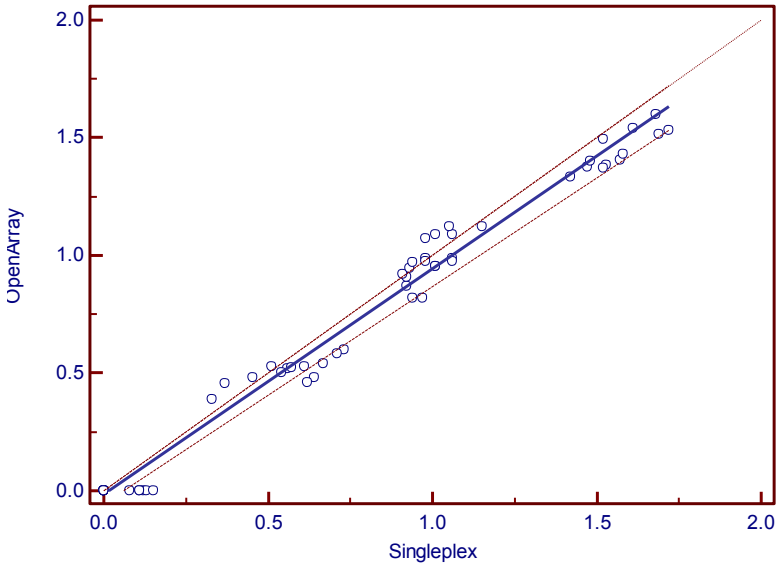

B)

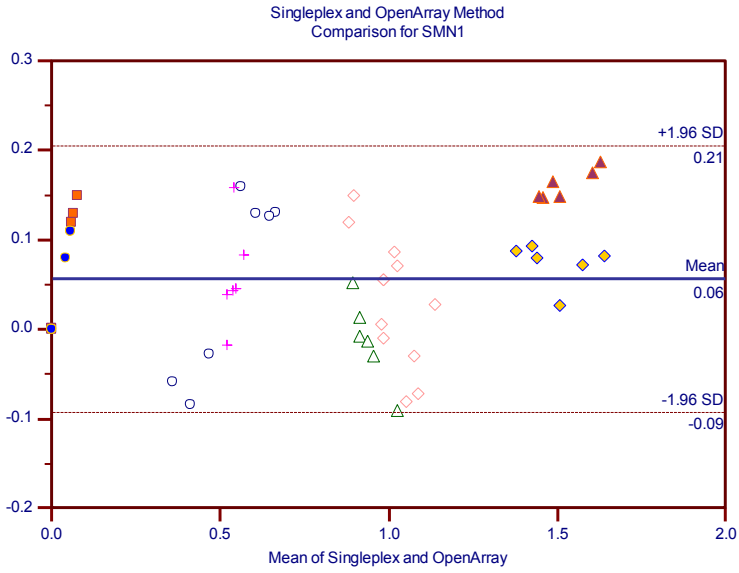

Figure 25 A-B. (A) Passing and Bablok regression analysis of the SMN1-G singleplex versus OpenArray assay. The scatter diagram shows the regression line (solid blue line) and confidence bands (dashed red lines). Cusum test for linearity indicates no significant deviation from linearity as P = 0.32 (P >0.05). (B) Bland-Altman plot of sample RQ values obtained from the singleplex reaction versus the OpenArray. Solid blue line represents the mean RQ ratio and the dashed red lines represent ±1.96 SD from the mean. Open pink diamonds=wild-type, solid yellow diamonds= sample 1, open circles=NA03814, solid orange squares =NA09677, open green triangles=sample 13,

solid purple triangles=sample 38, pink plus signs= sample 24 and solid blue circles=NA10684

6.3.8 DNA extraction optimization for TREC and CMV

Initial validation experiments using DNA extracted from a single DBS demonstrated amplification of only the highest TREC calibrator (100 000 TRECs/ 3.2 mm DBS) for TREC-E, with no amplification of any calibrators for TREC-C (data not shown). Amplification failures for all CMV calibrators were noted for all three CMV assays, *US17, UL54* and *UL55*. The relative high precision and sensitivity needed to accurately quantify both TRECs and CMV viral DNA within a background of genomic DNA prompted us to look at whether the number of dried blood spots needed to be increased, thereby improving DNA yield needed for successful amplification to occur.

OpenArray plates loaded with DNA extracted from 3 DBS had the best and most reproducible results (Figure 26 A-B, p.120). The TREC-E assay had successful amplification of six calibrators (Cal 1 to Cal 6) ranging from 100 000 to 1 000 TREC copies/3.2 mm DBS. (Figure 26A, p. 120) The slope (-2.13) and efficiency (194%) demonstrated considerable amplification inhibition with poor data correlation (R^2= 0.805). In an attempt to remove possible interfering compounds extracted concurrently with the DNA, we chose to use the Zymo clean and concentrator columns on DNA extracted from three DBS using the modified method. Samples were then loaded onto a plate for analysis. Excellent amplification was noted for the highest four TREC in-house calibrators amplified using TREC-E (Figure 26B, p.120). No amplification was ever detected for the TREC-C assay or the CMV assays on the OpenArray.

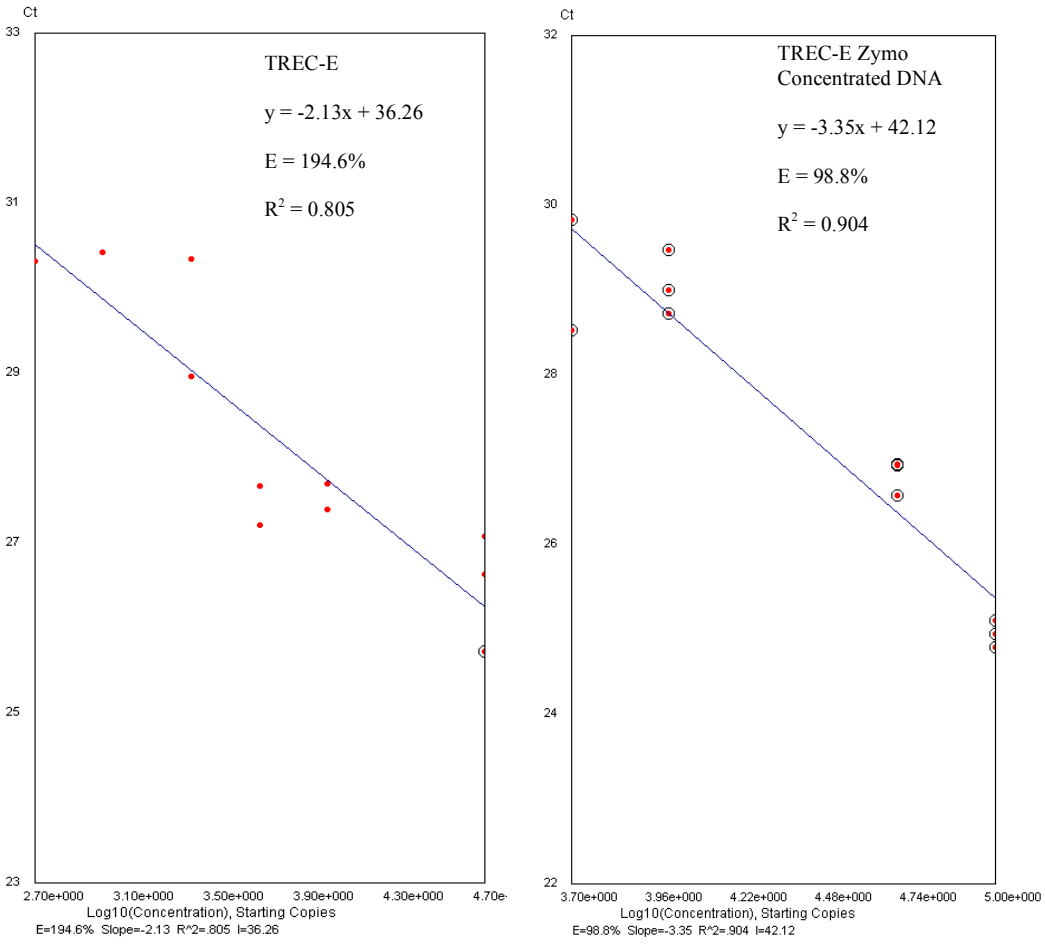

Figure 26 A-B. Calibration curves for TREC-E using DNA extracted from 3 DBS loaded directly after isolation (A) and after post-isolation concentration using the Zymo clean and concentrate spin column (B) analyzed on the OpenArray. (A) Amplification inhibition is detected leading to a decreased slope (-2.13) and increased efficiency (194.6%). (B) The concentrated and cleaned DNA greatly increased amplification efficiency (98.8%) but only for the highest four TREC calibrators.

6.4 Discussion

A number of nano-qPCR strategies have been developed in the last decade with the goal of reducing reagent cost, minimizing turn-around-time, all while trying to maximize throughput. Here, we chose to evaluate the OpenArray system for potential use in a newborn screening setting, incorporating assays needing absolute quantification, genotyping and relative quantification. System performance was accessed through method comparisons employing the singleplex TaqMan assays as "gold standard" tests by which we would then compare all OpenArray results. The goal of method comparison is to estimate constant and proportional errors between methods, thus determining if significant statistical differences in accuracy exist between the two clinical methods. We were able to successfully detect homozygous and single gene deletions and duplications (± 2-fold difference) in *SMN1* and all six deletion 22q11.2 assays using the OpenArray platform, with comparable accuracy and precision to the singleplex assays, as demonstrated by the Passing and Bablok regression analysis. Assay bias was not detected in the Bland-Altman plots for any of the CNV or SNP assays. Similar gene copy number results were obtained for the donated SMA samples using the SMN1-G assay on the OpenArray, when compares to those obtained by the singleplex assay and those calculated by the SMA MLPA kit (Figure 24, p.115). Based on the reproducibility and accuracy of the gene quantification results for all CNV assays, we can surmise that the OpenArray would be very amenable for use in detecting homozygous and hemizygous gene deletions as well as duplication.

Genomic-based assays amplified consistently well on the OpenArray with Cq values ranging from 19 to 24 cycles, which enabled accurate gene copy number quantification without the need to incorporate amplification efficiencies in the ΔΔCq calculations. On the other hand, non-genomic assays, such as for TRECs and CMV viral DNA had considerable difficulty amplifying due in part to very low starting copies of genetic material and to the presence of PCR inhibitors, such as heme, found in high abundance in dried blood spots (Figure 26 A-B, p.120). This is apparent with amplification failures in the TREC in-house calibrators with TREC counts of less than <5000 TREC/ 3.2 mm DBS and with the failure to amplify any of the CMV calibrators, all with estimated Cq values > 31 cycles based on the results from the singleplex assays. Previous OpenArray work done by Dixon *et al.* demonstrated a notable decline in both sensitivity and power of analysis of samples with Cq >22 cycles, with amplification efficiencies decreasing exponentially as Cq values increased (Dixon et al., 2009). Such findings suggest that accurately quantify clinically significant concentrations of TREC and CMV viral DNA may not be feasible, as each of these assays require detection of large dynamic ranges needed to maintained sensitivity even at the lower end of their analytical ranges. The increase in LOD for the TREC assay and the inability to amplify even the largest CMV calibrator preclude the use of the OpenArray for absolute quantification in a clinical setting.

We explored further testing strategies by developing multiplexed assays for high resolution 22q11.2 CNV detection using *UFD1L, COMT* and *CRKL*; for absolute quantification of TREC and CMV; and for both quantification TREC and CNV detection of *TBX1* for simultaneous SCID and deletion 22q11.2 screening. The *RNASEP* assay was

included in each separate multiplex for use as an amplification control and as a reference assay for relative quantification.

Part C: Multiplexing qPCR TaqMan assay

7.1 Introduction

Multiplexing qPCR assays is often time consuming and complex, requiring lengthy optimization. Many elements must be taken into consideration before beginning the assay design such as; i) limiting primer and probe concentrations within the reaction to minimize primer-dimer formation, primer-probe binding, ii) selecting fluorophores whose excitation and emission wavelength do not overlap, iii) designing the primers and probes to work optimally at the same annealing temperature, iv) optimizing the concentration of dNTPs, magnesium and PCR additives, and v) selecting quencher molecules with low background fluorescence, which absorb different wavelengths to reduce quenching of probes in solution.

The increased interest in multiplexing qPCR assays has driven many biotechnology companies to create reaction master mixes with optimized concentrations of dNTPs, magnesium ions (Mg^{+2}) and buffering salts (KCl). Several include mutant hot-start *Taq* DNA polymerase for increased fidelity and functionality for use on DNA samples containing high concentrations of PCR inhibitors. Many of the new generation of qPCR master mixes contain PCR additives such as FBS, glycerol (5-10%), non-ionic detergents (Triton-X) or even proprietary PCR enhancing solutions, all with the intentions of both increasing overall yield and increasing fidelity of SNP assays. Such master mixes reduce and often eliminate the need for extensive optimization of reaction conditions, saving time and ultimately money, while increasing the fidelity of results.

We elected to create three separate multiplex reactions for this portion of the study; (A) 22q11.2 copy number multiplex (*UFD1L, COMT* and *CRKL*); (B) TREC and CMV quantification multiplex; and (C) a deletion 22q11.2 copy number assay (*TBX1*) with TREC which will allow us to simultaneously discern those patients with classical SCID and those with self-resolving T-cell lymphopenias caused by 22q11.2 deletion syndrome. Deletion 22q11.2 and WT DBS QC material were created to provide quality control material for use in newborn screening, thus enabling relative quantification of neonatal DBS.

7.2 Material and Methods

7.2.1 qPCR 5'-hydrolysis probe and primer restriction

Separate primers and probes were purchased s to be able to conduct primer and probe restriction tests during initial multiplex optimization. BHQPlus-Quasar 670 labelled probes were purchased from Biosearch technologies, while all other probes were obtained from LifeTechnologies. *UL54* was selected as the CMV target due to the incompatibility of the TREC primers and probe sequences with those of *UL55* and *US17*. Real-time quantitative PCR for gene copy number detection was performed in a total volume of 20 uL containing 1X QuantiTect Multiplex master mix (Qiagen), varying concentrations of primers and probes listed in Table 19 (p.126), 100 ng of Coriell DNA or 8 uL of DNA extracted from DBS using the modified extraction method (Section 4.2.2, p.59) and molecular grade water. The reactions were carried out on a ViiA 7 Real-Time PCR System (LifeTechnologies). Cycling conditions were as follows; 1 cycle of 5 minutes at 60°C; 1 cycle of 15 minutes at 95°C and 45 cycles of 60 seconds at 94°C and 90 seconds at 60°C. A fixed cycle threshold (Cq) was set at the exponential phase of PCR amplification.

7.2.2 Validation of multiplexed assays

Amplification efficiencies of each of the assays using the restricted primer and probe concentrations were determined using the same serially diluted wild-type DNA (50

ng, 100 ng, 150 ng, 200 ng and 250 ng), which was setup in triplicate along with an NTC control. Calibration curve slope, Y-intercept and amplification efficiency were calculated

Table 19. Primers and probes with accompanying fluorophores used in the multiplex assays.

Assay	Sense Primer (5'→3')	Antisense Primer (5'→3')	MGB Probe (5'→3') – Reporter	Final Con. Primers/ Probe nM
Multiplex A				
UFL1D	GAGGCAGATTCGT CGCTTTC	CAATCAGCCAA CAGTCCTCACT T	TCTGGAGAAGGAC AGTCAT-FAM	400 nM/ 200nM
COMT	CAGTTGTGGTTACT TTCTGGAGAGAG	GGCCGCCCAG GAAGAC	CTCCTGCATGCCA CATG- Quasar 670	400 nM/ 200 nM
CRKL	TAGAGAAGCCTGA AGAACAGTGG	CTTTTCGACAT AAGGGACAGG AAT	CCGGAACAAGGAT G-NED	400 nM/ 200 nM
RNASEP		RnaseP_VIC_CCBJWM6		0.5 uL
Multiplex B				
TREC-E	TGCTGACACCTCTG GTTTTTGTAA	GCCAGCTGCAG GGTTTAGG	ATGCATAGGCACC TGCAC-Quasar 670	950 nM/ 250 nM
UL54	GCTGACGCGTTTG GTCATC	ACGATTCACGG AGCACCAG	ATCGGCGGATCAC CA-FAM	900 nM/ 250 nM
RNASEP		RnaseP_VIC_CCBJWM6		0.5 uL
Multiplex C				
TBX1		Hs01313390_cn FAM		0.5 uL
TREC-E	TGCTGACACCTCTG GTTTTTGTAA	GCCAGCTGCAG GGTTTAGG	ATGCATAGGCACC TGCAC-Quasar 670	900 nM/ 250 nM
RNASEP		RnaseP_VIC_CCBJWM6		0.5 uL

for each assay within the multiplex. Those values were then compared to the same measures taken from the singleplex assay during initial assay validation. We compared slope values, Y-intercepts and efficiencies for all assays using the serially diluted DNA calibrators, calculated using the ViiA 7 software. Amplification efficiencies were used during RQ_{EA} calculations.

7.2.3 Creation of DBS deletion 22q11.2 QC material

A total of 8 mL of whole blood were drawn in sodium heparin blood collection tubes from a single donor, with 2 mL spotted onto filter paper for use as WT DBS QC and the remaining 6 mL treated in a similar fashion as previously described but with the complete removal of the buffy coat, leaving only the red blood cells (Section 4.2.5, p.64). Immortalized B-cell lines GM07939, GM17938 and GM17942 (Coriell) grown in T25 flasks were poured into 50 mL Falcon tubes and centrifuges at 3000 rpm for 10 minutes to pellet the cells. The cells were then washed twice in 1X PBS, with resuspension and centrifugation between each wash. The final supernatant was removed, leaving < 50 uL of 1X PBS. A total of 2 mL of red blood cells reconstituted to 50% hematocrit was pipetted into the tubes to resuspend the cell pellet. The blood mixture was then placed in a 4 mL glass borosilicate vial and allowed to mix on a nutator for 2 hours. A small 75 uL volume of blood from the washed whole blood was applied to Whatman 903 Protein Saver cards (VWR) using a pipette and allowed to dry for 4 hours. Each DBS QC and a

WT DBS sample analyzed in triplicate on the ViiA 7 in conjunction with the liquid DNA from their corresponding cell line using multiplex A and C to compare RQ values.

7.2.4 Relative and absolute quantification using all three multiplexes

Deletion 22q11.2 Samples:

The same six 22q11.2 deletion samples (Coriell); NA17942, NA17938, NA13325, NA05401, NA07939, NA03479 were used to validate the multiplex reactions. Wild-type DNA extracted during initial assay validations was used as the control sample during copy number quantification.

TREC and CMV Samples:

The TREC in-house and CMV in-house calibrators were extracted using the modified DNA extraction protocol using one 3.2 mm DBS punches. Each calibrator was analyzed in duplicate (CMV) or triplicate (TREC) and analyzed on two consecutive plates. The blinded QCMD samples (CMVDBS11-01 to CMVDBS11-10) were analyzed in duplicate along with an NTC control and the results converted into CMV viral copies/mL. Forty of the blinded MPES SCID samples provided by the CDC will be analyzed in duplicate for both Multiplex B and C. All results will be compared to their singleplex counterparts using Passing and Bablok regression analysis and Bland-Altman comparisons. Assay means, slope and Y-intercept were compared to those from other newborn screening laboratories.

7.2.5 Statistical analysis

Statistical analysis was performed using the MedCalc® statistical software (http:/www.medcalc.org) as described in section 6.2.4 (p.99).

7.3 Results

7.3.1 Initial multiplex validations

Initial primer and probe restriction assays were conducted to reveal the minimum concentration of each needed to maintain similar slope and amplification efficiency as their singleplex counter parts, while reducing the possibility of primer-dimer formation or fluorescent spectral overlap (data not shown). The slope, E% and R^2 of each assay within their corresponding multiplexes were compared to those obtained from the singleplex reactions and from the OpenArray (Table 20, p.130). Very little difference in slope values were observed between the singleplex and the multiplexed assays, both setup in 96-well, 20 uL format. Linearity, as demonstrated by the R^2 value, remains quite constant for all three qPCR methods, regardless of manual or automated reagent dispensing. Calibration curves for *UFD1L, COMT, CRKL*, *RNASEP*, TREC and *UL54* are presented in Appendix XIV and XV.

Table 20. Comparison of amplification efficiencies of all singleplex, multiplex and OpenArray assays.

TaqMan Assays								
	Platforms	***TBX1***	**TREC-E**	***UL54***	***UFD1L***	***COMT***	***CRKL***	**RnaseP**
Slope	Singleplex	-3.57	-3.33	-3.66	-3.55	-3.33	-3.33	-3.484
	OpenArray	-3.79	-3.35	NA	-3.97	-3.75	-4	-3.86
	Multiplex A				-3.67	-3.65	-3.54	-3.738
	Multiplex B		-3.305	-3.679				-3.544
	Multiplex C	-3.441	-3.343					-3.583
Efficiency %	Singleplex	90.47%	99.89%	87.56%	91.38%	99.49%	99.64%	93.64%
	OpenArray	82.50%	98.80%	NA	78.70%	84.90%	77.90%	81.60%
	Multiplex A				87.20%	88.00%	91.50%	85.13%
	Multiplex B		100.70%	86.99%				91.50%
	Multiplex C	95.26%	99.13%					90.15%
R^2	Singleplex	0.996	0.94	0.932	0.997	0.985	0.986	0.994
	OpenArray	0.959	0.904	NA	0.973	0.927	0.959	0.968
	Multiplex A				0.99	0.991	0.986	0.996
	Multiplex B		0.964	0.94				0.973
	Multiplex C	0.99	0.952					0.993

7.3.2 Gene quantification for Multiplex A and Multiplex B

The mean RQ values obtained for *UFD1L, COMT* and *CRKL* in multiplex A and *TBX1* in multiplex C using the *RNASEP* as the reference assay are depicted in the bar graphs, shown in Figures 27 A and B (p.132). All samples, except for NA03479, had values ranging from ~0.304 to 0.74, showing hemizygous deletions for all targets. Sample NA05401, displayed two copies of the distal *CRKL* gene, with an RQ value of 1.02, suggestive of the smaller ~ 1.5 Mb deletion. Interestingly, NA05401 has higher RQ values for *UFD1L, COMT* and *TBX1* compared to the other Coriell samples when analyzed using multiplex A. This finding was also observed when each assay was run in singleplex as well (Figure 8 A-B, p.38) but was not observed on the OpenArray (Figure 20, p.105). Low-level cell mosaicism may be present in the culture caused by the complex translocation carried by NA05401 involving chromosome 22 [45,XY,der(4)t(4pter>4q35::22q11>22qter)mat,-22], for which multiple different chromosomal break-points may exist either naturally in the donor individual or accrued over time due to multiple cell passages at the facility. The overall mean RQ values for the deletion 22q11.2 samples for *UFD1L* and *CRKL* within multiplex A were quite similar ranging from ~0.50 to 0.62, while the mean RQ for *COMT* was significantly lower at ~ 0.3 to 0.53 (Figure 27A, p. 132). This indicates a preferential amplification of the larger *UFD1L* (85 bp), *CRKL* (83 bp) and *RNASEP* (87 bp) PCR products over the smaller 70 bp *COMT* product.

A)

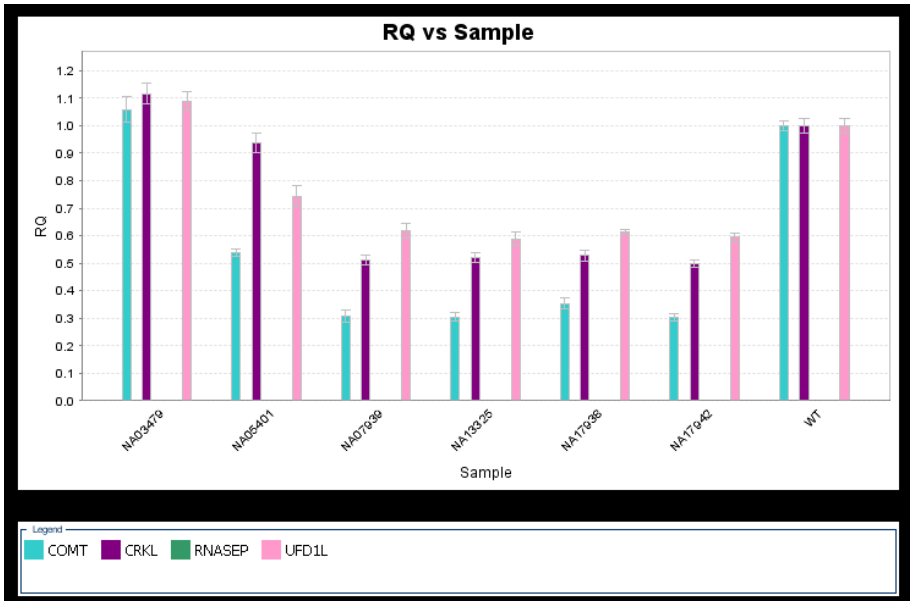

B)

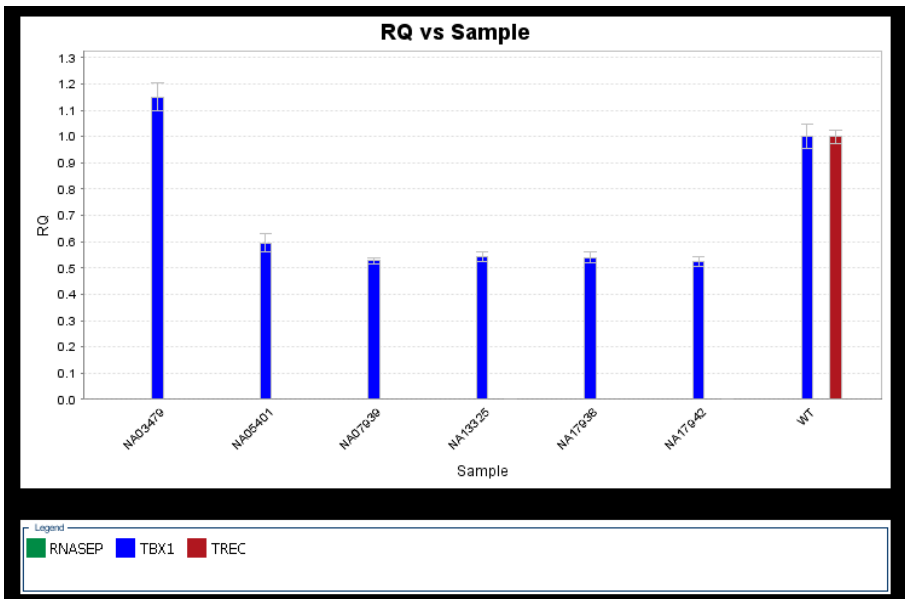

Figure 27 A-B. (A)Mean RQ values calculated for *UFD1L* (pink), *COMT* (blue) and *CRKL* (purple) in multiplex A normalized using *RNASEP* as a reference assay. (B) Mean

RQ values calculated for *TBX1*(blue) and *TREC* (red) in multiplex C. Samples were analyzed in triplicate on the ViiA 7. Error bars indicate ±1SD from the mean.

7.3.3 Statistical analysis of the multiplexed CNV assays

The values of both the RQ and RQ_{EA} calculation methods were compared by one-way ANOVA to determine if there were any statistically significant differences between the analytical methods (Appendix XVI). The P- value used to demonstrate the probability of statistically significance differences between analytical methods was >0.44 for every assay, demonstrating good correlation between the RQ numbers obtained using the classical ΔΔCq and the efficiency adjusted ΔΔCq method. Based on the results obtained through ANOVA analysis, we chose to rely on RQ values to perform further statistical analysis.

Further replicate experiments using the same samples were analyzed over several days to enable additional statistical analysis and to determine assay reproducibility. Mean, SD and CV for the RQ values were calculated for each assay (Table 21, p.134). There were no overlapping 95% CI for the normal and deletion samples amongst all of the 22q11.2 assays, demonstrating high accuracy of the copy number calculations. The mean RQ value for the normal non-deleted samples were significantly lower (0.82) for *UFD1L*, compared to those of the other deletion 22q11.2 assays within multiplex A. Assay cut-off values were determine using the area under the ROC curve (Table 22, p.134). *UFD1L* had 95.8% specificity due to a single sample outlier for NA05401, which presented as a false negative, with RQ above the ≤ 0.75 cut-off (RQ of 0.76), where as all other assay within multiplex A demonstrated 100% specificity and sensitivity.

Gaussian distribution plots located in Appendix XVII demonstrate the separate bi-modal distribution of the deletion and the normal samples, in between which the ROC cut-off values were chosen to maximize the accuracy of disease detection.

Table 21. Statistical calculations of the mean, SD, CV and 95% confidence interval calculated for each 22q11.2 copy number assays in multiplex A and C. There were no overlapping 95% CI for the WT and the deleted results indicating high accuracy of copy number quantification.

Multiplex Reaction	Assay	Result	N	Mean RQ	95% CI	SD	CV
A	*UFD1L*	WT	22	0.821	0.767 - 0.875	0.1923	0.2341
		Deletion	29	0.561	0.546 - 0.577	0.0411	0.0732
	COMT	WT	14	0.994	0.966 - 1.021	0.0475	0.0478
		Deletion	37	0.369	0.341 - 0.398	0.0866	0.2345
	CRKL	WT	22	1.13	1.085 - 1.175	0.1009	0.0892
		Deletion	29	0.561	0.546 - 0.577	0.0411	0.0732
C	*TBX1*	WT	12	1.077	1.019 - 1.134	0.0908	0.0843
		Deletion	36	0.543	0.532 - 0.554	0.0326	0.06

Table 22. Assay cut-off determination using the area under the ROC curve analysis method for which the cut-off was selected to maximize specificity and sensitivity. All assays, except for *UFD1L* had 100% specificity and sensitivity.

Multiplexed Assays	RQ Cut-Off (ROC)	Specificity	False -ve	False +ve	Sensitivity	PPV	NPV
UFD1L	≤0.75	**95.80%**	**2.6%**	**0.0%**	**100.0%**	**97.4%**	**100.0%**
COMT	≤0.56	**100%**	**0%**	**0.0%**	**100.0%**	**100%**	**100.0%**
CRKL	≤0.61	**100%**	**0%**	**0.0%**	**100.0%**	**100%**	**100.0%**

TBX1	≤0.66	**100%**	**0%**	**0.0%**	**100.0%**	**100%**	**100.0%**

7.3.4 Validation of the deletion 22q11.2 DBS QC material

DBS material spiked with immortalized B-cell cultures from line GM07939 (NA07939), GM17938 (NA17938) and GM17942 (NA17942) created from donors with 22q11.2 deletion syndrome were extracted and a WT DBS were analyzed in triplicate using multiplex C along side their liquid DNA counterparts (Figure 28, p. 136). All three DBS QC demonstrate clear hemizygous deletions of *TBX1* ranging from a mean RQ of 0.53 (GM17938) to 0.68 (GM07939). The mean RQ values were slightly higher than those of the liquid DNA controls, which had mean RQs of < 0.47.

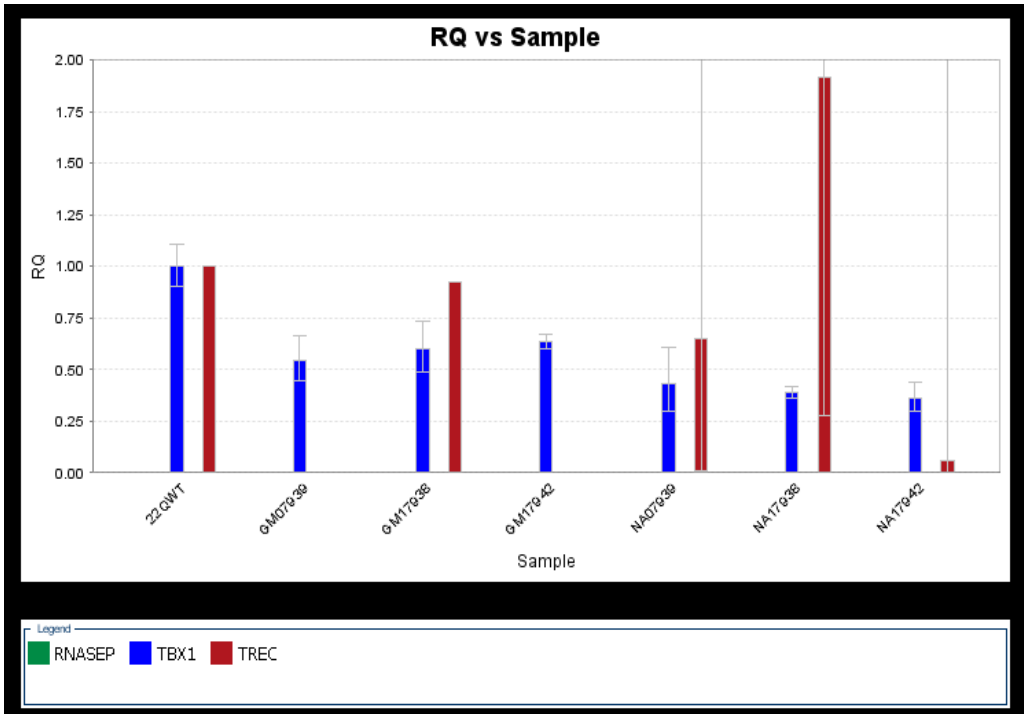

Figure 28. Mean RQ values for the 22q11.2 deletion DBS QC and the corresponding liquid DNA samples extracted from the same cell lines were calculated for *TBX1*(blue) and *TREC*(red) in multiplex C. Samples were analyzed in triplicate on the ViiA 7. Error bars indicate ±1SD from the mean.

7.3.5 Deletion 22q11.2 method comparisons

The Passing and Bablok regression revealed excellent method agreement for all three assays in multiplex A (*UFD1L, COMT* and *CRKL*) (Figure 29 A-C, p.138). Slight skewing of the regression line for *UFD1L* and *CRKL* is caused by slightly higher RQ values for the 22q11.2 deleted samples in the multiplex reaction compared to the singleplex reaction. *TBX1* also demonstrated slight regression line skewing due to lower mean RQ values using multiplex C compared to RQ value obtained by its singleplex reaction (Figure 30, p.139).

The Bland-Altman plots detected no method bias when comparing the 22q11.2 deletion assays in multiplex A and their singleplex counterparts, as the mean differences of each of the assays (Figure 29 D-F, p.138) were at or near 0 demonstrated by the solid center blue line, flanked by the 95% limits of agreement (dashed red lines).

To determine result concordance, we compared the relative quantification results obtained throughout our study for *UFD1L* and *TBX1* with those of previously published studies performed by Tomita-Mitchell *et al.* and by Kariyazono *et al.*, in which they separately multiplexed a 22q11.2 gene target and a reference gene to calculate gene copy number (Tomita-Mitchell et al., 2010). Results displayed in Table 23 (p.140) demonstrate excellent concordance with mean RQ values for the normal population and those with deletion 22q11.2 syndrome for *TBX1* and for *UFD1L* using all three platforms

investigated in this study. The assay cut-off values determined through ROC analysis are also very similar between our values and those from both independent studies.

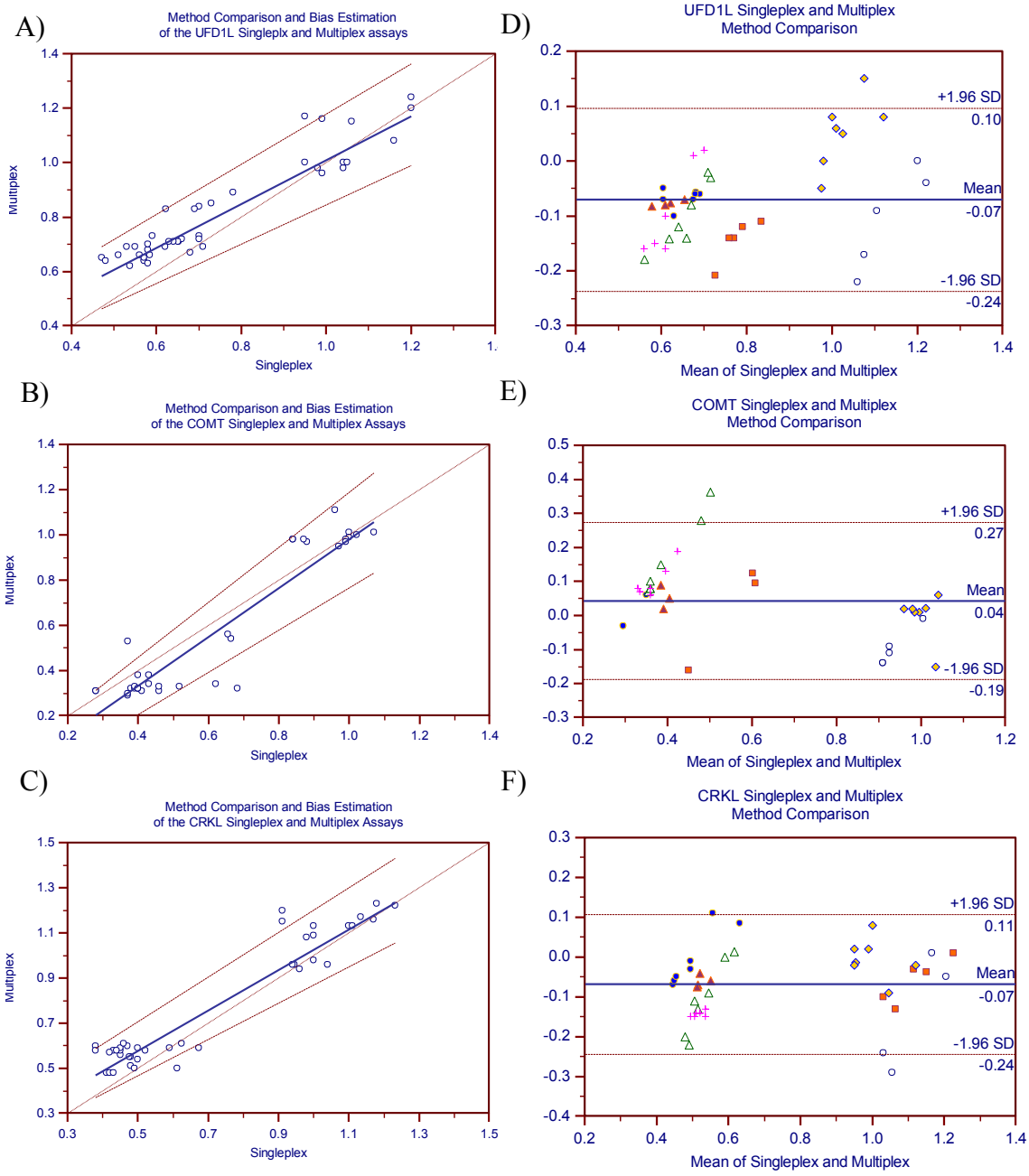

Figure 29 A-F. (A-C) Passing and Bablok regression analysis of the *UFD1L, COMT* and *CRKL* singleplex versus multiplex A. The scatter diagram shows the regression line

(solid blue line) and confidence bands (dashed red lines) (D-F) Bland-Altman plots of sample RQ values obtained from the singleplex reaction versus multiplex A Solid blue line represents the mean RQ ratio and the dashed red lines represent ±1.96 SD from the mean. Solid yellow diamonds= wild-type, open circles=NA03479, solid orange squares=NA05401, open green triangles=NA07939, solid purple triangles=NA13325, pink plus signs= NA17942 and solid blue circles=NA17938

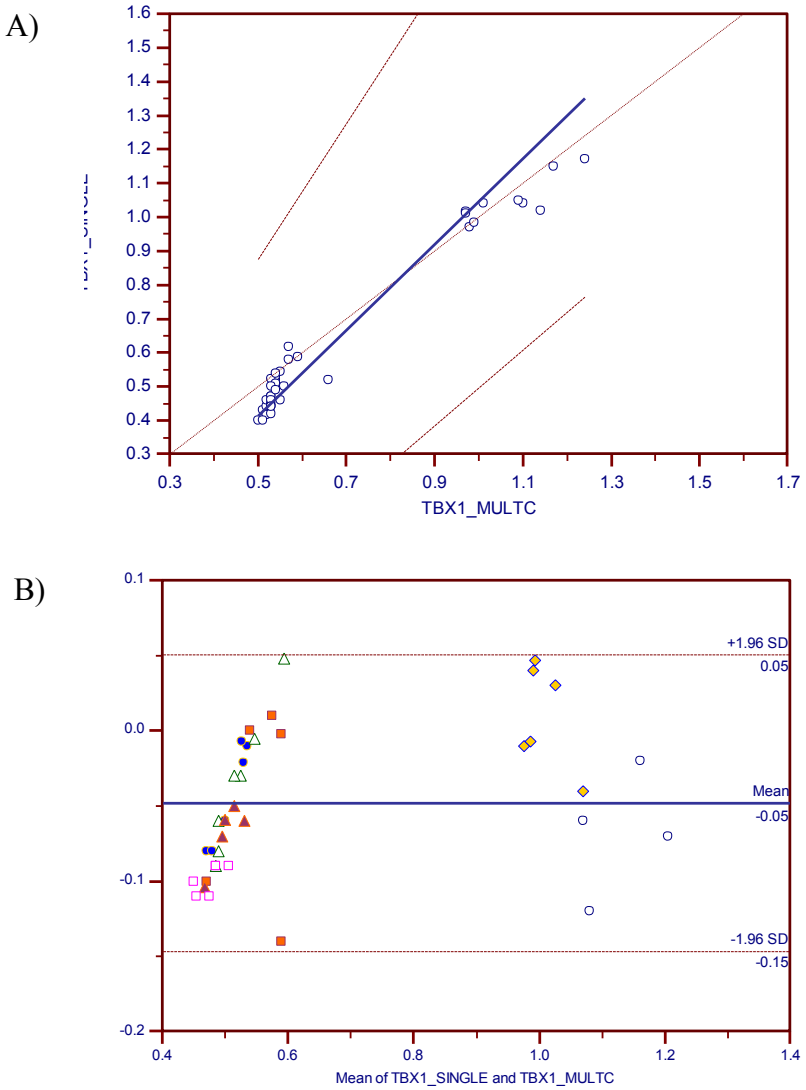

Figure 30 A-B. (A) Passing and Bablok regression analysis of the *TBX1* singleplex versus multiplex C. The scatter diagram shows the regression line (solid blue line) and confidence bands (dashed red lines) (B) Bland-Altman plots of sample RQ values obtained from the singleplex reaction versus multiplex C. Solid blue line represents the

mean RQ ratio and the dashed red lines represent ±1.96 SD from the mean. Solid yellow diamonds= wild-type, open circles=NA03479, solid orange squares=NA05401, open green triangles=NA07939, solid purple triangles=NA13325, pink plus signs= NA17942 and solid blue circles=NA17938

Table 23. Result comparison of published RQ values for TBX1 and UFD1L with those obtained in our study using analyzed in singleplex, on the OpenArray and in multiplex A and C, using RnaseP as the reference assay.

Results		N	Target	RQ Cut-off	Mean WT RQ	Mean deletion RQ
Singleplex	**This Study**	48	*UFD1L*	≤ 0.78	1.05	0.64
			TBX1	≤ 0.63	1.00	0.49
OpenArray		146	*UFD1L*	≤0.68	0.95	0.535
			TBX1	≤ 0.72	0.97	0.52
Multiplex A		48	*UFD1L*	≤ 0.75	0.82	0.56
Multiplex C		48	*TBX1*	≤ 0.66	1.07	0.54
Kariyazono *et al.*, 2001	**Published Results**	69	*UFD1L*	≤ 0.76	1.01	0.507
Tomita-Mitchel *et al.*, 2010		382	*TBX1*	≤ 0.65	1.07	0.5

7.3.6 Comparison of TREC results

We sought to compare our calibration curve results obtained using the in-house plasmid-spiked DBS with published results from other newborn screening facilities using liquid plasmid calibrators (Table 24, p.144). As expected, our slope values and amplification efficiency for the TREC-E assay closely mirrored those from the newborn screening facilities in New England, Wisconsin and California (Baker et al., 2009; Gerstel-Thompson et al., 2010). The Y-intercept values are notably higher (44.96) for the DBS calibrators compared to those obtained using liquid based plasmid calibrators (39 to 42), demonstrating both the loss of TREC plasmids during the extraction process and mild amplification inhibition caused by the presence of interfering substances in the blood.

Results for the CDC MPES samples for multiplex B and C were compared to those obtained by the singleplex reaction. The mean TREC concentrations for the normal CDC samples for the singleplex reaction and multiplex C were very similar (Figure 31, p. 143), while mean TREC concentration calculated using multiplex B were considerably lower. Such quantification differences at the upper end of the analytical range were present at the lower end, where all three assays successfully detected the SCID positive samples.

Assay cut-off values determined through ROC curve analysis were also compared, with only the New England lab demonstrating a considerably higher cut-off than those calculated for our study and those determined by the other newborn screening facilities (Table 24, p.144). ROC curves for the multiplexed TREC-E are located in Appendix XVIII. Interestingly, the singleplex TREC-E assay, based on the Dr. Comeau's assay, has cut-off values similar to those stated by the Wisconsin and California newborn screening programs, suggesting that the differences observed might be due to the use of liquid calibrators in the other laboratories. Multiplex C did not amplify any of the SCID positive CDC samples, therefore a very low cut-off of ≤ 0 was established.

The Passing and Bablok regression revealed good method agreement for both multiplex B and C (Figure 32 A-B, p.145). Slight skewing of the regression line for multiplex B is caused by slightly higher TREC concentrations noted for the singleplex reaction. The Bland-Altman plots demonstrated a fixed bias for both multiplex assays as the mean value of the differences, shown as the horizontal blue line, remains consistently greater > 0. Higher TREC concentrations were observed for the singleplex assay for all 20 CDC samples compared to the multiplex B and C, with a negative bias of nearly -122 TRECs/mL blood for multiplex C and a smaller negative bias of -38 TRECs/mL of blood (Figure 32 C-D, p.145). Such result indicated a closer concordance of quantification results between multiplex C and the singleplex reaction.

A)

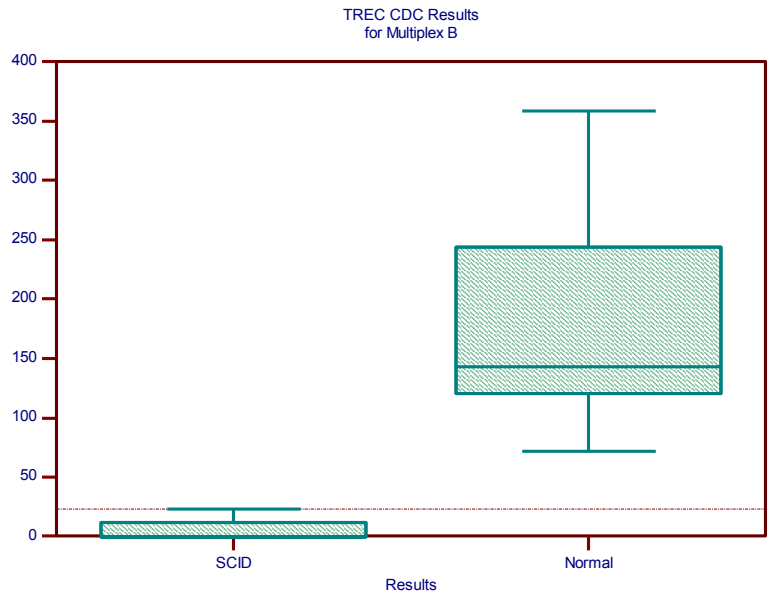
TREC CDC Results
for Multiplex B
400
350
300
250
200
150
100
50
0
SCID
Normal
Results

B)

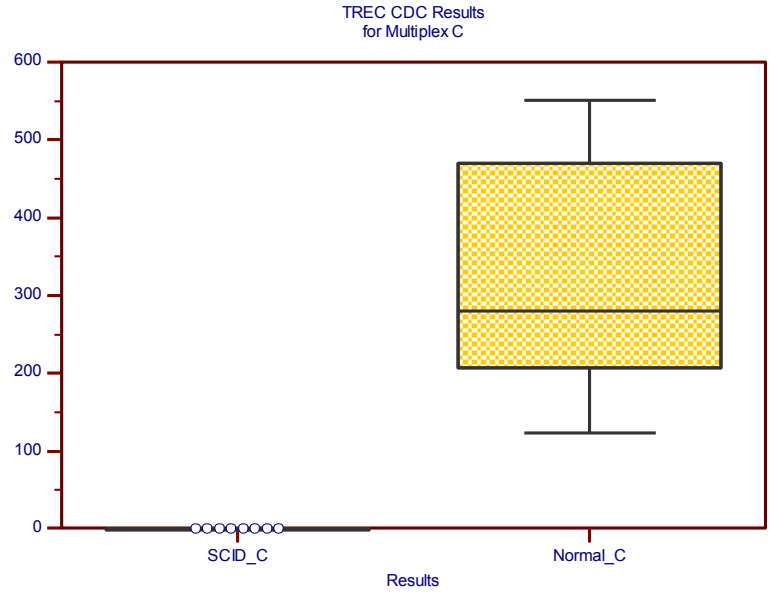
TREC CDC Results
for Multiplex C
600
500
400
300
200
100
0
SCID_C
Normal_C
Results

Figure 31 A-B. Box-and-whisker plots of the results for the CDC SCID samples using Multiplex B (A) and Multiplex C (B). The whiskers represent ± 1SD, with the centerline in each box representing the mean. The dashed orange line shows the assay cut-off for each assay.

Table 25. Data comparison of published data calculated using liquid TREC plasmid calibrators and our study using dried blood spot calibrators.

Results		N	TREC/ uL Cut-off	Mean TREC /uL	Slope	Efficiency	Y-Intercept	R^2
Singleplex	This Study	40	≤ 46	304	- 3.413	96.8%	44.96	0.924
Multiplex B		40	≤ 23	180	-3.305	100.70%	43.94	0.964
Multiplex C		40	≤ 0	324	-3.343	99.13%	45.39	0.952
New England(Gerstel-Thompson et al., 2010)	Published Results	129	≤ 252	2000	-3.35	99 .0%	39.28	0.99
Wisconsin(Baker et al., 2009)		75	≤ 30	827	-3.52	NA	41.54	0.996
California*		NA	≤ 25	742	-3.306	100.4%	42.21	0.948

NA: data not available; *presentation by Dr. Ajit Bhandal given at the SCID symposium hosted by the CDC, October 2010

A)

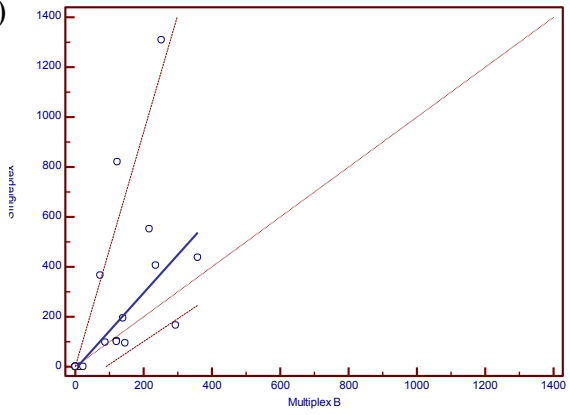
Singleplex
Multiplex B
0
200
400
600
800
1000
1200
1400

C)

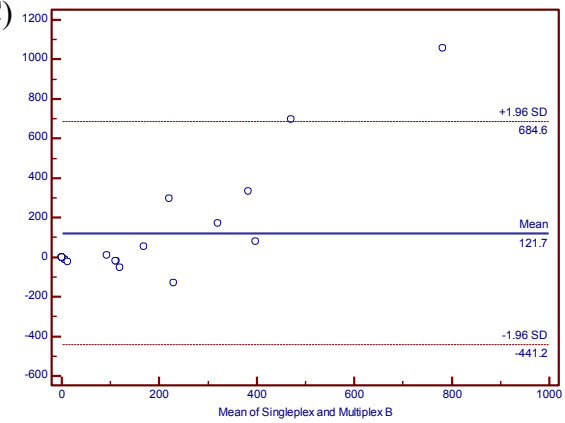
+1.96 SD
684.6
Mean
121.7
-1.96 SD
-441.2
Mean of Singleplex and Multiplex B
-600
-400
-200
0
200
400
600
800
1000
1200

B)

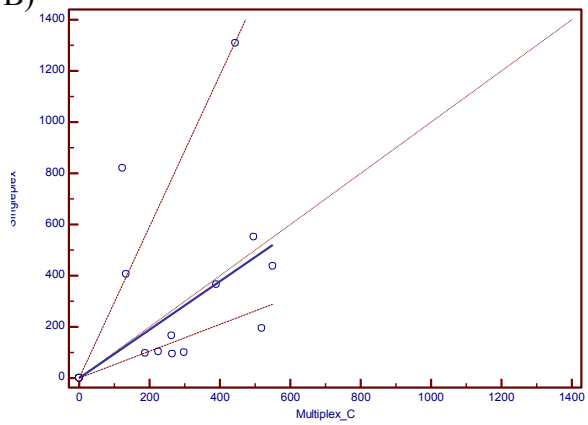
Singleplex
Multiplex_C
0
200
400
600
800
1000
1200
1400

D)

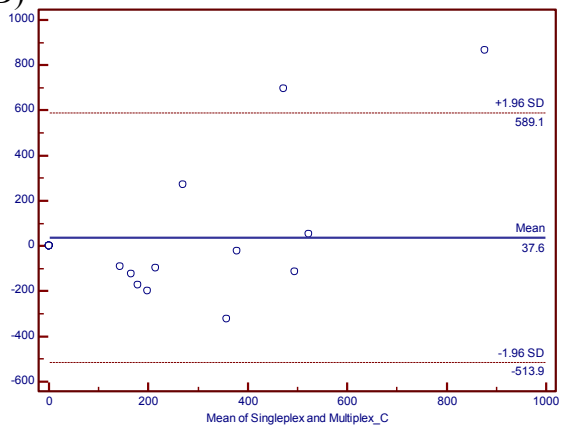
+1.96 SD
589.1
Mean
37.6
-1.96 SD
-513.9
Mean of Singleplex and Multiplex_C
-600
-400
-200
0
200
400
600
800
1000

Figure 32 A-D. (A-B) Passing and Bablok regression analysis of the TREC-E singleplex versus multiplex B (A) and multiplex C (B). The scatter diagram shows the regression line (solid blue line) and confidence bands (dashed red lines). (C-D) Bland-Altman plot of sample RQ values obtained from the TREC-E singleplex reaction versus multiplex B (C) and multiplex C (D). Solid blue line represents the mean TREC/mL concentration and the dashed red lines represent ±1.96 SD from the mean.

7.3.7 Comparison of results for the CMV QCMD samples

We wanted to compare results of the ten CMV QCMD samples analyzed with the singleplex *UL54* assay and as a multiplexed reaction with TREC-E and RnaseP to determine if the multiplex reaction would be appropriate for use in newborn screening. Multiplex B has a markedly lower sensitivity compared to the stand-alone *UL54* assay, as demonstrated by its inability to amplify both BS11-02 and BS11-09, both of which had CMV concentrations of 2500 viral copies/mL samples (Table 25, p.147). The estimated concentration of CMV viral copy number was noticeably lower for all ten QCMD samples when analyzed using multiplex B. Large variations in calculated CMV viral concentrations were noted for BS11-10, potentially caused by the uneven application of the CMV virus over-top the already dry blood spot. Uneven application would lead to variations in CMV concentration depending on the location of the 3.2 mm dried blood spot punch within the larger 50 mm blood spot. The decrease in LOD of the multiplex, when compared with the results for the singleplex *UL54*, indicated a significant loss of sensitivity. *US17* and *UL55* were precluded them from further use in multiplex reactions due to primer and probe interactions with the TREC-E assay.

Table 25. Method comparison between the singleplex and multiplexed *UL54*, which analyzed ten DBS QCMV CMV samples.

Samples	**Sample Con. Copies/mL**	**Core Proficiency**	**Singleplex *UL54* (Copies/mL)**	**Multiplexed *UL54* (Copies/mL)**
BS11-06	**0**	**Core**	0	0
BS11-04	**625**		**NA**	**NA**
BS11-07	**1 250**		2 803	**NA**
BS11-02	**2 500**	**Core**	**NA***	**NA***
BS11-09	**2 500**	**Core**	2 775	**NA***
BS11-01	**5 000**	**Core**	10 517	7 639
BS11-05	**5 000**	**Core**	12 819	7 331
BS11-08	**10 000**	**Core**	23 612	23 307
BS11-10	**10 000**	**Core**	30 309	9 749
BS11-03	**20 000**	**Core**	20 000	13 418

7.4 Discussion

We chose to label the probes with a wide selection of fluorophores and quencher molecules to prevent signal cross-talk (Table 19, p.126). As neonatal DBS contains heme and other contaminants known to inhibit qPCR reactions, we opted to use the QuantiTect Multiplex kit for our master mix. We also increased both the annealing and elongation times, which promoted the amplification of all PCR products within the multiplex, thereby increasing the overall detection limit of the combined assays similar those of the singleplex reactions. We demonstrated excellent concordance between *UFD1L, COMT* and *CRKL* in multiplex A and *TBX1* in multiplex C when compared to their singleplex counterparts (Figure 29 and 30, p.138-139) as depicted by both the Passing and Bablok regression curves and the Bland-Altman bias assessments. Limiting both primers and probes of each of the 22q11.2 assays did not hinder amplification, nor did it affect CNV detection in either multiplex A or C as established in Table 24 (p.144).

We additionally compared the *TBX1* results obtained from our study with those of the published study done by Tomita-Mitchel *et al.*(Tomita-Mitchell et al., 2010). The mean RQ values for both the normal and abnormal samples from our study were indistinguishable from those published by the Wisconsin newborn screening facility, with

the predicted assay cut-offs for our singleplex assay and multiplex C also identical to the published. A similar comparison was made between our *UFD1L* results with those obtained by Kariyazono *et al.* at Kyushu University (Japan) (Kariyazono et al., 2001). Almost identical relative quantification results were obtained from all three platforms used in our study when compared those obtained using the *UFD1L/S100β* multiplex from the published source.

The successful creation of the artificial 22q11.2 deletion QC material using washed red blood cells spiked with a B-cell culture established that CNV can accurately be detected using dried blood spots (Figure 28, p.136), as both QC material (WT and deletion control) and for future use on neonatal DBS samples in a newborn screening environment.

Results from multiplex B were lower for both the TREC and CMV targets compared to their singleplex assays, suggesting possible primer-dimmer or primer/probe interactions due to the higher concentration of both oligonucleotides needed for optimal amplification of their respective targets (Figure 32, p. 145). The CMV viral genome and TRECs are both non-genomic targets that must be amplified and detected, despite the large amount of available background DNA detected by the *RNASEP* assay, which may not be possible using a multiplex reaction. All the assays compete for dNTPs, enzyme and Mg^{+2} within the reactions, suggesting the more easily amplified *RNASEP* assay may diminish the available resources. The published mean TREC concentrations are nearly double those from our study reflecting both the wider range of normal values found in the neonatal population compared to the limited CDC samples and reflecting values calculated using liquid calibrators.

Similarly, the CMV results from multiplex B are much lower than those obtained using *UL54* as a singleplex reaction. The failure to identify the QCMD core samples using the multiplexed assay has negated its use for population-wide newborn screening newborn screening and further multiplexing studies would require the selection of a different CMV target such as *US17* or *UL55*, with the hope of increasing the lower limit of detection.

The reproducibility and accuracy of multiplex A, combining *UFD1L, COMT*, *CRKL* and *RNASEP* would make the assay quite amenable for implementation in the newborn screening program as the inclusion of additional 22q11.2 markers increasing specificity and enabling the identification of smaller deletions as well as duplications. The higher resolution multiplex identified classical 22q11.2 deletion carriers and patients carrying complex translocations involving the DGCR.

Multiplex C also demonstrates promise as a potential primary or secondary screening assay, owing to its ability to the positively identify SCID positive samples with comparable results to both the singleplex reaction and to published values, along with the capability of determining 22q11.2 deletion status. Simultaneous quantification of a disease biomarker along with the potential confirmation of one of the disease causing mutation is a novel diagnostic approach and offers a wide range of potential uses. Large-scale population studies would need to be conducted to determine the reference ranges for the normal population and for the 22q11.2 deletion syndrome infants and classical SCID positive cohorts before a definitive cut-off value can be determined.

General Discussion

8.1 Significance of results

The major focus of our study was to develop 5'-hydrolysis assays for use on the nano-fluidic OpenArray system, and in multiplexed qPCR reactions, for the future goal of implementation in the newborn screening program. Ideally, each design would decrease the costs associated with molecular diagnostics by decreasing reagent costs through multiplexing disease targets, decreasing DBS sample usage and turn-around-time. Maintaining assay sensitivity and specificity throughout development is of the utmost importance, with the goal of lowering or eliminating the possibility of false negative and false positive results.

The OpenArray system proved to be ideally suited to genomic-based assays such as SNP genotyping and CNV assay. We were able to demonstrate accurate relative gene quantification with the detection of homozygous and heterozygous deletions as well as gene duplications involved in the 22q11.2 deletion syndrome and in SMA. The platform is sensitive enough to detect as little as a 2-fold difference in amplification in as many as 54 separate assays run in parallel on a single array in less than three hours. The gene copy numbers calculated for *TBX1* and *UFD1L* on the OpenArray were quite comparable to

those of other published results using qPCR techniques (Table 23, p.144) (Tomita-Mitchell et al., 2010; Kariyazono et al., 2001). Similarly, relative quantification results for SMA on the OpenArray using donated samples with known *SMN1* and *SMN2* gene copy numbers correlated well with results obtained using MLPA (Figure 24, p.115). The use of both SNP assays and CNV assays for relative quantification is a novel use of the OpenArray platform, thus facilitating further studies on its use as a diagnostic tool in clinical laboratories.

On the other hand, assays designed to quantify non-genomic targets did not amplify samples containing lower concentrations of either TREC or CMV, indicating a significant decrease in the limit of detection and the inability to detect clinically significant lower biomarker concentrations on the OpenArray. Assays requiring absolute quantification for precise detection of sample concentrations seem to be more sensitive to DNA yield and purity as seen by the significant increase in amplification of the TREC calibrators when three DBS were used during DNA extraction, which were then further purified using spin columns (Figure 26 A-B, p.120). Therefore, we surmise that the OpenArray platform would not be viable for use in absolute quantification of very low copy number targets such as TRECs or CMV, without further concentrating DNA samples or without pre-amplification of targets prior to loading on the array. Whole genome amplification adapted from single-cell qPCR methods, would entail target specific sample amplification before loading and cycling, thereby exponentially increasing the starting template (Roberts et al., 2009). Pre-amplification would increase the probability of introducing amplification artifacts due to non-specific amplification, leading to false-positive CMV results or false-negative SCID results. Unfortunately,

concentrating filter plates and pre-amplification kits would be quite expensive to implement for large-scale population screening and would increase the turn-around-time.

Three distinct multiplexed reactions, analyzed on the ViiA 7, were created with the long-term goal of potentially being utilized in newborn screening with the motivation being the inclusion of SCID to the primary panel of screening disorders in Ontario in 2012. Multiplex A enabled the co-amplification of three deletion 22q11.2 gene targets, thereby increasing diagnostic accuracy of the assay without sacrificing sensitivity or specificity, as compared to their singleplex counterparts. Samples containing the smaller 1.5 Mb deletion were well differentiated from those with the larger 3 Mb deletion (Figure 27, p.132). The multiplexing of TREC, *UL54* and *RNASEP* in multiplex B functioned well but demonstrated a decrease in overall calculated target concentrations for both analytes. Such a decrease prevented the identification of core CMV samples with concentration < 5000 viral copies/mL (Table 25, p.147). The TREC assay mirrored the decrease in mean TREC copies/mL but was still able to accurately identify the SCID positive CDC samples (Table 24, p.144). The need to maintain the high concentration of primers and probes for both the TREC and CMV assay increases the possibility of primer-dimer and primer-probe interactions, reducing the overall amount of PCR products being produced during cycling, which could in turn affect quantification results. Multiplex C proved to be surprisingly successful, combining both relative quantification of *TBX1* using *RNASEP* as the reference assay, and absolute quantification of TRECs within a single assay. The restricted concentrations of primers and probes from the CNV assays did not hamper TREC amplification, thus allowing accurate *TBX1* copy number determination as well as TREC quantification comparable to both the singleplex assays

and to published values from numerous newborn screening laboratories. Multiplex C would enable the simultaneous SCID determination with positive identification of one of the genetic causes of the condition, possibly establishing a new trend in potential future assay design.

As the majority of the genetic diseases targeted by newborn screening are rare within the population, obtaining dried blood spot samples for use as positive controls samples is very difficult. Currently all newborn screening facilities performing qPCR for SCID and congenital CMV infection use liquid-based calibrators (Baker et al., 2009; Chan and Puck, 2005; Gerstel-Thompson et al., 2010; Morinishi et al., 2009). Possible plasmid and viral contamination in the laboratory are a real concern for high throughput diagnostic laboratories as well as the possibility of underestimating the true number of TRECs and CMV copies within a sample due to phenomenon called the matrix effect. The matrix effect is most notably referred to in the field of mass spectrometry, where the material or solution in which the target of interest is found, can affect a number of different method parameters such as limit of detection, limit of quantification, linearity, accuracy, and precision due to the presence of interfering substances, which is also applicable to qPCR techniques (Matuszewski et al., 1998; Trufelli et al., 2011). It is for these reasons that creating accurate DBS calibrators and QC material are of the utmost importance. The serially diluted in-house DBS TREC calibrators created through the addition of the TREC plasmids into TREC-free blood have proven themselves to be a stable and accurate means by which to successfully quantify TREC levels in neonatal DBS with 100% sensitivity and 100% specificity. Similarly, the serially diluted in-house CMV DBS calibrators created through the addition of the CMV Towne$_{\Delta 147}$ BAC into

CMV-free blood enabled the differentiation between infected and uninfected samples, but with divergent results compared to stated values (Table 12, p. 89). Such differences in sample concentrations may be due to use of single 3.2 mm DBS used during the study instead of the 50 mm larger spot, historically used for CMV DBS qPCR and the use of liquid calibrators for quantification (Barbi et al., 2006; Barbi et al., 2000; Binda et al., 2004; Choi et al., 2009). The creation of artificial QC material for mutation analysis through the mixing of packed red blood cells with cultured lymphocytes will enhance molecular analysis in newborn screening facilities, as obtaining considerable amounts of whole blood from individuals with SMA or deletion 22q11.2 may prove difficult and require careful ethics review. Whole blood is often applied unevenly onto the filter paper and leading to variations in DNA concentration once extracted. The artificial QC was applied in a uniform manor using precise volumes, thereby increasing the reproducibility of the results, which is extremely important when using the samples as quality indicators. Unlimited quantities of DBS material can be created and stored long-term with very little decline in sample quality if stored under appropriate laboratory conditions. The deletion 22q11.2 DBS QC material showed similar deletion RQ values compared to values calculated using liquid Coriell DNA extracted from the same cell lines (Figure 28, p.136). To completely mimic normal whole blood, macrophages and monocytes would have to be removed from the remaining red blood cells to decrease the RQ value to those of the purified Coriell samples. We were able to demonstrate relative quantification using DBS using a wild-type DBS sample as the control sample by which we were then able to detect the *Tbx1* deletions in the artificial DBS QC as well as in the liquid DNA sample.

A variety of obstacles and issues have to be addressed before selecting qPCR technologies for use in newborn screening laboratories. Many of the new analytical qPCR technologies such as digital PCR and microfluidic digital chips, have a limited sample throughput ranging from one sample to twelve samples, due to the potential of cross-contamination, which can occur when analyzing samples through a common fluidic channel (Brenan and Morrison, 2005). Analytical capacity and the elimination of potential sources of cross-contamination are extremely important in a newborn screening laboratory. Secondly, almost all nanotechnologies for quantitative PCR perform end-point fluorescence detection, amenable to SNP and CNV detection but not highly accurate for absolute quantification of viral, bacterial or plasmid targets, which require real-time collection of fluorescent data (Hilton et al., 2012; Brenan and Morrison, 2005; Dahl et al., 2007; Pak et al., 2012). Sample quality, including DNA yield and purity is also a limiting factor, with precise concentrations and considerable volume needed for many of these platforms, which is often difficult to obtain from neonatal dried blood spots (DBS). The presence of inhibiting substances as well as the smaller and highly variable amount of DNA found within a 3.2 mm DBS must be taken into account when selecting a new analytical platform. There are also intrinsic limitations to qPCR centered primarily on the limited detection capabilities of the primer and probe pairs. CNV assays, created for the purpose of detecting specific regional deletions and duplication, cannot detect small nucleotide polymorphisms or deletions/duplications outside of the primer and probe binding sites. Gene deletion syndromes, such as deletion 22q11.2, display phenotypic variability due to smaller interstitial deletions that may not be detected using single target CNV assays. SNP assays, used to detect single base-pair changes, may not

detect additional disease-causing SNPs lying upstream or downstream from the probe-binding site. In assays such as those developed for TREC and CMV detection, mutations within the probe or primer binding sites lead to amplification failure, resulting in false positive SCID result or a false negative CMV results. The heterogeneous nature of the DBS may also pose significant issues; that without the inclusion of amplification controls such as *RNASEP* or β-Actin, the lack of amplification of a target such a TREC, would lead to a false positive screen of SCID but could be simply due to poor sample quality and yield. Single-tube multiplexes and qPCR arrays that perform concurrent multi-target amplification offer solutions to many classical qPCR restrictions.

8.2 Future direction

Following the inclusion of SCID in the Ontario newborn screening panel, we are looking to develop further TREC-based multiplexed reactions. Recently, the Karolinska Institute in Stockholm, Sweden, developed a screening assay combining TRECs and κ-deleting excision circles (KRECs) to detect both T-cell and B-cell deficiencies such as X-linked agamaglobulinemia, ataxia-telanglectasia and Nijmegen-breakage syndrome (Borte et al., 2012). Creating a multiplex assay combining TREC, KREC and *RNASEP* for future use as a first-tier screening assay for primary immunodeficiency would be beneficial for the Ontario newborn screening program by increasing assay specificity through the identification of additional infants with idiopathic immunodeficiencies that would benefit from early HSCT transplant or immunoglobulin replacement therapy without entailing additional cost to the program.

The OpenArray system may be further explored at a later date for use in CNV and SNP detection as a platform for second-tier confirmatory testing of inborn errors of metabolism. Additional studies would need to be performed using neonatal dried blood spots to confirm the sensitivity and specificity of the plated assays.

We are exploring additional DNA-based technologies for inclusion in the newborn screening laboratory that offer the ability to miniaturize and to multiplex assays, such as the MassARRAY Analyzer (Sequenom) and the MiSeq system (Illumina) for targeted Next-Generation sequencing. The MassARRAY provides MALDI-TOF-based mutation and methylation detection, which will enable the development of assays for diseases such as Fragile X which have proven difficult to adapt to population-wide screening and the development of multiplexed disease panels such as those involved in sensorineural hearing loss (SNHL) (Coffee et al., 2009; Nagy et al., 2010). A hearing-loss panel developed for the OpenArray or above-mentioned instruments would complement the CMV qPCR assays related in this study with the goal of identifying neonates who may benefit from early intervention (De Keulenaer et al., 2012; Tang et al., 2012; Han et al., 2013; Linden Phillips et al., 2013). Further inclusion of high-throughput technologies with multiplexing capabilities will enable continued expansion of DNA-based screening targets.

8.3 Future implementation into the newborn screening program

Newborn Screening Ontario commenced screening for Severe Combined Immunodeficiency in August 2013, selecting the singleplex TREC-E assay as the primary SCID assay, with multiplex C selected as the second-tier confirmatory assay. The primary screening assay is used to calculate initial TREC concentrations in all neonatal

dried blood spots samples, with patients whose TREC values fall below the calculated cut-off sent for further screening confirmatory screening. The secondary screening assay confirms initial TREC concentrations and determines both *TBX1* deletion status and DNA quality using *RNASEP* as an amplification control. TREC and *TBX1* RQ reference ranges for our population were determined, after which assay cut-off values for each target were calculated, using ROC curve analysis. Dried blood spot samples from infants with known cases of SCID and deletion 22q11.2 carriers, obtained from various newborn screening centers or pulled from our archived samples, were analyzed to reconfirm assay reproducibility and sensitivity. Multiplex A is currently being employed to confirm the 22q11.2 deletion status of patients screened positive for combined SCID and *TBX1* deletion, as the high density multiplex assay includes additional 22q11.2 deletion markers, thus increasing the sensitivity of the CNV determination.

As several newborn screening facilities in the United States and around the world have pursued retrospective studies on the frequency of congenital CMV infection within their population, we are also looking at initiating a pilot project to screen for the most common causes of syndromic and non-syndromic hearing loss and as well screening for congenital CMV infection (Stehel et al., 2008; Soetens et al., 2008; Grosse et al., 2009). Both qPCR and MassArray will be used for mutation analysis and targeted quantification.

In 2011, the American College of Medical Genetics recommended the inclusion of SMA in population-based screening to begin first as an initial pilot project to access the feasibility of both the screening strategy and treatment options (Muralidharan et al., 2011). The implementation of SMA screening remains bound to the success of current clinical trials in the United States and in Canada, but at the present time, a pilot screening

project for Ontario has yet to be proposed. With more than 95% of severe denervation occurring within the first three months of life, a progressive newborn screening initiative may be the only way to demonstrate drug efficacy and prevent further neuronal loss (Prior, 2010; MacKenzie, 2012; Muralidharan et al., 2011; Ben-Shachar et al., 2011).

Conclusion

The miniaturization on the OpenArray platform and at the macro-level using multiplexed assays has proven quite successful in combining the analysis of separate DNA-based targets using a variety of quantification techniques. We developed the OpenArray for copy number detection of the deletion 22q11.2 gene targets, *DGCR2, HIRA, TBX1, UFD1L, COMT* and *CRKL*; and for the *SMN1* gene in SMA through relative quantification, employing CNV and an ASA-based SNP qPCR assays. The ability of the OpenArray to concurrently analyze up to 54 different CNV and SNP qPCR assays, using nanoliters of reagents, makes it highly amenable for screening of genomic based targets needing limited analytical range. The TREC and CMV assays did not fair well when miniaturized on the OpenArray, as the larger dynamic ranges needed to detect the clinically relevant lower concentrations could not be attained using this platform.

Lastly, we successfully quantified multiple targets for the purpose of CNV detection of a wider region of the DGCR; the quantification of both TREC and CMV viral targets; and the concomitant quantification of TREC and relative quantification of *TBX1*, in single-tube multiplexed reactions. The simultaneous quantification of different DNA-based targets using both relative and absolute quantification methods is a novel

analytical concept with potential clinical applications for other screening assays. With the creation of the singleplex TREC assay and the construction of multiplex C, Newborn Screening Ontario began neonatal SCID screening in Ontario as of August, 2013 and will continue exploring additional DNA-based techniques and high throughput technologies for future disease targets.

References

American College of Medical Genetics (ACMG) (2006). Newborn screening: toward a uniform screening panel and system. Genetics in Medicine : Official Journal of the American College of Medical Genetics. 8 Suppl 1, 1S-252S.

Afonina, I., M. Metcalf, A. Mills, et al. (2008). Evaluation of 5'-MGB hybridization probes for detection of Bordetella pertussis and Bordetella parapertussis using different real-time PCR instruments. Diagnostic Microbiology and Infectious Disease. 60, 429-432.

Agergaard, P., C. Olesen, J.R. Østergaard, et al. (2012). Chromosome 22q11.2 duplication is rare in a population-based cohort of Danish children with cardiovascular malformations. American Journal of Medical Genetics, Part A. 158 A, 509-513.

Al-Harthi, L., G. Marchetti, C.M. Steffens, et al. (2000). Detection of T cell receptor circles (TRECs) as biomarkers for de novo T cell synthesis using a quantitative polymerase chain reaction-enzyme linked immunosorbent assay (PCR-ELISA). Journal of Immunological Methods. 237, 187-197.

Alias, L., S. Bernal, M.J. Barcelo, et al. (2011). Accuracy of marker analysis, quantitative real-time polymerase chain reaction, and multiple ligation-dependent probe amplification to determine SMN2 copy number in patients with spinal muscular atrophy. Genetic Testing and Molecular Biomarkers. 15, 587-594.

Also-Rallo, E., L. Alias, R. Martinez-Hernandez, et al. (2011a). Treatment of spinal muscular atrophy cells with drugs that upregulate SMN expression reveals inter- and intra-patient variability. European Journal of Human Genetics. 19, 1059-1065.

Also-Rallo, E., L. Alías, R. Martínez-Hernández, et al. (2011b). Treatment of spinal muscular atrophy cells with drugs that upregulate SMN expression reveals inter- and intra-patient variability. European Journal of Human Genetics. 19, 1059-1065.

Al-Tamemi, S., B. Mazer, D. Mitchell, et al. (2005). Complete DiGeorge anomaly in the absence of neonatal hypocalcemia and velofacial and cardiac defects. Pediatrics. 116, e457-e460.

Anhuf, D., T. Eggermann, S. Rudnik-Schöneborn, et al. (2003). Determination of SMN1 and SMN2 copy number using TaqMan™ technology. Human Mutation. 22, 74-78.

Baker, M.W., W.J. Grossman, R.H. Laessig, et al. (2009). Development of a routine newborn screening protocol for severe combined immunodeficiency. Journal of Allergy and Clinical Immunology. 124, 522-527.

Baker, M.W., R.H. Laessig, M.L. Katcher, et al. (2010). Implementing routine testing for severe combined immunodeficiency within Wisconsin's newborn screening program. Public Health Reports. 125, 88-95.

Bales, A.M., C.A. Zaleski, and E.W. McPherson. (2010). Newborn screening programs: should 22q11 deletion syndrome be added? Genetics in Medicine : Official Journal of the American College of Medical Genetics. 12, 135-144.

Barbi, M., S. Binda, and S. Caroppo. (2006). Diagnosis of congenital CMV infection via dried blood spots. Reviews in Medical Virology. 16, 385-392.

Barbi, M., S. Binda, S. Caroppo, et al. (2003). A wider role for congenital cytomegalovirus infection in sensorineural hearing loss. Pediatric Infectious Disease Journal. 22, 39-42.

Barbi, M., S. Binda, S. Caroppo, et al. (2006a). Multicity Italian study of congenital cytomegalovirus infection. Pediatric Infectious Disease Journal. 25, 156-159.

Barbi, M., S. Binda, S. Caroppo, et al. (2006b). Neonatal screening for congenital cytomegalovirus infection and hearing loss. Journal of Clinical Virology. 35, 206-209.

Barbi, M., S. Binda, S. Caroppo, et al. (2001). CMV gB genotypes and outcome of vertical transmission: study on dried blood spots of congenitally infected babies. Journal of Clinical Virology. 21, 75-79.

Barbi, M., S. Binda, V. Primache, et al. (2000). Cytomegalovirus DNA detection in Guthrie cards: A powerful tool for diagnosing congenital infection. Journal of Clinical Virology. 17, 159-165.

Barbi, M., W.G. MacKay, S. Binda, et al. (2008). External quality assessment of cytomegalovirus DNA detection on dried blood spots. BMC Microbiology. 8, .

Bassett, A.S., D.M. McDonald-Mcginn, K. Devriendt, et al. (2011). Practical guidelines for managing patients with 22q11.2 deletion syndrome. Journal of Pediatrics. 159, 332-339.e1.

Bearden, C.E., A.F. Jawad, D.R. Lynch, et al. (2005). Effects of COMT genotype on behavioral symptomatology in the 22q11.2 Deletion Syndrome. Child Neuropsychology. 11, 109-117.

Bearden, C.E., A.F. Jawad, D.R. Lynch, et al. (2004). Effects of a functional COMT polymorphism on prefrontal cognitive function in patients with 22q11.2 deletion syndrome. American Journal of Psychiatry. 161, 1700-1702.

Ben-Shachar, S., A. Orr-Urtreger, E. Bardugo, et al. (2011). Large-scale population screening for spinal muscular atrophy: Clinical implications. Genetics in Medicine. 13, 110-114.

Bertrandy, S., P. Burlet, O. Clermont, et al. (1999). The RNA-binding properties of SMN: Deletion analysis of the zebrafish orthologue defines domains conserved in evolution. Human Molecular Genetics. 8, 775-782.

Beuten, J., T.J. Payne, J.Z. Ma, et al. (2006). Significant association of catechol-O-methyltransferase (COMT) haplotypes with nicotine dependence in male and female smokers of two ethnic populations. Neuropsychopharmacology. 31, 675-684.

Bi, W., F.J. Probst, J. Wiszniewska, et al. (2012). Co-occurrence of recurrent duplications of the digeorge syndrome region on both chromosome 22 homologues due to inherited and de novo events. Journal of Medical Genetics. 49, 681-688.

Bilio-Zulle, L. (2011). Comparison of methods: Passing and Bablok regression. Biochemia Medica. 21, 49-52.

Binda, S., S. Caroppo, P. Didò, et al. (2004). Modification of CMV DNA detection from dried blood spots for diagnosing congenital CMV infection. Journal of Clinical Virology. 30, 276-279.

Binda, S., V. Primache, S. Caroppo, et al. (1999). The typing of the HCMV strains responsible for congenital infection by molecular analysis of the UL55 gene. Annali Di Igiene : Medicina Preventiva e Di Comunita. 11, 527-531.

Bittel, D.C., S. Yu, H. Newkirk, et al. (2009). Refining the 22q11.2 deletion breakpoints in DiGeorge syndrome by aCGH. Cytogenetic and Genome Research. 124, 113-120.

Bland, J.M., and D.G. Altman. (1986). Statistical method for assessing agreement between two methods of clinical measurement. The Lancet. i:307-310.

Blennow, E., K. Lagerstedt, S. Malmgren, et al. (2008). Concurrent microdeletion and duplication of 22q11.2. Clinical Genetics. 74, 61-67.

Booth, C., H.B. Gaspar, and A.J. Thrasher. (2011). Gene therapy for primary immunodeficiency. Current Opinion in Pediatrics. 23, 659-666.

Boppana, S.B., K.B. Fowler, W.J. Britt, et al. (1999). Symptomatic congenital cytomegalovirus infection in infants born to mothers with preexisting immunity to cytomegalovirus. Pediatrics. 104, 55-60.

Boppana, S.B., K.B. Fowler, R.F. Pass, et al. (2005). Congenital cytomegalovirus infection: Association between virus burden in infancy and hearing loss. Journal of Pediatrics. 146, 817-823.

Boppana, S.B., K.B. Fowler, Y. Vaid, et al. (1997). Neuroradiographic findings in the newborn period and long-term outcome in children with symptomatic congenital cytomegalovirus infection. Pediatrics. 99, 409-414.

Boppana, S.B., L.B. Rivera, K.B. Fowler, et al. (2001). Intrauterine transmission of cytomegalovirus to infants of women with preconceptional immunity. New England Journal of Medicine. 344, 1366-1371.

Borte, S., U. Von Döbeln, A. Fasth, et al. (2012). Neonatal screening for severe primary immunodeficiency diseases using high-throughput triplex real-time PCR. Blood. 119, 2552-2555.

Borte, S., N. Wang, S. Óskarsdóttir, et al. (2011). Newborn screening for primary immunodeficiencies: Beyond SCID and XLA. Annals of the New York Academy of Sciences. 1246, 118-130.

Breckpot, J., B. Thienpont, M. Bauters, et al. (2012). Congenital heart defects in a novel recurrent 22q11.2 deletion harboring the genes CRKL and MAPK1. American Journal of Medical Genetics, Part A. 158 A, 574-580.

Brenan, C., T. Morrison, D. Roberts, et al. (2008). A nanofluidic system for massively parallel PCR. Proceedings of SPIE - the International Society for Optical Engineering. 6886, .

Brenan, C.J.H. (2002). DNA-based molecular lithography for nanoscale fabrication. IEEE Engineering in Medicine and Biology Magazine. 21, 164.

Brenan, C.J.H., D. Roberts, and J. Hurley. (2009). Nanoliter high-throughput PCR for DNA and RNA profiling. Methods in Molecular Biology. 496, 161-174.

Brenan, C., and T. Morrison. (2005). High throughput, nanoliter quantitative PCR. Drug Discovery Today: Technologies. 2, 247-253.

Brown, L., J. Xu-Bayford, Z. Allwood, et al. (2011). Neonatal diagnosis of severe combined immunodeficiency leads to significantly improved survival outcome: The case for newborn screening. Obstetrical and Gynecological Survey. 66, 398-399.

Buckley, R.H. (2011). Transplantation of hematopoietic stem cells in human severe combined immunodeficiency: Longterm outcomes. Immunologic Research. 49, 25-43.

Buckley, R.H. (2002). Primary cellular immunodeficiencies. Journal of Allergy and Clinical Immunology. 109, 747-757.

Buckley, R.H. (2000). Advances in the understanding and treatment of human severe combined immunodeficiency. Immunologic Research. 22, 237-251.

Buckley, R.H., R.I. Schiff, S.E. Schiff, et al. (1997). Human severe combined immunodeficiency: Genetic, phenotypic, and functional diversity in one hundred eight infants. Journal of Pediatrics. 130, 378-387.

Burlet, P., C. Huber, S. Bertrandy, et al. (1998). The distribution of SMN protein complex in human fetal tissues and its alteration in spinal muscular atrophy. Human Molecular Genetics. 7, 1927-1933.

Burnett, B.G., T.O. Crawford, and C.J. Sumner. (2009a). Emerging treatment options for spinal muscular atrophy. Current Treatment Options in Neurology. 11, 90-101.

Burnett, B.G., E. Muñoz, A. Tandon, et al. (2009b). Regulation of SMN protein stability. Molecular and Cellular Biology. 29, 1107-1115.

Bustin, S.A. (2010). Why the need for qPCR publication guidelines?-The case for MIQE. Methods. 50, 217-226.

Bustin, S.A., V. Benes, J.A. Garson, et al. (2009). The MIQE guidelines: Minimum information for publication of quantitative real-time PCR experiments. Clinical Chemistry. 55, 611-622.

Campbell, L., A. Potter, J. Ignatius, et al. (1997). Genomic variation and gene conversion in spinal muscular atrophy: Implications for disease process and clinical phenotype. American Journal of Human Genetics. 61, 40-50.

Candotti, F., C. Roifman, and J.M. Puck. (2006). Immunodeficiencies: Injecting some safety into SCID gene therapy? Gene Therapy. 13, 741-743.

Carlson, C., H. Sirotkin, R. Pandita, et al. (1997). Molecular definition of 22q11 deletions in 151 velo-cardio-facial syndrome patients. American Journal of Human Genetics. 61, 620-629.

Chan, K., and J.M. Puck. (2005). Development of population-based newborn screening for severe combined immunodeficiency. Journal of Allergy and Clinical Immunology. 115, 391-398.

Chan, V., B. Yip, I. Yam, et al. (2004). Carrier incidence for spinal muscular atrophy in southern Chinese. Journal of Neurology. 251, 1089-1093.

Cheeran, M.C.-., J.R. Lokensgard, and M.R. Schleiss. (2009). Neuropathogenesis of congenital cytomegalovirus infection: Disease mechanisms and prospects for intervention. Clinical Microbiology Reviews. 22, 99-126.

Chen, T.,J., Chang, Y. Yang, et al. (2010). Randomized, double-blind, placebo-controlled trial of hydroxyurea in spinal muscular atrophy. Neurology. 75, 2190-2197.

Chiang, P.-., W.-. Song, K.-. Wu, et al. (1996). Use of a fluorescent-PCR reaction to detect genomic sequence copy number and transcriptional abundance. Genome Research. 6, 1013-1026.

Choi, K.Y., L.A. Schimmenti, A.M. Jurek, et al. (2009). Detection of cytomegalovirus DNA in dried blood spots of minnesota infants who do not pass newborn hearing screening. Pediatric Infectious Disease Journal. 28, 1095-1098.

Coady, T.H., and C.L. Lorson. (2011). SMN in spinal muscular atrophy and snRNP biogenesis. Wiley Interdisciplinary Reviews: RNA. 2, 546-564.

Coffee, B., K. Keith, I. Albizua, et al. (2009). Incidence of Fragile X Syndrome by Newborn Screening for Methylated FMR1 DNA. American Journal of Human Genetics. 85, 503-514.

Coll, O., G. Benoist, Y. Ville, et al. (2009). Guidelines on CMV congenital infection. Journal of Perinatal Medicine. 37, 433-445.

Corti, S., M. Nizzardo, C. Simone, et al. (2012). Genetic correction of human induced pluripotent stem cells from patients with spinal muscular atrophy. Science Translational Medicine. 4, .

Cusco, I., M.J. Barcelo, E. Del Rio, et al. (2001). Characterisation of SMN hybrid genes in Spanish SMA patients: De novo, homozygous and compound heterozygous cases. Human Genetics. 108, 222-229.

Cusco, I., M.J. Barcelo, R. Rojas-Garcia, et al. (2006). SMN2 copy number predicts acute or chronic spinal muscular atrophy but does not account for intrafamilial variability in siblings. Journal of Neurology. 253, 21-25.

da Silva, L.R.J., M.E.S. Colovati, B. Coprerski, et al. (2013). Spinal muscular atrophy due to a "de novo" 1.3Mb deletion: Implication for genetic counseling. Neuromuscular Disorders. 23, 388-390.

Dahl, A., M. Sultan, A. Jung, et al. (2007). Quantitative PCR based expression analysis on a nanoliter scale using polymer nano-well chips. Biomedical Microdevices. 9, 307-314.

De Keulenaer, S., J. Hellemans, S. Lefever, et al. (2012). Molecular diagnostics for congenital hearing loss including 15 deafness genes using a next generation sequencing platform. BMC Medical Genomics. 5,

DeLong, E.R., D.M., DeLong, D.L. Clarke-Pearson. (1988). Comparing the areas under two or more correlated receiver operating characteristic curves: a nonparametric approach. Biometrics. 44:837-845.

Deng, J.-., Z.-. Zhang, J.-. Li, et al. (2011). Evaluation of detection and analysis of chromosome 22q11. 2 microdeletion by multiple ligation-dependent probe amplification assay. Chinese Journal of Medical Genetics. 28, 190-194.

Dhondt, J.-. (2007). Neonatal screening: From the 'Guthrie age' to the 'genetic age'. Journal of Inherited Metabolic Disease. 30, 418-422.

Dixon, J.M., M. Lubomirski, D. Amaratunga, et al. (2009). Nanoliter high-throughput RT-qPCR: A statistical analysis and assessment. BioTechniques. 46, ii-viii.

Donnelly, E.M., and N.M. Boulis. (2012). Update on gene and stem cell therapy approaches for spinal muscular atrophy. Expert Opinion on Biological Therapy. 12, 1463-1471.

Douek, D.C., R.D. McFarland, P.H. Keiser, et al. (1998). Changes in thymic function with age and during the treatment of HIV infection. Nature. 396, 690-695.

Driscoll, D.A., M.L. Budarf, and B.S. Emanuel. (1992). A genetic etiology for DiGeorge syndrome: Consistent deletions and microdeletions of 22q11. American Journal of Human Genetics. 50, 924-933.

Driscoll, D.A., J. Salvin, B. Sellinger, et al. (1993). Prevalence of 22q11 microdeletions in DiGeorge and velocardiofacial syndromes: Implications for genetic counselling and prenatal diagnosis. Journal of Medical Genetics. 30, 813-817.

Driscoll, D.A., N.B. Spinner, M.L. Budarf, et al. (1992). Deletions and microdeletions of 22q11.2 in velo-cardio-facial syndrome. American Journal of Medical Genetics. 44, 261-268.

Dunham, I., N. Shimizu, B.A. Roe, et al. (1999). The DNA sequence of human chromosome 22. Nature. 402, 489-495.

Edelmann, L., R.K. Pandita, E. Spiteri, et al. (1999). A common molecular basis for rearrangement disorders on chromosome 22q11. Human Molecular Genetics. 8, 1157-1167.

Emanuel, B.S. (2008). Molecular mechanisms and diagnosis of chromosome 22q11.2 rearrangements. Developmental Disabilities Research Reviews. 14, 11-18.

Ensenauer, R.E., A. Adeyinka, H.C. Flynn, et al. (2003). Microduplication 22q11.2, an Emerging Syndrome: Clinical, Cytogenetic, and Molecular Analysis of Thirteen Patients. American Journal of Human Genetics. 73, 1027-1040.

Er, T.-., T.-. Kan, Y.-. Su, et al. (2012). High-resolution melting (HRM) analysis as a feasible method for detecting spinal muscular atrophy via dried blood spots. Clinica Chimica Acta. 413, 1781-1785.

Farrell, M.J., H. Stadt, K.T. Wallis, et al. (1999). HIRA, a DiGeorge syndrome candidate gene, is required for cardiac outflow tract septation. Circulation Research. 84, 127-135.

Fernandes, J.F., V. Rocha, M. Labopin, et al. (2012). Transplantation in patients with SCID: Mismatched related stem cells or unrelated cord blood? Blood. 119, 2949-2955.

Fernhoff, P.M. (2009). Newborn Screening for Genetic Disorders. Pediatric Clinics of North America. 56, 505-513.

Finlayson, H. (2008). Severe combined immunodeficiency (SCID) - Advances in molecular diagnosis, neonatal screening and long-term management. Current Allergy and Clinical Immunology. 21, 20-24.

Freeman, W.M., S.J. Walker, and K.E. Vrana. (1999). Quantitative RT-PCR: Pitfalls and potential. BioTechniques. 26, 112-125.

Gaspar, H.B., K.C. Gilmour, and A.M. Jones. (2001). Severe combined immunodeficiency - Molecular pathogenesis and diagnosis. Archives of Disease in Childhood. 84, 169-173.

Gerstel-Thompson, J.L., J.F. Wilkey, J.C. Baptiste, et al. (2010). High-throughput multiplexed T-cell-receptor excision circle quantitative PCR assay with internal controls for detection of severe combined immunodeficiency in population-based newborn screening. Clinical Chemistry. 56, 1466-1474.

Griffiths, P.D., and S. Walter. (2005). Cytomegalovirus. Current Opinion in Infectious Diseases. 18, 241-245.

Grosse, S.D., S. Dollard, D.S. Ross, et al. (2009). Newborn screening for congenital cytomegalovirus: Options for hospital-based and public health programs. Journal of Clinical Virology. 46, S32-S36.

Guris, D.L., G. Duester, V.E. Papaioannou, et al. (2006). Dose-dependent interaction of Tbx1 and Crkl and locally aberrant RA signaling in a model of del22q11 syndrome. Developmental Cell. 10, 81-92.

Habbal, W., F. Monem, and B.C. Gartner. (2009). Comparative evaluation of published cytomegalovirus primers for rapid real-time PCR: Which are the most sensitive? Journal of Medical Microbiology. 58, 878-883.

Han, B., L. Zong, Q. Li, et al. (2013). Newborn genetic screening for high risk deafness-associated mutations with a new Tetra-primer ARMS PCR kit. International Journal of Pediatric Otorhinolaryngology.

Han, J.J., and C.M. McDonald. (2008). Diagnosis and Clinical Management of Spinal Muscular Atrophy. Physical Medicine and Rehabilitation Clinics of North America. 19, 661-680.

He, J., Q.-. Zhang, Q.-. Lin, et al. (2013). Molecular analysis of SMN1, SMN2, NAIP, GTF2H2, and H4F5 genes in 157 Chinese patients with spinal muscular atrophy. Gene. 518, 325-329.

Heimall, J., M. Keller, R. Saltzman, et al. (2012). Diagnosis of 22q11.2 deletion syndrome and artemis deficiency in two children with T-B-NK+ Immunodeficiency. Journal of Clinical Immunology. 32, 1141-1144.

Higuchi, R., G. Dollinger, P.S. Walsh, et al. (1992). Simultaneous amplification and detection of specific DNA sequences. Nature Biotechnology. 10, 413-417.

Hillis, S.L., N.A. Obuchowski, K.M. Schartz, et al. (2005). A comparison of the Dorfman-Berbaum-Metz and Obuchowski-Rockette methods for receiver operating characteristic (ROC) data. Statistics in Medicine. 24, 1579-1607.

Hilton, J.P., T. Nguyen, M. Barbu, et al. (2012). Bead-based polymerase chain reaction on a microchip. Microfluidics and Nanofluidics. 13, 749-760.

Iannaccone, S.T., S.A. Smith, and L.R. Simard. (2004). Spinal muscular atrophy. Current Neurology and Neuroscience Reports. 4, 74-80.

Jablonka, S., and M. Sendtner. (2003). Molecular and cellular basis of spinal muscular atrophy. Amyotrophic Lateral Sclerosis and Other Motor Neuron Disorders. 4, 144-149.

Jakubikova, J., Z. Kabatova, G. Pavlovcinova, et al. (2009). Newborn hearing screening and strategy for early detection of hearing loss in infants. International Journal of Pediatric Otorhinolaryngology. 73, 607-612.

Jalali, G.R., J.A.S. Vorstman, A. Errami, et al. (2008). Detailed analysis of 22q11.2 with a high density MLPA probe set. Human Mutation. 29, 433-440.

Jones, C.H., and M.J. Gawronski. (2002). The genetics of 22q11.2 deletion syndrome. Progress in Pediatric Cardiology. 15, 99-101.

Just, H.L., M. Deleuran, C. Vestergaard, et al. (2008). T-cell receptor excision circles (TREC) in CD4+ and CD8 + T-cell subpopulations in atopic dermatitis and psoriasis show major differences in the emission of recent thymic emigrants. Acta Dermato-Venereologica. 88, 566-572.

Kariyazono, H., T. Ohno, K. Ihara, et al. (2001). Rapid detection of the 22q11.2 deletion with quantitative real-time PCR. Molecular and Cellular Probes. 15, 71-73.

Kelly, D., R. Goldberg, D. Wilson, et al. (1993). Confirmation that the velo-cardio-facial syndrome is associated with haplo-insufficiency of genes at chromosome 22q11. American Journal of Medical Genetics. 45, 308-312.

Kersseboom, R., A. Brooks, and C. Weemaes. (2011). Educational paper : Syndromic forms of primary immunodeficiency. European Journal of Pediatrics. 170, 295-308.

Kishore, R., W. Reef Hardy, V.J. Anderson, et al. (2006). Optimization of DNA extraction from low-yield and degraded samples using the BioRobot® EZ1 and BioRobot® M48. Journal of Forensic Sciences. 51, 1055-1061.

Knutsen, A.P., M.W. Baker, and M.L. Markert. (2011). Interpreting low T-cell receptor excision circles in newborns with DiGeorge anomaly: Importance of assessing naive T-cell markers. Journal of Allergy and Clinical Immunology. 128, 1375-1376.

Korver, A.M.H., J.J.C. de Vries, S. Konings, et al. (2009). DECIBEL study: Congenital cytomegalovirus infection in young children with permanent bilateral hearing impairment in the Netherlands. Journal of Clinical Virology. 46, S27-S31.

Kutyavin, I., S. Lokhov, E. Lukhtanov, et al. (2003). Chemistry of minor groove binder-oligonucleotide conjugates. Current Protocols in Nucleic Acid Chemistry / Edited by Serge L.Beaucage ...[Et Al.]. Chapter 8, .

Kutyavin, I.V., I.A. Afonina, A. Mills, et al. (2000). 3'-Minor groove binder-DNA probes increase sequence specificity at PCR extension temperatures. Nucleic Acids Research. 28, 655-661.

Laczmanska, I., K. Pesz, and L. Laczmanski. (2009). Application of selected methods based on the polymerase chain reaction in medical molecular diagnostics. Advances in Clinical and Experimental Medicine. 18, 85-92.

Lee, T.-., S.-. Kim, K.-. Lee, et al. (2004). Quantitative analysis of SMN1 gene and estimation of SMN1 deletion carrier frequency in korean population based on real-time PCR. Journal of Korean Medical Science. 19, 870-873.

Lefebvre, S., L. Burglen, S. Reboulliet, et al. (1997a). Identification and characterization of a spinal muscular atrophy- determining gene; Genetic mapping of chronic childhood-onset spinal muscular atrophy to chromosome 5q11.2-13.3; Proceedings of the National Academy of Sciences of the United States of America. 80; 344- 348.

Lefebvre, S., P. Burlet, Q. Liu, et al. (1997b). Correlation between severity and SMN protein level in spinal muscular atrophy. Nature Genetics. 16, 265-269.

Li, L., D.L. Guris, M. Okura, et al. (2003). Translocation of CrkL to focal adhesions mediates integrin-induced migration downstream of Src family kinases. Molecular and Cellular Biology. 23, 2883-2892.

Lima, K., T.G. Abrahamsen, I. Foelling, et al. (2010a). Low thymic output in the 22q11.2 deletion syndrome measured by CCR9 +CD45RA+ T cell counts and T cell receptor rearrangement excision circles. Clinical and Experimental Immunology. 161, 98-107.

Lima, K., I. Følling, K.L. Eiklid, et al. (2010b). Age-dependent clinical problems in a Norwegian national survey of patients with the 22q11.2 deletion syndrome. European Journal of Pediatrics. 169, 983-989.

Lin, Z., J.G. Suzow, J.M. Fontaine, et al. (2005). A simple automated DNA extraction method for dried blood specimens collected on filter paper. Journal of the Association of Laboratory Automation. 10, 310-314.

Linden Phillips, L., M. Bitner-Glindzicz, N. Lench, et al. (2013). The future role of genetic screening to detect newborns at risk of childhood-onset hearing loss. International Journal of Audiology. 52, 124-133.

Lipstein, E.A., S. Vorono, M.F. Browning, et al. (2010). Systematic evidence review of newborn screening and treatment of severe combined immunodeficiency. Pediatrics. 125, e1226-e1235.

Liu, H.-., N. Ramalingam, Y. Jiang, et al. (2009). Rapid distribution of a liquid column into a matrix of nanoliter wells for parallel real-time quantitative PCR. Sensors and Actuators, B: Chemical. 135, 671-677.

Livak, K.J., and T.D. Schmittgen. (2001). Analysis of Relative Gene Expression Data Using Real-Time Quantitative PCR and the $2-\Delta\Delta CT$ Method. Methods. 25, 402-408.

Lombardi, G., F. Garofoli, P. Villani, et al. (2009). Oral valganciclovir treatment in newborns with symptomatic congenital cytomegalovirus infection. European Journal of Clinical Microbiology and Infectious Diseases. 28, 1465-1470.

Lorson, C.L., J. Strasswimmer, J.-. Yao, et al. (1998). SMN oligomerization defect correlates with spinal muscular atrophy severity. Nature Genetics. 19, 63-66.

Lunn, M.R., and C.H. Wang. (2008). Spinal muscular atrophy. The Lancet. 371, 2120-2133.

Machida, U., M. Kami, T. Fukui, et al. (2000). Real-time automated PCR for early diagnosis and monitoring of cytomegalovirus infection after bone marrow transplantation. Journal of Clinical Microbiology. 38, 2536-2542.

MacKenzie, A. (2012). Sense in antisense therapy for spinal muscular atrophy. New England Journal of Medicine. 366, 761-763.

MacKenzie, A. (2010). Genetic therapy for spinal muscular atrophy. Nature Biotechnology. 28, 235-237.

Magnaghi, P., C. Roberts, S. Lorain, et al. (1998). HIRA, a mammalian homologue of saccharomyces cerevisiae transcriptional co-repressors, interacts with Pax3. Nature Genetics. 20, 74-77.

Markert, M.L., D.S. Hummel, H.M. Rosenblatt, et al. (1998). Complete DiGeorge syndrome: Persistence of profound immunodeficiency. Journal of Pediatrics. 132, 15-21.

Markowitz, J.A., M.B. Tinkle, and K.H. Fischbeck. (2004). Spinal muscular atrophy in the neonate. JOGNN - Journal of Obstetric, Gynecologic, and Neonatal Nursing. 33, 12-20.

Matsubara, Y., K. Kerman, M. Kobayashi, et al. (2004). On-chip nanoliter-volume multiplex TaqMan polymerase chain reaction from a single copy based on counting fluorescence released microchambers. Analytical Chemistry. 76, 6434-6439.

Matuszewski, B.K., M.L. Constanzer, and C. Chavez-Eng. (1998). Matrix Effect in Quantitative LC/MS/MS Analyses of Biological Fluids: A Method for Determination of Finasteride in Human Plasma at Picogram Per Milliliter Concentrations. Analytical Chemistry. 70, 882-889.

Maynard, T.M., D. Gopalakrishna, D.W. Meechan, et al. (2013). 22q11 Gene dosage establishes an adaptive range for sonic hedgehog and retinoic acid signaling during early development. Human Molecular Genetics. 22, 300-312.

McDonald-McGinn, D., S. Fahiminiya, T. Revil, et al. (2013). Hemizygous mutations in SNAP29 unmask autosomal recessive conditions and contribute to atypical findings in patients with 22q11.12Ds. Journal of Medical Genetics. 50, 80-90.

McDonald-McGinn, D.M., D. LaRossa, E. Goldmuntz, et al. (1997). The 22q11.2 deletion: Screening, diagnostic workup, and outcome of results; report on 181 patients. Genetic Testing. 1, 99-108.

McDonald-Mcginn, D.M., and K.E. Sullivan. (2011). Chromosome 22q11.2 deletion syndrome (DiGeorge syndrome/velocardiofacial syndrome). Medicine. 90, 1-18.

Meechan, D.W., T.M. Maynard, Y. Wu, et al. (2006). Gene dosage in the developing and adult brain in a mouse model of 22q11 deletion syndrome. Molecular and Cellular Neuroscience. 33, 412-428.

Meechan, D.W., E.S. Tucker, T.M. Maynard, et al. (2009). Diminished dosage of 22q11 genes disrupts neurogenesis and cortical development in a mouse model of 22q11 deletion/DiGeorge syndrome. Proceedings of the National Academy of Sciences of the United States of America. 106, 16434-16445.

Moon, A.M., D.L. Guris, J. Seo, et al. (2006). Crkl deficiency disrupts Fgf8 signaling in a mouse model of 22q11 deletion syndromes. Developmental Cell. 10, 71-80.

Morinishi, Y., K. Imai, N. Nakagawa, et al. (2009). Identification of severe combined immunodeficiency by T-cell receptor excision circles quantification using neonatal Guthrie cards. Journal of Pediatrics. 155, 829-833.

Morrison, T., J. Hurley, J. Garcia, et al. (2006). Nanoliter high throughput quantitative PCR. Nucleic Acids Research. 34, .

Mulder, M.P., M. Wilke, A. Langeveld, et al. (1995). Positional mapping of loci in the DiGeorge critical region at chromosome 22q11 using a new marker (D22S183). Human Genetics. 96, 133-141.

Muralidharan, K., R.B. Wilson, S. Ogino, et al. (2011). Population Carrier Screening for Spinal Muscular Atrophy: A Position Statement of the Association for Molecular Pathology. The Journal of Molecular Diagnostics. 13, 3-6.

Nagy, A.L., R. Csáki, J. Klem, et al. (2010). Minimally invasive genetic screen for GJB2 related deafness using dried blood spots. International Journal of Pediatric Otorhinolaryngology. 74, 75-81.

Obuchowski, N.A. (2006). An ROC-type measure of diagnostic accuracy when the gold standard is continuous-scale. Statistics in Medicine. 25, 481-493.

Obuchowski, N.A., M.L. Lieber, and F.H. Wians Jr. (2004). ROC curves in Clinical Chemistry: Uses, misuses, and possible solutions. Clinical Chemistry. 50, 1118-1125.

Óskarsdóttir, S., C. Persson, B.O. Eriksson, et al. (2005). Presenting phenotype in 100 children with the 22q11 deletion syndrome. European Journal of Pediatrics. 164, 146-153.

Óskarsdóttir, S., M. Vujic, and A. Fasth. (2004). Incidence and prevalence of the 22q11 deletion syndrome: A population-based study in Western Sweden. Archives of Disease in Childhood. 89, 148-151.

Oskoui, M., and P. Kaufmann. (2008). Spinal Muscular Atrophy. Neurotherapeutics. 5, 499-506.

Oskoui, M., G. Levy, C.J. Garland, et al. (2007). The changing natural history of spinal muscular atrophy type 1. Neurology. 69, 1931-1936.

Pak, N., D.C. Saunders, C.R. Phaneuf, et al. (2012). Plug-and-play, infrared, laser-mediated PCR in a microfluidic chip. Biomedical Microdevices. 14, 427-433.

Passing, H., and W. Bablok. (1983). A new biometric procedure for testing the equality of measurements from two different analytical methods. Application of linear regression procedures for method comparison studies in Clinical Chemistry, Part I. Journal of Clinical Chemistry and Clinical Biochemistry. 21:709-720.

Pizzuti, A., G. Novelli, A. Ratti, et al. (1997). UFD1L, a developmentally expressed ubiquitination gene, is deleted in CATCH 22 syndrome. Human Molecular Genetics. 6, 259-265.

Prior, T.W. (2010). Spinal muscular atrophy: A time for screening. Current Opinion in Pediatrics. 22, 696-702.

Prior, T.W. (2007). Spinal muscular atrophy diagnostics. Journal of Child Neurology. 22, 952-956.

Prior, T.W., N. Nagan, E.A. Sugarman, et al. (2011). Technical standards and guidelines for spinal muscular atrophy testing. Genetics in Medicine. 13, 686-694.

Prior, T.W., P.J. Snyder, B.D. Rink, et al. (2010). Newborn and carrier screening for spinal muscular atrophy. American Journal of Medical Genetics, Part A. 152, 1608-1616.

Puck, J.M. (2012). Laboratory technology for population-based screening for severe combined immunodeficiency in neonates: The winner is T-cell receptor excision circles. Journal of Allergy and Clinical Immunology. 129, 607-616.

Puck, J.M. (2011). The case for newborn screening for severe combined immunodeficiency and related disorders. Annals of the New York Academy of Sciences. 1246, 108-117.

Puck, J.M. (2007). Neonatal screening for severe combined immune deficiency. Current Opinion in Allergy and Clinical Immunology. 7, 522-527.

Pyatt, R.E., D.C. Mihal, and T.W. Prior. (2007). Assessment of liquid microbead arrays for the screening of newborns for spinal muscular atrophy. Clinical Chemistry. 53, 1879-1885.

Rauch, A., S. Zink, C. Zweier, et al. (2005). Systematic assessment of atypical deletions reveals genotype-phenotype correlation in 22q11.2. Journal of Medical Genetics. 42, 871-876.

Roberts, D.G., T.B. Morrison, S.N. Liu-Cordero, et al. (2009). A nanoliter fluidic platform for large-scale single nucleotide polymorphism genotyping. BioTechniques. 46, ix-xiii.

Russman, B.S. (2007). Spinal muscular atrophy: Clinical classification and disease heterogeneity. Journal of Child Neurology. 22, 946-951.

Saito, T., D.F. Papolos, D. Chernak, et al. (1999). Analysis of GNAZ gene polymorphism in bipolar affective disorder. American Journal of Medical Genetics - Neuropsychiatric Genetics. 88, 324-328.

Saitta, S.C., S.E. Harris, D.M. McDonald-McGinn, et al. (2004). Independent De Novo 22q11.2 Deletions in First Cousins with DiGeorge/Velocardiofacial Syndrome. American Journal of Medical Genetics. 124 A, 313-317.

Sanchez, J.L., and G.A. Storch. (2002). Multiplex, quantitative, real-time PCR assay for cytomegalovirus and human DNA. Journal of Clinical Microbiology. 40, 2381-2386.

Sanghavi, S.K., K. Abu-Elmagd, M.C. Keightley, et al. (2008). Relationship of cytomegalovirus load assessed by real-time PCR to pp65 antigenemia in organ transplant recipients. Journal of Clinical Virology. 42, 335-342.

Scambler, P.J., D. Kelly, E. Lindsay, et al. (1992). Velo-cardio-facial syndrome associated with chromosome 22 deletions encompassing the DiGeorge locus. Lancet. 339, 1138-1139.

Scanga, L., S. Chaing, C. Powell, et al. (2006). Diagnosis of human congenital cytomegalovirus infection by amplification of viral DNA from dried blood spots on perinatal cards. Journal of Molecular Diagnostics. 8, 240-245.

Schulze, A., M. Lindner, D. Kohlmüller, et al. (2003). Expanded newborn screening for inborn errors of metabolism by electrospray ionization-tandem mass spectrometry: Results, outcome, and implications. Pediatrics. 111, 1399-1406.

Seymour, C.A., M.J. Thomason, R.A. Chalmers, et al. (1997). Newborn screening for inborn errors of metabolism: a systematic review. Health Technology Assessment (Winchester, England). 1, i-iv, 1-95.

Shaikh, T.H., H. Kurahashi, and B.S. Emanuel. (2001). Evolutionarily conserved low copy repeats (LCRs) in 22q11 mediate deletions, duplications, translocations, and genomic instability: An update and literature review. Genetics in Medicine. 3, 6-13.

Shaikh, T.H., H. Kurahashi, S.C. Saitta, et al. (2000). Chromosome 22-specific low copy repeats and the 22q11.2 deletion syndrome: Genomic organization and deletion endpoint analysis. Human Molecular Genetics. 9, 489-501.

Shaw, K.J., L. Thain, P.T. Docker, et al. (2009). The use of carrier RNA to enhance DNA extraction from microfluidic-based silica monoliths. Analytica Chimica Acta. 652, 231-233.

Shen, F., W. Du, E.K. Davydova, et al. (2010). Nanoliter multiplex pcr arrays on a slipchip. Analytical Chemistry. 82, 4606-4612.

Soetens, O., C. Vauloup-Fellous, I. Foulon, et al. (2008). Evaluation of different cytomegalovirus (CMV) DNA PCR protocols for analysis of dried blood spots from consecutive cases of neonates with congenital CMV infections. Journal of Clinical Microbiology. 46, 943-946.

Sorensen, K.M., P.S. Andersen, L.A. Larsen, et al. (2008). Multiplex ligation-dependent probe amplification technique for copy number analysis on small amounts of DNA material. Analytical Chemistry. 80, 9363-9368.

Stedtfeld, R.D., S.W. Baushke, D.M. Tourlousse, et al. (2008). Development and experimental validation of a predictive threshold cycle equation for quantification of virulence and marker genes by high-throughput nanoliter-volume PCR on the OpenArray platform. Applied and Environmental Microbiology. 74, 3831-3838.

Stehel, E.K., A.G. Shoup, K.E. Owen, et al. (2008). Newborn hearing screening and detection of congenital cytomegalovirus infection. Pediatrics. 121, 970-975.

Stuppia, L., I. Antonucci, G. Palka, et al. (2012). Use of the MLPA assay in the molecular diagnosis of gene copy number alterations in human genetic diseases. International Journal of Molecular Sciences. 13, 3245-3276.

Sullivan, K.E. (2008). Chromosome 22q11.2 Deletion Syndrome: DiGeorge Syndrome/Velocardiofacial Syndrome. Immunology and Allergy Clinics of North America. 28, 353-366.

Tang, W., D. Qian, S. Ahmad, et al. (2012). A low-cost exon capture method suitable for large-scale screening of genetic deafness by the massively-parallel sequencing approach. Genetic Testing and Molecular Biomarkers. 16, 536-542.

Tapia, O., R. Bengoechea, A. Palanca, et al. (2012). Reorganization of Cajal bodies and nucleolar targeting of coilin in motor neurons of type i spinal muscular atrophy. Histochemistry and Cell Biology. 137, 657-667.

Tarini, B.A., D.A. Christakis, and H.G. Welch. (2006). State newborn screening in the tandem mass spectrometry era: More tests, more false-positive results. Pediatrics. 118, 448-456.

Therrell Jr., B.L., C. Buechner, M.A. Lloyd-Puryear, et al. (2008). What's new in newborn screening? Pediatric Health. 2, 411-429.

Tichopad, A., M. Dilger, G. Schwarz, et al. (2003). Standardized determination of real-time PCR efficiency from a single reaction set-up. Nucleic Acids Research. 31, .

Tizzano, E.F., C. Cabot, and M. Baiget. (1998). Cell-specific survival motor neuron gene expression during human development of the central nervous system: Implications for the pathogenesis of spinal muscular atrophy. American Journal of Pathology. 153, 355-361.

Tomita-Mitchell, A., D.K. Mahnke, J.M. Larson, et al. (2010). Multiplexed quantitative real-time PCR to detect 22q11.2 deletion in patients with congenital heart disease. Physiological Genomics. 42 A, 52-60.

Tong, Y., W. Tang, H.-. Kim, et al. (2008). Development of isothermal TaqMan assays for detection of biothreat organisms. BioTechniques. 45, 543-557.

Trufelli, H., P. Palma, G. Famiglini, et al. (2011). An overview of matrix effects in liquid chromatography-mass spectrometry. Mass Spectrometry Reviews. 30, 491-509.

Van Doorn, R., M.M. Klerks, M.P.E. Van Gent-Pelzer, et al. (2009). Accurate quantification of microorganisms in PCR-inhibiting environmental DNA extracts by a novel internal amplification control approach using Biotrove OpenArrays. Applied and Environmental Microbiology. 75, 7253-7260.

van Doorn, R., M. Szemes, P. Bonants, et al. (2007). Quantitative multiplex detection of plant pathogens using a novel ligation probe-based system coupled with universal, high-throughput real-time PCR on OpenArrays™ . BMC Genomics. 8, .

Verbsky, J.W., M.W. Baker, W.J. Grossman, et al. (2011). Newborn Screening for Severe Combined Immunodeficiency; The Wisconsin Experience (2008-2011). Journal of Clinical Immunology.1-7.

Verhagen, J.M., K.E. Diderich, G. Oudesluijs, et al. (2012). Phenotypic variability of atypical 22q11.2 deletions not including TBX1. American Journal of Medical Genetics, Part A. 158 A, 2412-2420.

Vorstman, J.A.S., G.R. Jalali, E.F. Rappaport, et al. (2006). MLPA: A rapid, reliable, and sensitive method for detection and analysis of abnormalities of 22q. Human Mutation. 27, 814-821.

Walter, S., C. Atkinson, M. Sharland, et al. (2008). Congenital cytomegalovirus: Association between dried blood spot viral load and hearing loss. Archives of Disease in Childhood: Fetal and Neonatal Edition. 93, F280-F285.

Wang, W., C.E. Patterson, S. Yang, et al. (2004). Coupling generation of cytomegalovirus deletion mutants and amplification of viral BAC clones. Journal of Virological Methods. 121, 137-143.

Watterson, J.H., S. Raha, C.C. Kotoris, et al. (2004). Rapid detection of single nucleotide polymorphisms associated with spinal muscular atrophy by use of a reusable fibre-optic biosensor. Nucleic Acids Research. 32, .

Wee, C.D., L. Kong, and C.J. Sumner. (2010). The genetics of spinal muscular atrophies. Current Opinion in Neurology. 23, 450-458.

Weisfeld-Adams, J., L. Edelmann, I.K. Gadi, et al. (2012). Phenotypic heterogeneity in a family with a small atypical microduplication of chromosome 22q11.2 involving TBX1. European Journal of Medical Genetics. 55, 732-736.

Whelan, J.A., N.B. Russell, and M.A. Whelan. (2003). A method for the absolute quantification of cDNA using real-time PCR. Journal of Immunological Methods. 278, 261-269.

Wilming, L.G., C.A.S. Snoeren, A. Van Rijswijk, et al. (1997). The murine homologue of HIRA, a DiGeorge syndrome candidate gene, is expressed in embryonic structures affected in human CATCH22 patients. Human Molecular Genetics. 6, 247-258.

Wilson, J.M., and Y.G. Jungner. (1968). Principles and practice of mass screening for disease. Boletin De La Oficina Sanitaria Panamericana. 65, 281-393.

Yagi, H., Y. Furutani, H. Hamada, et al. (2003). Role of TBX1 in human del22q11.2 syndrome. Lancet. 362, 1366-1373.

Yamanaka, K.-., N. Yawalkar, D.A. Jones, et al. (2005). Decreased T-cell receptor excision circles in cutaneous T-cell lymphoma. Clinical Cancer Research. 11, 5748-5755.

Yobb, T.M., M.J. Somerville, L. Willatt, et al. (2005). Microduplication and triplication of 22q11.2: A highly variable syndrome. American Journal of Human Genetics. 76, 865-876.

Yu, Y., B. Li, C.A. Baker, et al. (2012). Quantitative polymerase chain reaction using infrared heating on a microfluidic chip. Analytical Chemistry. 84, 2825-2829.

Yuan, J.S., J. Burris, N.R. Stewart, et al. (2007). Statistical tools for transgene copy number estimation based on real-time PCR. BMC Bioinformatics. 8,

Yuan, J.S., D. Wang, and C.N. Stewart Jr. (2008). Statistical methods for efficiency adjusted real-time PCR quantification. Biotechnology Journal. 3, 112-123.

Zweygberg Wirgart, B., M. Brytting, A. Linde, et al. (1998). Sequence variation within three important cytomegalovirus gene regions in isolates from four different patient populations. Journal of Clinical Microbiology. 36, 3662-3669.

Appendix I A-B. Statistical equations for calculating both classical relative gene copy number quantification (ΔΔCq method) and the efficiency-adjusted quantification (RQE_A)

A) The following Livak ΔΔCq calculation (Livak and Schmittgen, 2001) was employed to derive the gene copy number:

Delta Cq (ΔCq) =
(Cq $_{ROI}$ patient - Cq $_{RNASEP}$ patient) and (Cq $_{ROI}$ Control- Cq $_{RNASEP}$ Control)

Delta Delta Cq (ΔΔCq) = ΔCq Patient – ΔCq Control

Relative Gene Copy Number (RQ) = $\mathbf{2^{-\Delta\Delta Cq}}$

$$= \mathbf{2^{-(\Delta Cq\ Patient\ -\ \Delta Cq\ Control)}}$$

B) The following Efficiency Adjusted ΔΔ Cq ($\Delta\Delta Cq_{EA}$) calculation was used to derive the relative gene copy number (Yuan et al., 2008):

(E_{ROI} * Cq ROI Patient - E_{RNASEP} * Cq $_{RNASEP}$ Patient) - (Cq E_{ROI} * ROI Control - E_{Rnasep} * Cq $_{RNASEP}$ Control)

Efficiency Adjusted Relative Gene Copy Number (RQ_{EA}) = $2^{-\Delta\Delta CqEA}$

; where E is the individual amplification efficiency set between 0 and 1 calculated by way of the calibration curves run during the initial validation; and where Cq represents the quantification cycle of each assay.

Appendix II. Results of the one-way Anova analysis of variation between the RQ and RQ_{EA} of the singleplex deletion 22q11.2 assays.

Assay	Variations	df	F	P
DGCR2	Between Group	1	0.00889	0.926
	Within Group	12		
	Total	13		
HIRA	Between Group	1	0.378	0.55
	Within Group	12		
	Total	13		
UFD1L	Between Group	1	0.0778	0.785
	Within Group	12		
	Total	13		
TBX1	Between Group	1	0.146	0.709
	Within Group	12		
	Total	13		
COMT	Between Group	1	0.00356	0.953
	Within Group	12		
	Total	13		
CRKL	Between Group	1	0.0872	0.773
	Within Group	12		
	Total	13		

df = degrees of freedom; F = variance ratio; P = probability

Appendix III A-F. Distribution curves for each of the 22q11.2 singleplex TaqMan assays. Note the distinct bi-modal distribution found between the deletion and normal populations for which the ROC cut-offs were calculated enabling accurate disorder detection.

A)

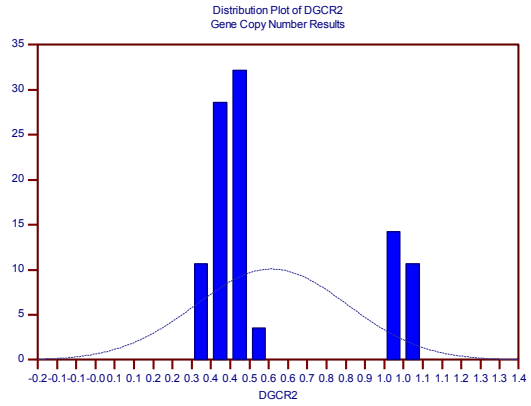

B)

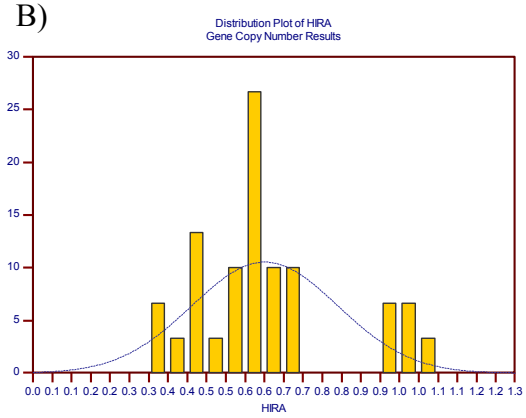

C)

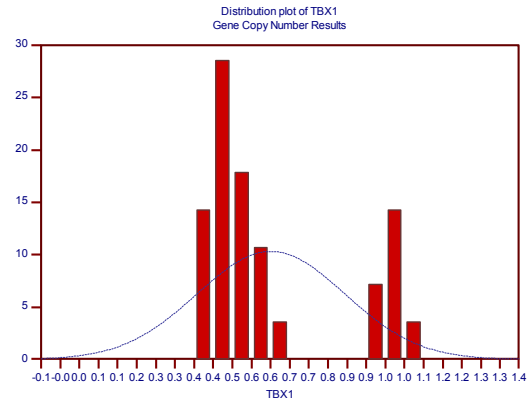

D)

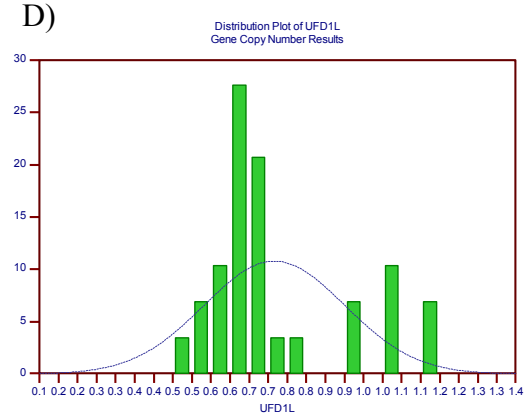

E)

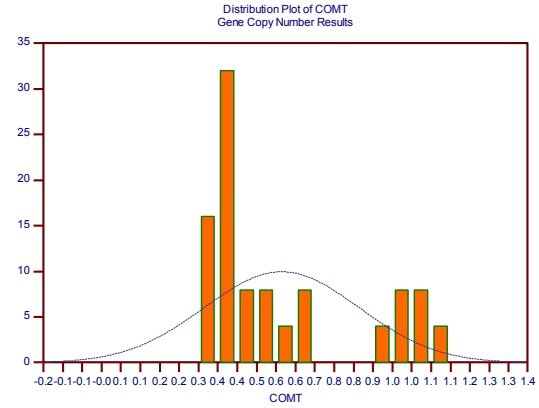

F)

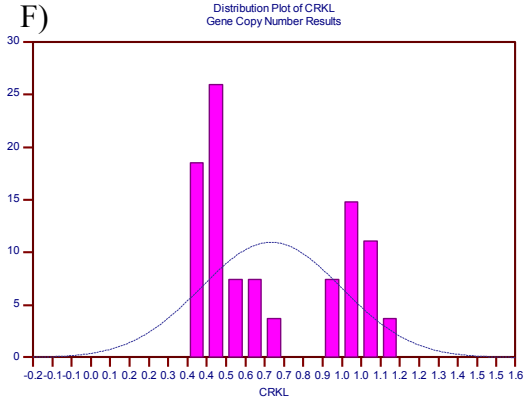

Appendix IV. Results of the one-way Anova analysis of variation of the singleplex SMN1-B and SMN1-G. Little variation (F) was noted between data points used to calculate the mean RQ and RQ_{EA} values for both *SMN*1 assays, with SMN1-G showing almost no variation between the classical RQ method and the efficiency adjusted RQ_{EA} method and higher copy number precision. The p- values were >0.87 for every assay, demonstrating excellent correlation between both gene copy number quantification methods.

Assay		df	F	P
SMN1-B	Between Group	1	0.0306	0.867
	Within Group	6		
	Total	7		
SMN1-G	Between Group	1	0.00524	0.945
	Within Group	6		
	Total	7		

df = degrees of freedom; F = variance ratio; P = probability

Appendix V A-B. Distribution curves for each of the *SMN1* singleplex TaqMan assays. (B) Triplication samples analyzed with SMN1-G demonstrate a third distinct population. Note the bi-modal distribution found between the deletion and normal populations for which the ROC cut-offs were calculated enabling accurate disorder detection. (Also-Rallo et al., 2011b)

A)

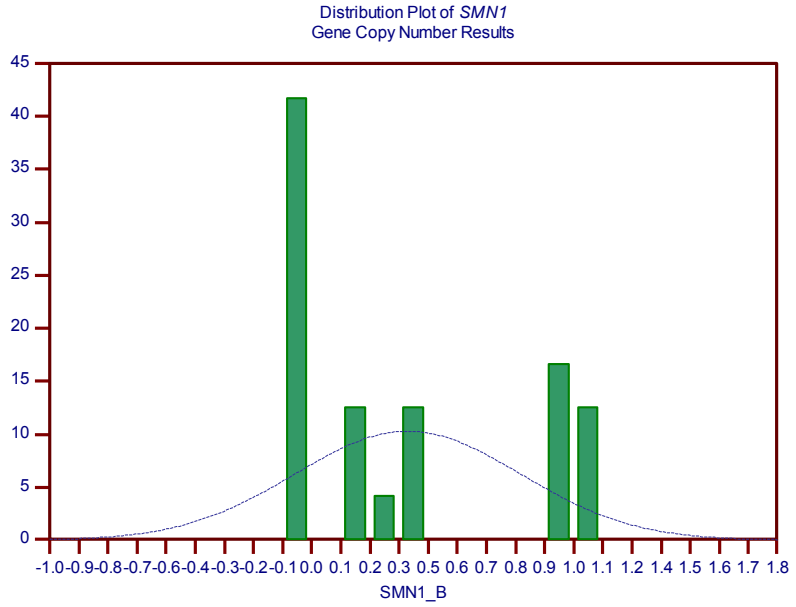

B)

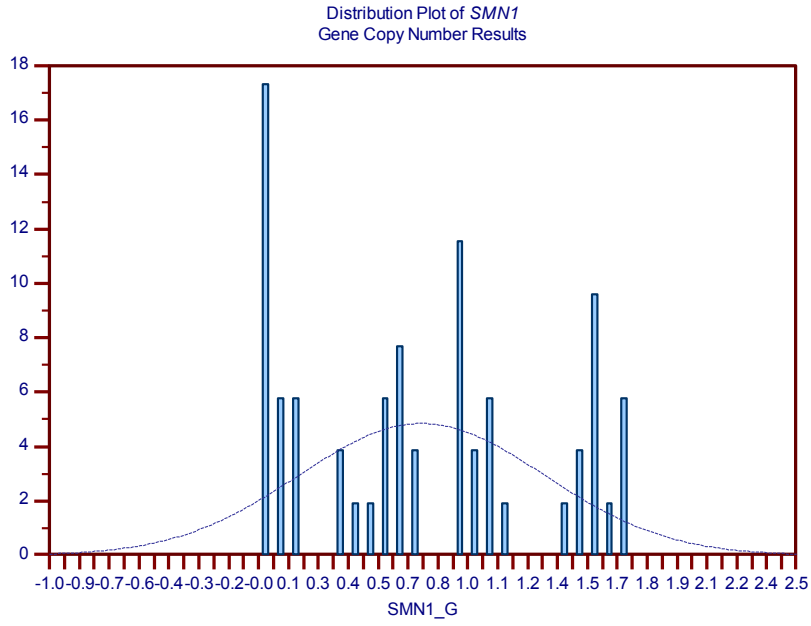

Appendix VI. Restriction enzyme digest of the TREC pGem-T Easy plasmid using *EcoRI* run on a 1.5% agarose gel stained with GelRed Nucleic Acid stain. Uncut plasmid was loaded into lane 1, while *EcoRI* digested plasmid was loaded into lane 2 and a 1:2 digested plasmid dilution was loaded into lane 3. Both lanes 2 and 3 have bands at ~3.1 Kb, indicating the presence of the fully of the linearized plasmid (**) and a much smaller band near the bottom of the gel confirming the presence of the removed 111 bp TREC insert (►). Loaded samples were flanked by the High DNA Mass Ladder (Invitrogen) to enable size estimation and for use as a secondary method for estimating plasmid concentration found to be > 80 ng < 120 ng according to the intensity comparisons between the linear plasmid (**) and the 2 Kb and 3 Kb size markers which is in accordance with the concentration determined by the spectrophotometer.

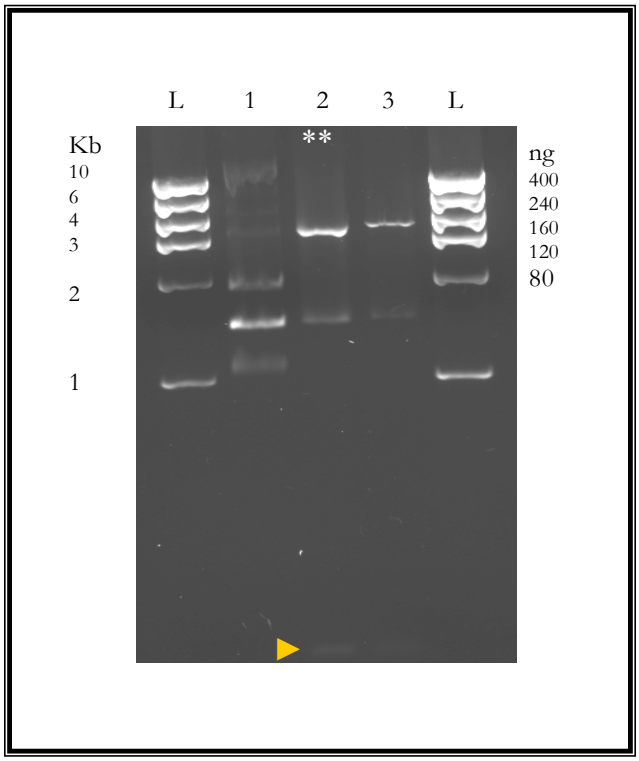

Appendix VII. Receiver Operating Characteristic (ROC) curve for the TREC-E singleplex assay.

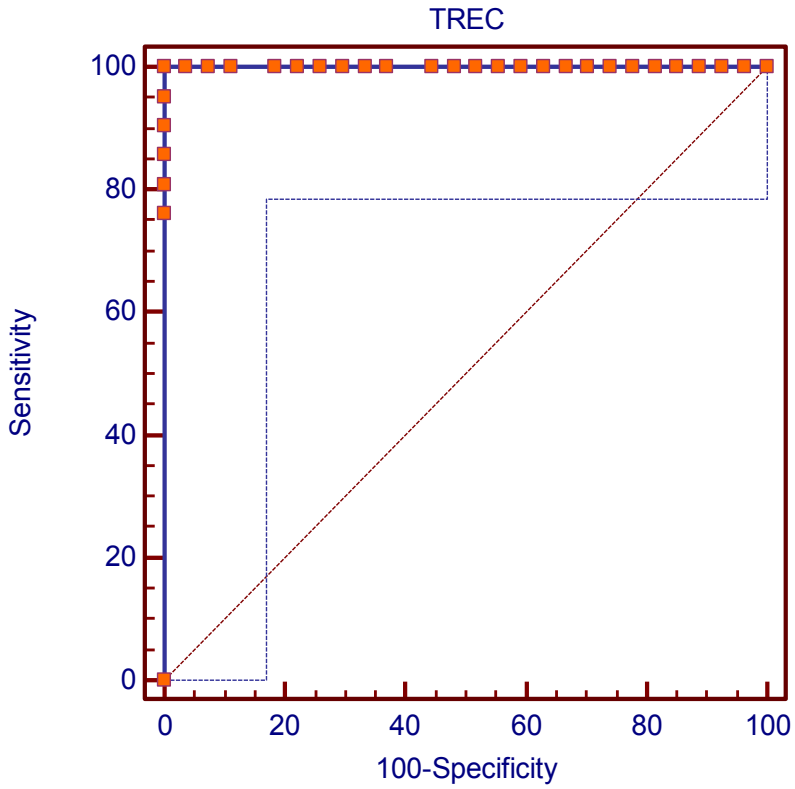

Appendix IIX A-B. Calibration curves for β-Actin and *RNASEP* reference assays. The re-designed custom β-Actin assay had comparable efficiency, slope and y-intercept values compared to the commercial *RNASEP* reference assay (LifeTechnologies). No calibrator data points were omitted and amplification was absent from all NTC through-holes.

A)

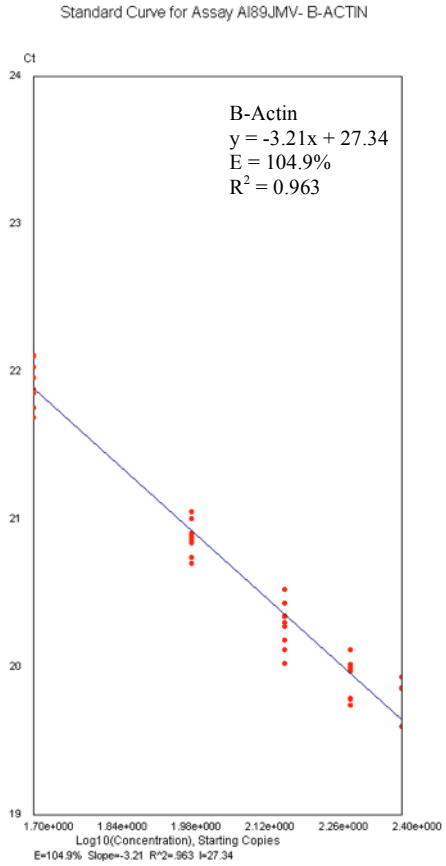

B)

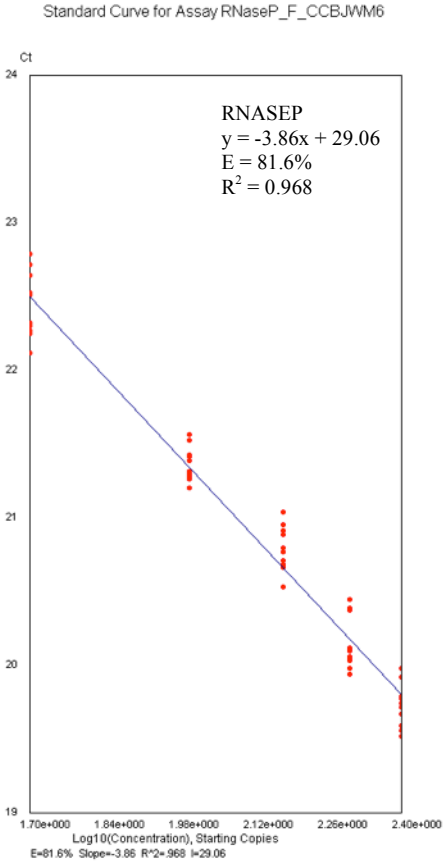

Appendix IX. Calibration curves for each of the six 22q11.2 TaqMan assays analyzed on the OpenArray. Re-designed custom assays (*UFD1L, COMT, CRKL* and *GNAZ*) had comparable efficiencies, slopes and y-intercept values compared to the commercial copy number variation (CNV). No calibrator data points were omitted and amplification was absent from all NTC wells for each assay.

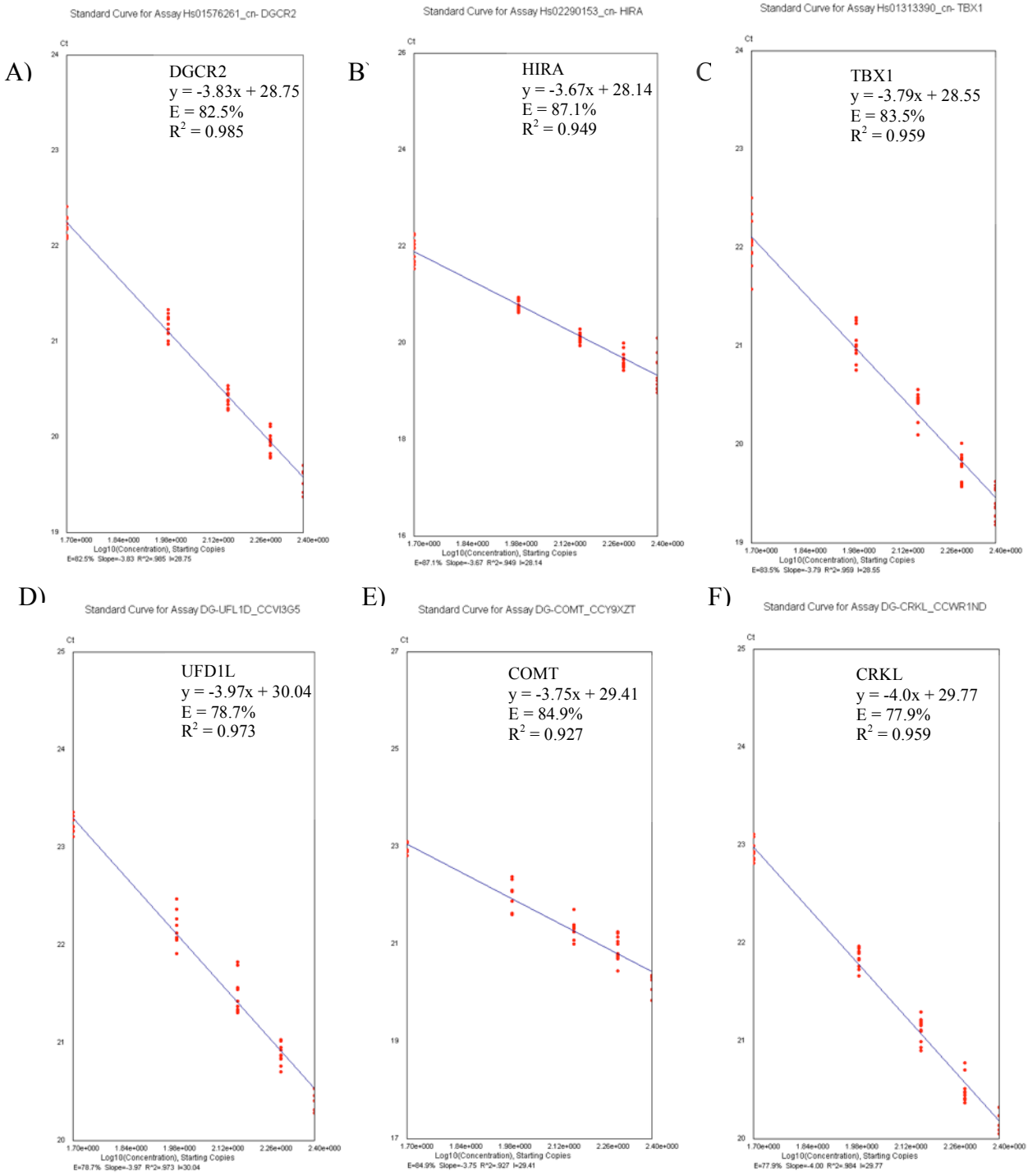

Appendix X. Results of the one-way ANOVA analysis of variation between the RQ and RQ_{EA} for the deletion 22q11.2 assays analyzed on the OpenArray.

Assay	Variations	df	F	P
DGCR2	Between Group	1	0.189	0.672
	Within Group	12		
	Total	13		
HIRA	Between Group	1	0.157	0.699
	Within Group	12		
	Total	13		
UFD1L	Between Group	1	0.155	0.701
	Within Group	12		
	Total	13		
TBX1	Between Group	1	0.243	0.631
	Within Group	12		
	Total	13		
COMT	Between Group	1	0.322	0.581
	Within Group	12		
	Total	13		
CRKL	Between Group	1	0.28	0.606
	Within Group	12		
	Total	13		

df = degrees of freedom; F = variance ratio; P = probability

Appendix XI. Population distribution curves of all the deletion 22q11.2 assays analyzed using the OpenArray system. Note the distinct bi-modal separations between the carriers and normal samples. ROC cut-off values fall in between each of the modes.

A)

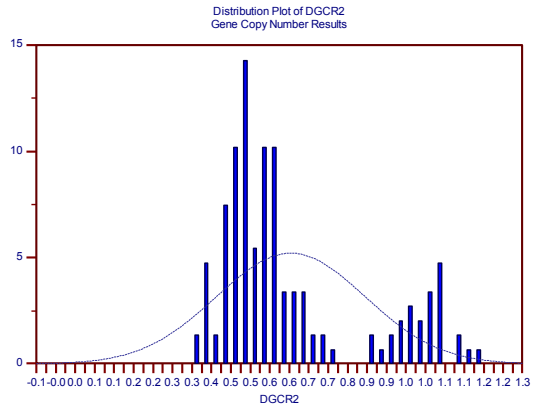

B)

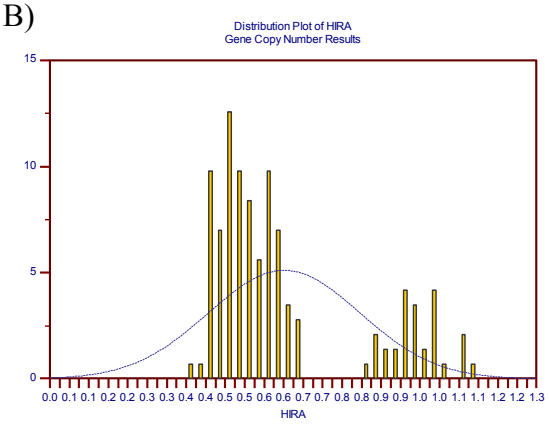

C)

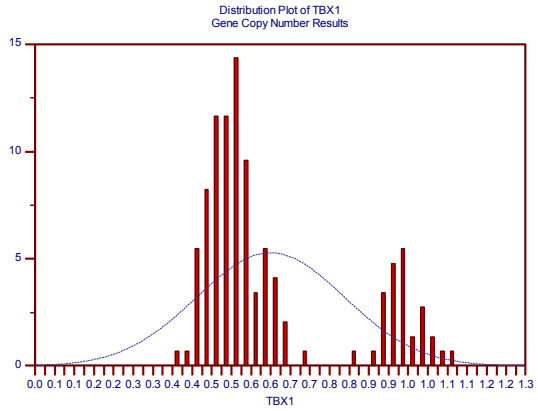

D)

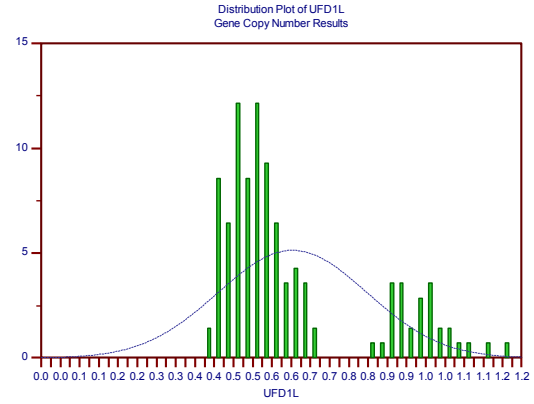

E)

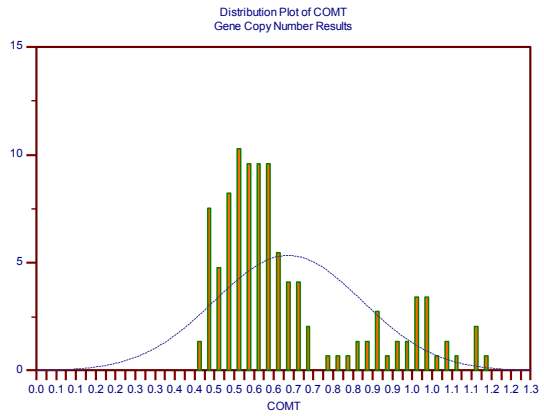

F)

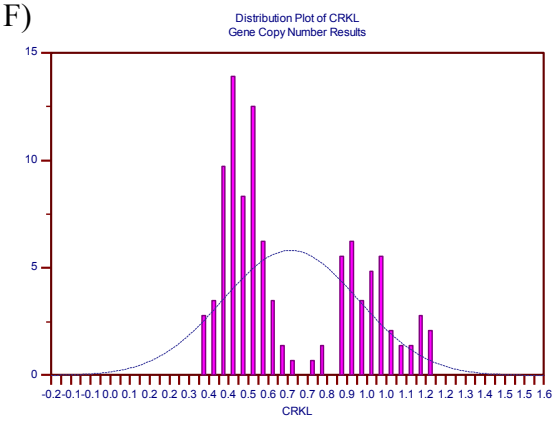

Appendix XII. Distribution plot of the SMN1-G assay using the OpenArray system. Note the distinct multi-modal separations between the SMA samples; carriers; normal and duplication samples. ROC cut-off values fall in between each of the modes.

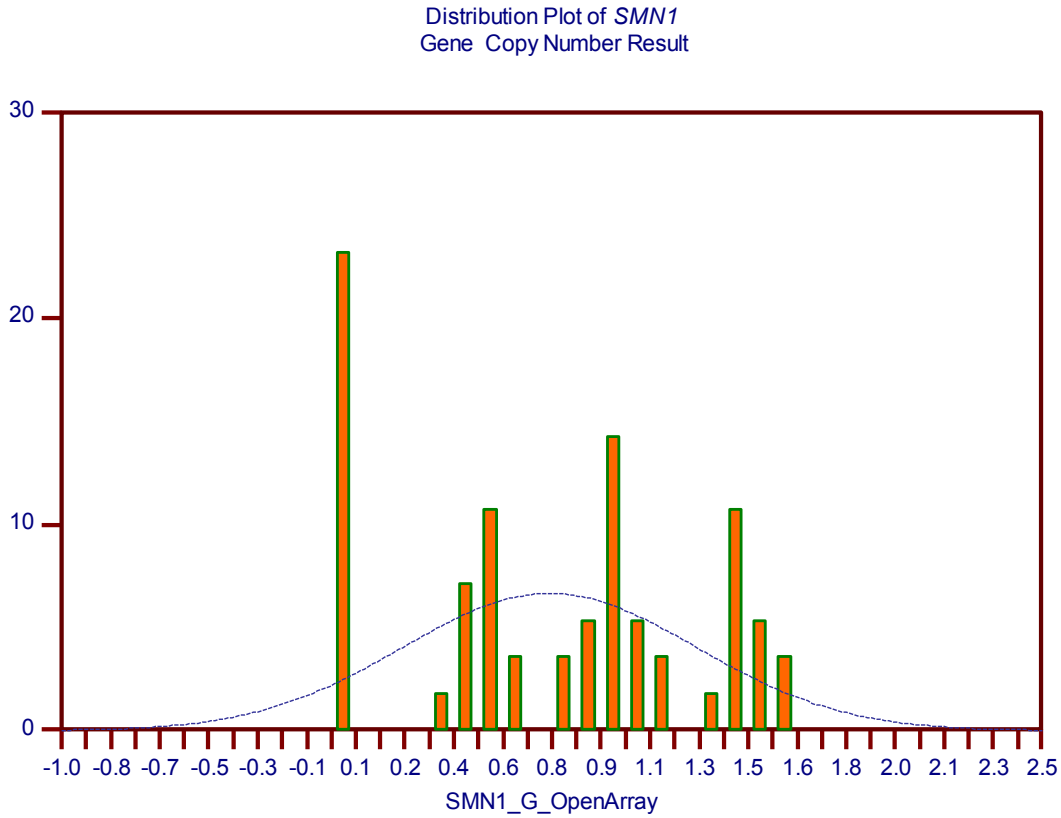

Appendix XIII. A list of excitation, emission and quenching wavelengths of the fluorophores and quenchers used in this study.

Fluorophore	Excitation	Emission	Quencher	Quenching Range λ nm
FAM	495	520	BHQ-0	130-520 nm
VIC	538	554	MGB	480-580 nm
NED	546	575	MGB	480-580 nm
Quasar 670	647	670	BHQ-3	620-730 nm

Appendix XIV A-D. Calibration curves of *RNASEP, UFD1L, COMT* and *CRKL* assays within Multiplex A. Each calibrator was analyzed in triplicate, with no amplification noted in the NTC.

A)

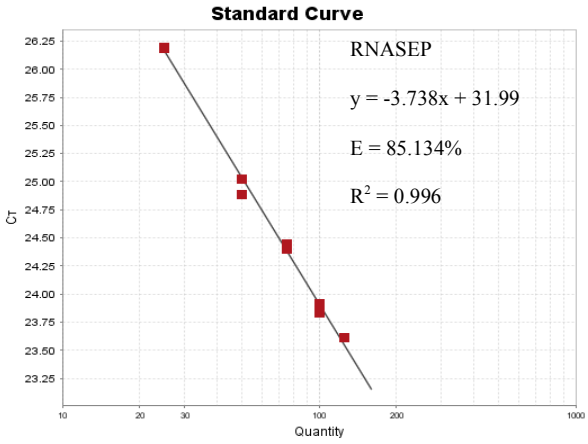

Target: RNASEP Slope: -3.738 Y-Inter: 31.39 R^2: 0.996 Eff%: 85.134 Error: 0.077

B)

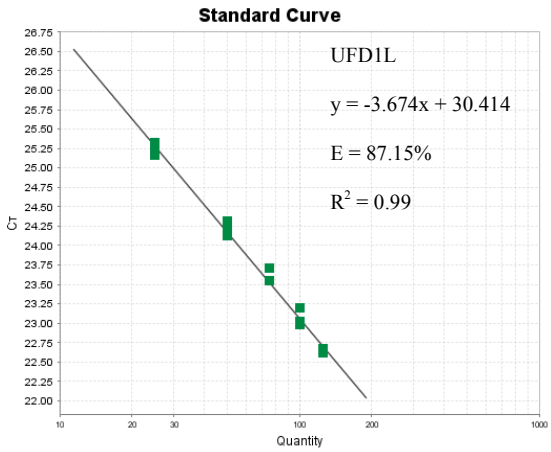

Target: UFD1L Slope: -3.674 Y-Inter: 30.414 R^2: 0.99 Eff%: 87.15 Error: 0.104

C)

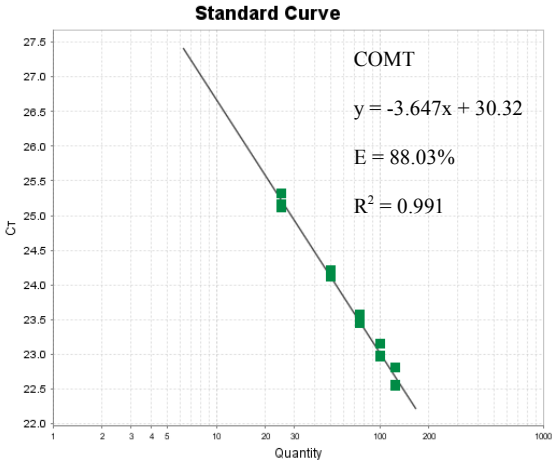

Target: COMT Slope: -3.647 Y-Inter: 30.32 R^2: 0.991 Eff%: 88.03 Error: 0.097

D)

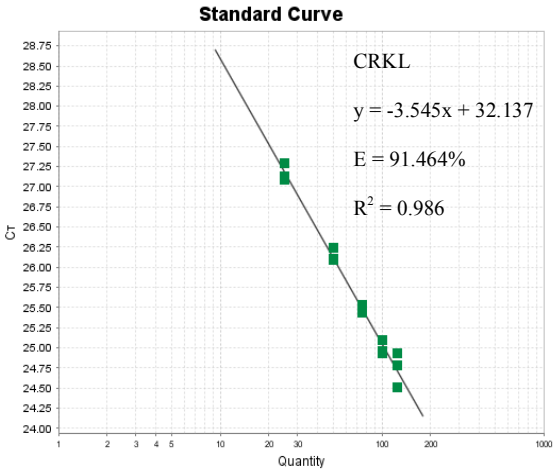

Target: CRKL Slope: -3.545 Y-Inter: 32.137 R^2: 0.986 Eff%: 91.464 Error: 0.122

Appendix XV A-C. Calibration curves of all *UL54, RNASEP* and TREC-E assays within multiplex B. The highest concentration calibrator (250 ng/ul) was removed from the *RNASEP* curve due to increased amplification inhibition. The CMV calibrators and WT DNA calibrators for *RNASEP* were setup in duplicate, while the TREC in-house calibrators were setup in triplicate.

A)

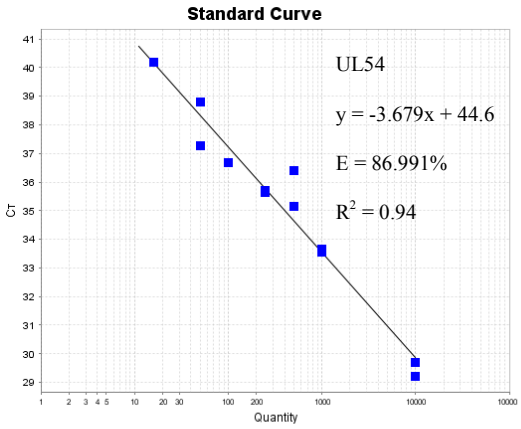

Target: CMV UL-54 Slope: -3.679 Y-Inter: 44.6 R^2: 0.94 Eff%: 86.991 Error: 0.31

B)

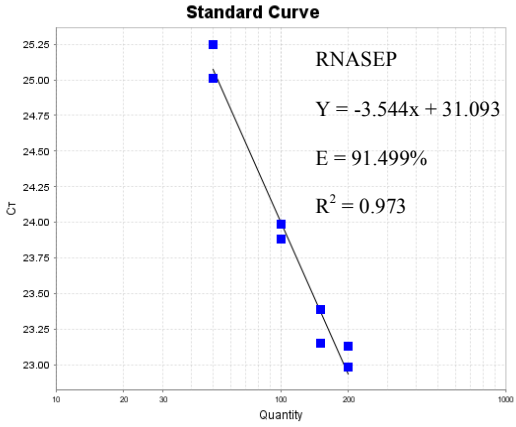

Target: RNASEP Slope: -3.544 Y-Inter: 31.093 R^2: 0.973 Eff%: 91.499 Error: 0.242

C)

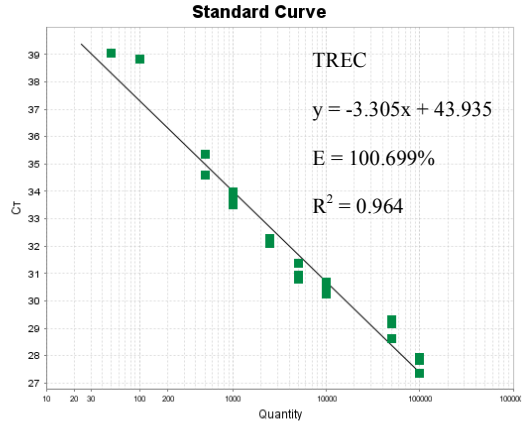

Target: TREC Slope: -3.305 Y-Inter: 43.935 R^2: 0.964 Eff%: 100.699 Error: 0.144

Appendix XVI A-C. Calibration curves for *RNASEP*, TREC-E and *TBX1* assays within multiplex C. The highest concentration calibrator (250 ng/ul) was removed from the *RNASEP* and *TBX1* curve due to increased amplification inhibition. The WT DNA calibrators for *RNASEP* and *TBX1* were setup in duplicate, while the TREC in-house calibrators were setup in triplicate.

A)

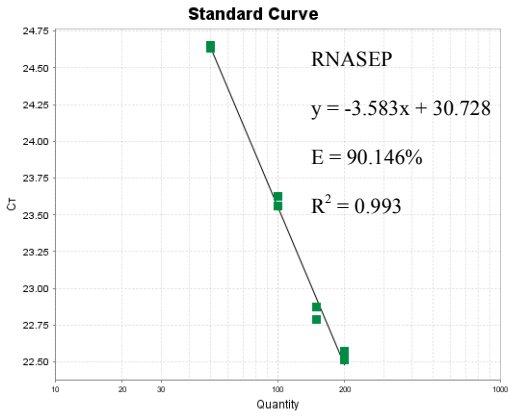

Target: RNAse P Slope: -3.583 Y-Inter: 30.728 R^2: 0.993 Eff%: 90.146 Error: 0.123

B)

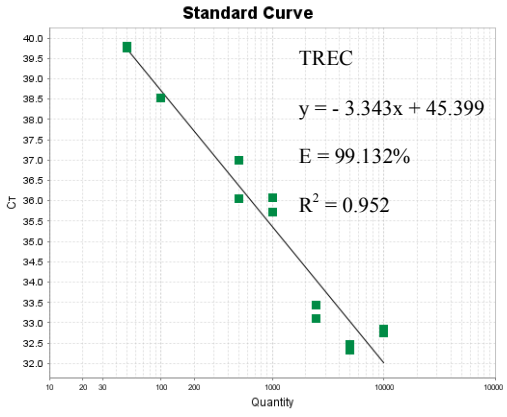

Target: TREC Slope: -3.343 Y-Inter: 45.399 R^2: 0.952 Eff%: 99.132 Error: 0.226

C)

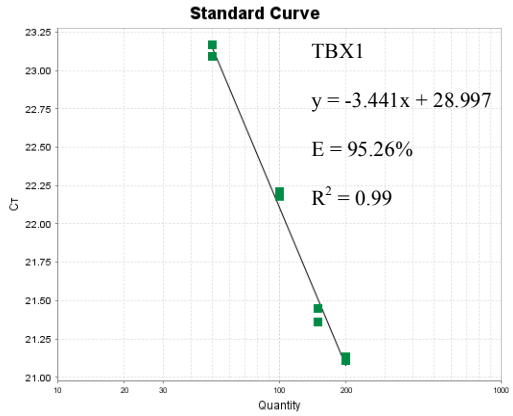

Target: TBX1 Slope: -3.441 Y-Inter: 28.997 R^2: 0.99 Eff%: 95.26 Error: 0.139

Appendix XVII. Results of the one-way ANOVA analysis of variation between the RQ and RQ_{EA} for *UFD1L, COMT* and *CRKL* from multiplex A and *TBX1* from multiplex C.

Assay	Variations	df	F	P
UFD1L	Between Group	1	0.579	0.449
	Within Group	100		
	Total	101		
TBX1	Between Group	1	0.0231	0.88
	Within Group	82		
	Total	83		
COMT	Between Group	1	0.565	0.454
	Within Group	100		
	Total	101		
CRKL	Between Group	1	0.352	0.554
	Within Group	100		
	Total	101		

df = degrees of freedom; F = variance ratio; P = probability

Appendix XVIII A-D. Distribution plots of multiplexed *UFD1L, COMT* and *CRKL* gene copy number from multiplex A, and *TBX1* from multiplex C. Note the distinct separations between the WT samples and 22q11.2 deletion carriers. ROC cut-off values fall in between each of the modes.

A)

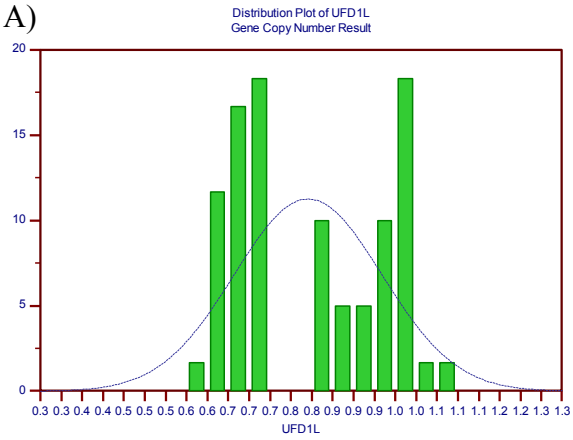

B)

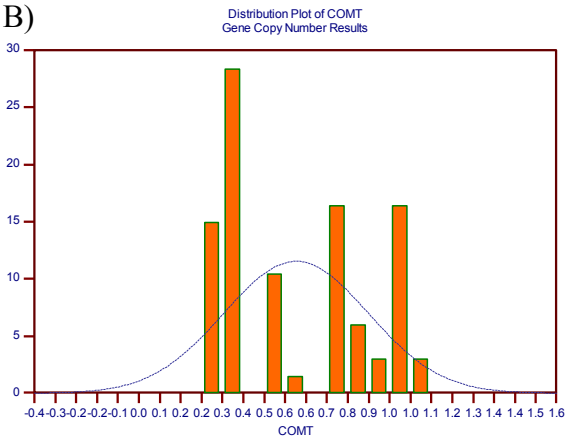

C)

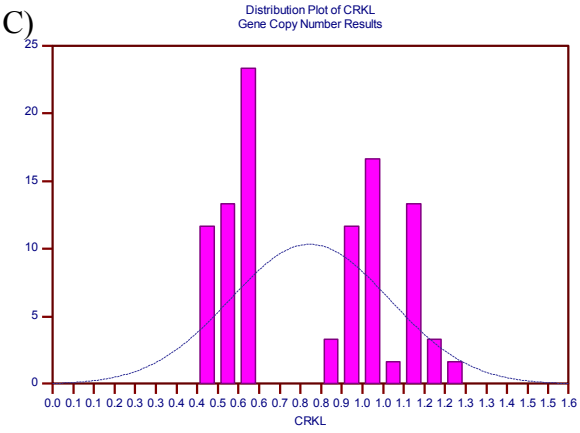

D)

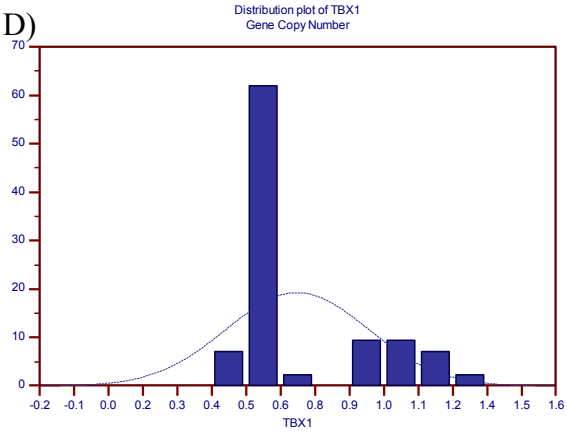

Appendix XIV A-B. The TREC ROC curves for both Multiplex B (A) and Multiplex C (B).

A)

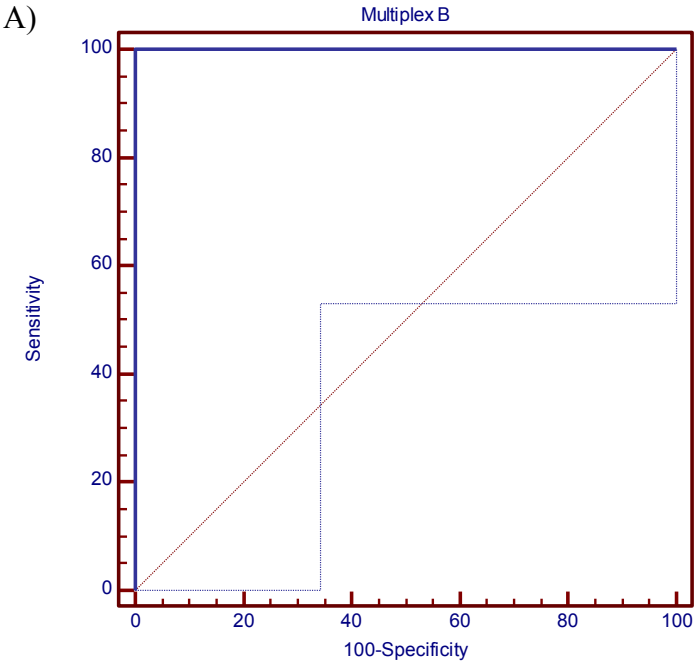

B)